SOME NOVEL HYDROGEN BONDED SUPRAMOLECULAR LIQUID CRYSTALS: SYNTHESIS AND STUDY OF LIQUID CRYSTALLINE AND PHOTOCHEMICAL PROPERTIES

THESIS SUBMITTED TO
THE UNIVERSITY OF KERALA
IN FULFILMENT OF THE REQUIREMENTS
FOR THE DEGREE OF
DOCTOR OF PHILOSOPHY
IN CHEMISTRY
UNDER THE FACULTY OF SCIENCE

BY

V. AJAYA MALLIA

PHOTOCHEMISTRY RESEARCH UNIT
REGIONAL RESEARCH LABORATORY (CSIR)
TRIVANDRUM-695 019. KERALA. INDIA

JUNE 2001

SOME NOVEL HYDROGEN BONDED SUPRAMOLECULAR LIQUID CRYSTALS: SYNTHESIS AND STUDY OF LIQUID CRYSTALLINE AND PHOTOCHEMICAL PROPERTIES

THESIS SUBMITTED TO
THE UNIVERSITY OF KERALA
IN FULFILMENT OF THE REQUIREMENTS
FOR THE DEGREE OF
DOCTOR OF PHILOSOPHY
IN CHEMISTRY
UNDER THE FACULTY OF SCIENCE

BY

V. AJAYA MALLIA

PHOTOCHEMISTRY RESEARCH UNIT
REGIONAL RESEARCH LABORATORY (CSIR)
TRIVANDRUM-695 019, KERALA, INDIA

JUNE 2001

STATEMENT

I hereby declare that the matter embodied in this thesis is the result of investigations carried out by me at the Photochemistry Research Unit of the Regional Research Laboratory (CSIR), Trivandrum, under the guidance of Dr. Suresh Das and the same has not been submitted elsewhere for a degree.

In keeping with the general practice of reporting scientific observations, due acknowledgement has been made wherever the work described is based on the findings of other investigators.

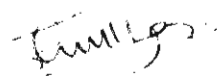V. Ajaya Mallia

Dr. SURESH DAS
SCIENTIST

June 19, 2001

CERTIFICATE

Certified that the work embodied in this thesis entitled: **"Some Novel Hydrogen Bonded Supramolecular Liquid Crystals: Synthesis and Study of Liquid Crystalline and Photochemical Properties"** has been carried out by Mr. V. Ajaya Mallia under my supervision and the same has not been submitted elsewhere for a degree.

Suresh Das

(Thesis Supervisor)

iii

ACKNOWLEDGEMENTS

Trivandrum

June 2001

V. Ajaya Mallia

iv

CONTENTS

PREFACE

The thesis entitled: "Some Novel Hydrogen Bonded Supramolecular Liquid Crystals: Synthesis and Study of Liquid Crystalline and Photochemical Properties" deals mainly with efforts on designing novel liquid crystalline (LC) materials containing photoactive chromophores. In order to achieve this we have used hydrogen bonding interactions between suitable donor and acceptor molecules to generate a variety of photoactive LCs showing smectic, nematic, cholesteric and cubic phases.

In the area of photonics, increasing attention is being paid to the study of molecules or molecular systems whose chemical or physical properties can be reversibly controlled using light as a stimulus, due to the importance of such systems in erasable direct read after write devices (EDRAW). LC materials are particularly suited for such applications since their liquid like nature provides the possibility of molecular motion in response to the properties of light. LC materials that can respond to light (optical switching) can have switching times of the order of microseconds. Such devices can find use in optical computing and real time holography.

The first Chapter of the thesis presents a brief review covering some aspects of hydrogen bonded LCs as well as the importance of LC materials in

display systems. The recent work on photoswitchable LC materials and devices is also briefly described.

The second Chapter deals with the synthesis and characterization of some supramolecular hydrogen bonded mesomorphic materials containing azopyridyl moieties, which exhibit smectic and nematic LC phases. These assemblies were prepared by the complexation of hydrogen bond acceptors such as 4-*n*-alkyloxyphenyl.4'-azopyridines (**3a-e**), 4-pyridylazo,4'-phenyl-*n*-alkanoates (**9a, b**) and 4,4'-azobipyridine (**11**) with hydrogen bond donors such as 4-*n*-alkyloxybenzoic acids (**4a-c**). It has been observed that these compounds exhibit well defined LC phases over wide range of temperatures in the heating, as well as in the cooling cycles which are distinctly different from those of the parent compounds. The mesogenic behaviour of materials containing varying proportions of hydrogen bond donors and acceptors were investigated in detail. The effect of the photochromic behaviour of the azo moiety on the LC behaviour has also been studied. Photoisomerization of the azo moiety in the hydrogen bonded complexes resulted in a marked change in its phase transition properties.

Chapter 3 describes our efforts to synthesize hydrogen bonded cholesteric LC materials whose helical super-structure can be preserved in the solid state. Recent studies suggest that such cholesteric glassy LCs can be used for developing full colour recording devices. Supramolecular hydrogen bonded LC materials containing

cholesterol groups have been synthesized and characterized. These assemblies were prepared by complexing cholest-5-en-3-ol-(3β)[4-phenyl,4'-pyridylazo]carbonate (4) with a series of hydrogen bond donors such as 4-n-alkyloxybenzoic acids (5a-e) and 4-n-alkyloxycinnamic acids (9a-e). The heterointermolecular hydrogen bonded complexes exhibit LC phases over a range of temperature. Sudden cooling of the complexes from cholesteric temperatures to 0 °C resulted in the formation of stable glasses. The glassy phases thus formed show characteristic cholesteric colours, which were extremely stable at room temperature (> 8 months). This is the first report on the formation of low molecular weight cholesteric glassy LCs *via* heterointermolecular hydrogen bonding between suitable hydrogen bond donor and acceptor molecules.

In Chapter 4, first- and second-generation supramolecular hydrogen bonded complexes containing dendrimeric materials have been synthesized. These assemblies were prepared by the intermolecular hydrogen bonding interaction between hydrogen bond donors such as 3,4,5-tri-n-dodecyloxybenzoic acid (6) and 3,4,5-tris[3',4',5'-tris(n-dodecane-1-yloxy)-benzyloxy]benzoic acid (13) with hydrogen bond acceptors such as 4,4'-azobipyridine (ABP), 4,4'-bipyridylethylene (BPE) and 4,4'-bipyridine (BP). Liquid crystalline properties of these materials were studied by polarizing optical microscope, differential scanning calorimetry

and small angled X-ray diffractrometry. These studies reveal that the second-generation hydrogen bonded materials exhibit cubic LC phases whereas the first-generation dendrimers do not possess any LC phases. Sudden cooling of the LC phases observed at high temperature to ~0 °C resulted in the formation of highly transparent ordered glassy phases, which were extremely stable at room temperature (> 1 year). Photochemical transformation of the chromophores (azo and stilbene moieties) in the cubic glassy LC phases have also been investigated.

Note: The compound numbers listed in this preface refer to those given in different Chapters of this thesis.

CHAPTER 1

INTRODUCTION

1.1. Liquid Crystals–Basic Aspects and Classification

Molecules, which show both the property of a well arranged crystal and highly disordered liquid state, are termed as liquid crystals (LC) or mesogens. These compounds show a series of transformations involving new phases possessing a state of aggregation intermediate between a crystal and liquid. LCs can broadly be classified into lyotropic and thermotropic, depending on their mode of formation.[1] Lyotropic LCs can be obtained by dissolving amphiphilic molecules in a solvent, which is most commonly water or some highly polar solvent. At intermediate concentrations (above the critical micellar concentration, CMC), they show anisotropic properties, characteristic of LCs. Common examples of such lyotropic LCs are those produced from soaps and other detergent systems in water. The molecular mechanism involved in these cases is the destruction of the three dimensional lattice by solvent penetration. Materials for which LC phases are obtained on heating their crystalline phase or cooling their liquid phase are termed as thermotropic LCs. Thermotropic LCs are formed from predominantly organic

compounds, which are mainly either rod-, disc- or board shaped.[2] In such materials the LC phases are formed due to dislocation of lattice positions as a result of thermal vibrations. Thus, in a thermotropic mesophase varying degrees of positional order are lost, giving rise to fluidity, while orientational (supramolecular) order is retained, giving rise to anisotropy. Hence the mesophases can have two or even three different refractive indices, magnetic susceptibilities and electric permittivities. As a result of this, applied electric or magnetic fields can orient some thermotropic molecules, which form the basis for their practical applications. The essential requirement for LC behaviour is that the molecule must possess geometric anisotropy.[1]

$$|\;|\;|\;|\;|\;|\;|\;|\;|\qquad /\;/\;/\;/\;/\;/\;/$$
$$|\;|\;|\;|\;|\;|\;|\;|\;|\qquad /\;/\;/\;/\;/\;/\;/$$
$$|\;|\;|\;|\;|\;|\;|\;|\qquad /\;/\;/\;/\;/\;/\;/$$

(a) (b)
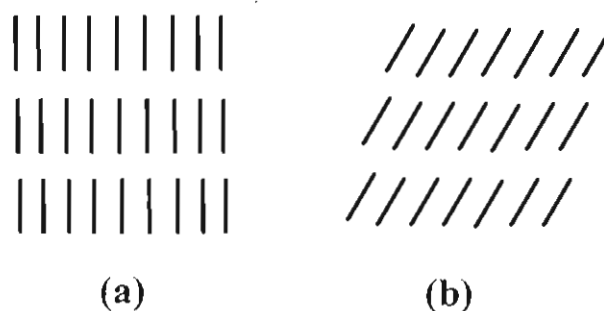
Figure 1.1. Molecular orientation: (a) S_A phase (b) S_C phase.

Thermotropic LCs can be further subdivided into three types, namely calamitic (rod like), discotic (D, disc like) and sanidic (board shaped). The vast majority of thermotropic liquid crystals are composed of rod like molecules and these can be further classified into three types, namely smectic (S), nematic (N)

and cholesteric mesophases.[3] The smectic mesophase is a turbid viscous state with certain properties reminiscent of those found for soaps. The term 'smectic' is derived from the Greek word, 'smectos' (soap like), because these phases were first discovered in soap solutions. They have stratified structures and a variety of molecular arrangements are possible within each stratification.[4,5] Smectic mesophases adopt three different textures depending on: (i) the nature of the compound under consideration, (ii) the way in which the mesophase is produced, e.g., by heating the crystals, by cooling the isotropic liquid, or by cooling the nematic mesophase, and (iii) the nature and cleanliness of the supporting surface employed to mount the specimen. Some smectic LCs have phases with the molecules perpendicular to the layers (S_A, Figure 1.1.a), whereas in others they are inclined to the plane (S_C, Figure 1.1.b). Depending on the molecular orientation, several types of higher order smectic phases are also described in the literature.[1] Discotic LC phases are obtained with disc like molecules wherein the director is perpendicular to the molecular plane.[6,7]

Nematic LCs have a high degree of long-range orientational order of molecules, but no long-range translational order (Figure 1.2.a). On surfaces such as glass, the mesophase frequently adopts a characteristic 'threaded' texture, clearly visible between crossed polaroids, and the word 'nematic' again stems from the Greek word, 'nematos', meaning thread-like. The point group symmetry

of the nematic phase is $D_{\infty h}$. A notable difference between the smectic and nematic mesophases lies in the way in which the two mesophase types separate from the isotropic liquid. Whilst the smectic mesophase appears in the shape of elongated rods (bâtönnets), the nematic mesophase separates as tiny, spherical droplets, which coalesce to form a nematic texture.[8]

The third class of thermotropic liquid crystals is very similar to nematics except that the molecules contain chiral groups. This type of LC phase is known as chiral nematic or cholesteric mesophase since this type of texture was first observed in derivatives of cholesterol or other steroids such as cholesteryl esters derived from open chain aliphatic acids.[9] However, compounds derived from other systems also exhibit cholesteric mesophase as in the case of optically active amyl *p*-(4-cyanobenzylidene-amino)cinnamate. It may also be noted that not all cholesterol containing compounds exhibit cholesteric LC phases. Many of the open-chain aliphatic esters of cholesterol exhibit smectic mesophases in addition to cholesteric mesophases. The difference between cholesteric and nematic mesophases is that in cholesterics the director (the unit vector describing the average direction of the molecular long axis) is not constant in space, but undergoes a helical distortion (Figure 1.2.b). The structure may be envisaged as composed of layers or sheets of nematic LC, as shown in Figure 1.2. The director of an individual layer is rotated through a small angle with respect to the director

in adjacent layers. As a succession of layers is passed through, the director turns

through 360° and this thickness represents the pitch length (p) for the helix. The

twist may be right handed or left handed depending on the molecular

conformation. The spiral arrangement of the molecules in the cholesteric phase is

responsible for its optical properties. Cholesteric LCs show selective reflection of

circularly polarized light and a rotatory power about a thousand times greater than

that of an ordinary optically active substance.

pitch length (p),
360° rotation of
director

(a)

(b)
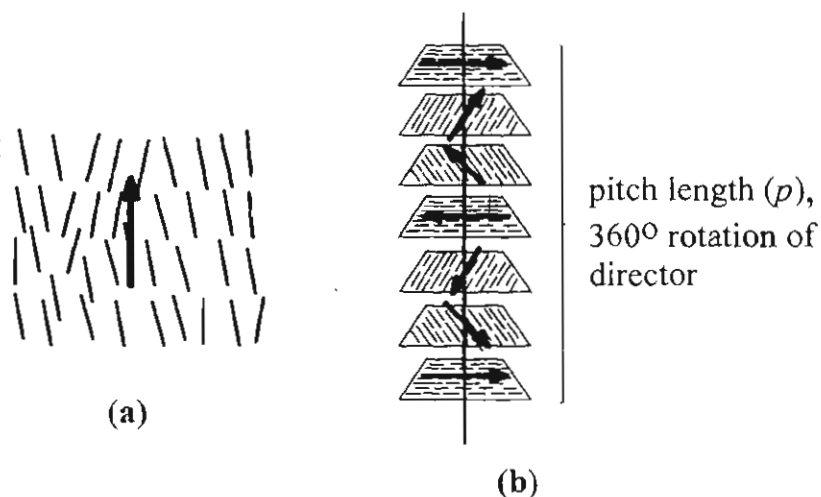
**Figure 1.2. Schematic representation of the molecular order in (a) nematic
LC, (b) helical structure of a cholesteric LC.**

1.2. Structure Property Relationship of Liquid Crystals

LC phases can be exhibited by molecules having several different

molecular shapes such as rod and disc shapes. Generally compounds possessing a

rigid core with a flexible chain show LC behaviour. A schematic representation of a LC forming molecule is as shown in Figure 1.3. Here 'B' can be an aromatic core, example, phenyl, 'A' a linker such as N=N, CH=CH, 'X' a flexible alkyl chain and 'Z' can be any lateral substituent.
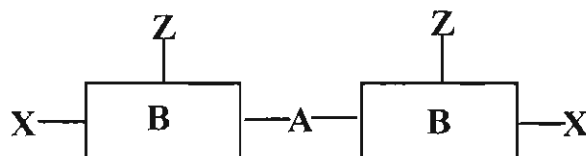
Figure 1.3.

1.3. Hydrogen Bonded Liquid Crystals

For inducing aggregation of molecules or molecular species hydrogen bonding is considered to be of great importance.[10,11] Hydrogen bonding was first recognized in the physical properties of liquids involving a hydrogen atom and electronegative atoms like fluorine, oxygen or nitrogen. The most well known example of hydrogen bonding in nature is the interaction of complementary nucleobases, which stabilizes the double helical structure of nucleic acids. Also in organic compounds hydrogen bonding is considered as the simplest way of linking two components in the preparation of new supramolecular assemblies.[10,11] However up to the last decade, synthesis of mesomorphic materials *via* hydrogen bonding has not been well appreciated. This may be due to the fact that in most

cases the magnitude and direction of these secondary interactions are not sufficient to keep the fluid state ordered. Also, many simple molecules that show hydrogen bonding do not exhibit LC behaviour.[12]

Emil Fischer in 1911 noted the double melting of some long alkyl chain *n*-alkyl pyranosides, and later it was recognized as evidence for the formation of a LC phase.[13-15] These carbohydrate derivatives could be the first compounds reported in the literature, which exhibit mesophases *via* intermolecular hydrogen bonding. The stacked chair form of carbohydrate groups (Chart 1.1.) can clearly favor hydrogen bonding between the overlapping hydroxyl groups.[15-17]
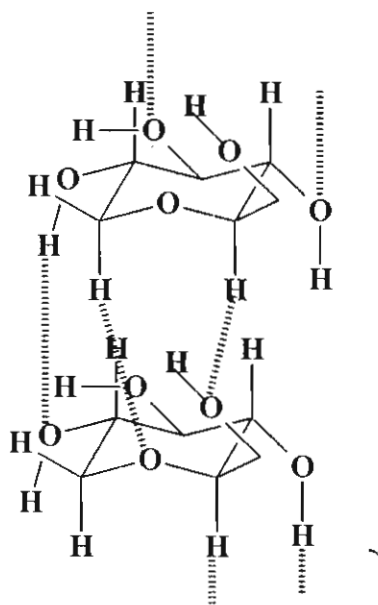
1

Chart 1.1.

In 1953, Gray *et al.* have reported the LC properties of 4-*n*-alkyloxybenzoic acids and 4-*n*-alkyloxycinnamic acids, and predicted the formation of the LC phase by hydrogen bonding.[18,19] Carboxylic acids can dimerize either in a closed chain form or in an open chain form, both of which stabilize the LC phase by lengthening the rigid rod moiety (**2**, Chart 1.2.).[20]

2
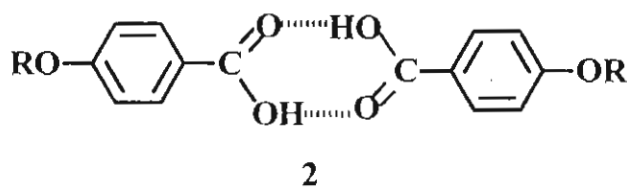
Chart 1.2.

Aliphatic acids do not generally exhibit LC properties, however 2,4-nondienoic acid is liquid crystalline due to the presence of double bonds which increase the intermolecular attraction due to high polarizability of the molecule.[1,12]

A series of aromatic and aliphatic polyesteramides also show thermotropic liquid crystallinity through lateral hydrogen bonding interactions between amide linkages. The lateral hydrogen bonding interaction is also effective in generating S_C phases for tropone derivatives.[21] A columnar mesophase is observed for trialkyloxybenzamides.[22] In all the above compounds intermolecular hydrogen bonding between identical molecules is responsible for the occurrence of LC phases.

In 1989, Kato *et al.* have reported the formation of supramolecular LC assemblies *via* heterointermolecular hydrogen bonding between a hydrogen bond donor and a hydrogen bond acceptor.[23,24] In view of the ease of synthesis of novel LC materials by hydrogen bonding, a wide variety of LC materials have since been synthesized by this method.

1.3.1. Hydrogen Bonded Liquid Crystals from Monomeric Molecules

The general structural requirement of a molecule to show LC property is that it must contain a rigid core and a flexible chain.[1] In hydrogen bonded supramolecular assemblies these can be achieved *via* intermolecular hydrogen bonding. These systems are composed of hydrogen bond acceptors such as pyridyl or bipyridyl moieties and hydrogen bond donors such as carboxylic acids, alcohols or amines. A typical interaction of this type is shown schematically in Figure 1.4.[12,23-25]
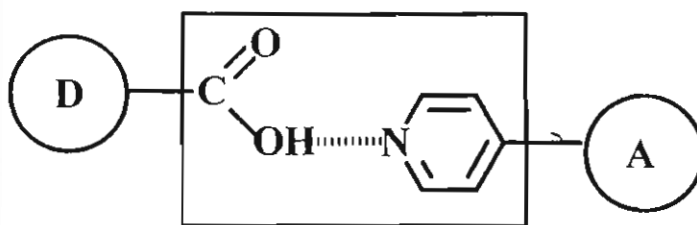
Figure 1.4. Schematic representation of the interaction of pyridyl and carboxyl groups.

The LC complex **3** was formed by the intermolecular interaction of 4-*n*-butyloxybenzoic acid with *trans*-4[(4-ethoxybenzoyl)oxy]-4'-stilbazole (**3**, Chart 1.3.).[23] This complex exhibits a S phase as evidenced by its focal conic texture, which was not exhibited by either of the individual components. The stabilization of the mesophase of the 1:1 complex **3** was attributed to the formation of a new and elongated mesogen through intermolecular hydrogen bonding which allows **3** to behave as a single component liquid crystalline material.

3
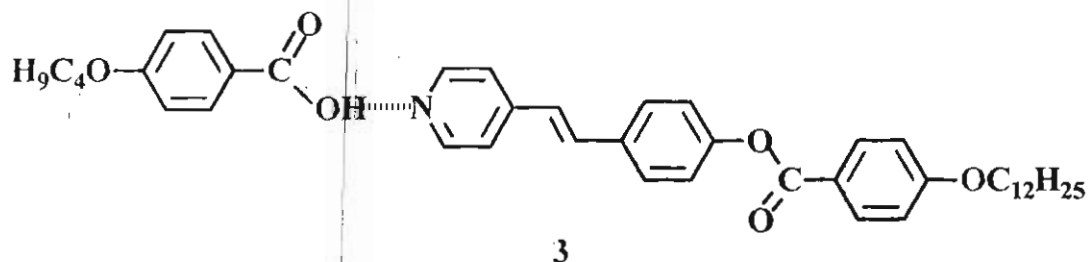
Chart 1.3.

In a similar manner, the hydrogen bonded complexes formed between a nonmesogenic dicarboxylic acid with mesogenic *trans*-4-[4-(ethoxy-benzoyl)oxy]-4'-stilbazole also exhibit LC properties.[26] LC complexes were formed by treating 4-*n*-alkyloxybenzoic acids or 4-*n*-alkylbenzoic acids with bipyridine or *trans*-1,2-bis(4-pyridyl)ethylene.[27-29] These complexes show sharp phase transitions which are very different from those of the parent components. The hydrogen bonded complex between 4,4'-bipyridine and 4-*n*-butylbenzoic acid

exhibits a S phase while the supramolecular assembly between 4,4'-bipyridine and 4-*n*-butyloxybenzoic acid possess N and S phases. The interaction of phthalic acid or isophthalic acid with *trans*-4-alkoxy-4'-stilbazole leads to complexes with bent structures (**4**, Chart 1.4.).[25] These complexes exhibit LC properties even though they are not linear in shape. It is interesting to note that compounds consisting of covalently bonded nonlinear structures generally do not exhibit LC properties.

4
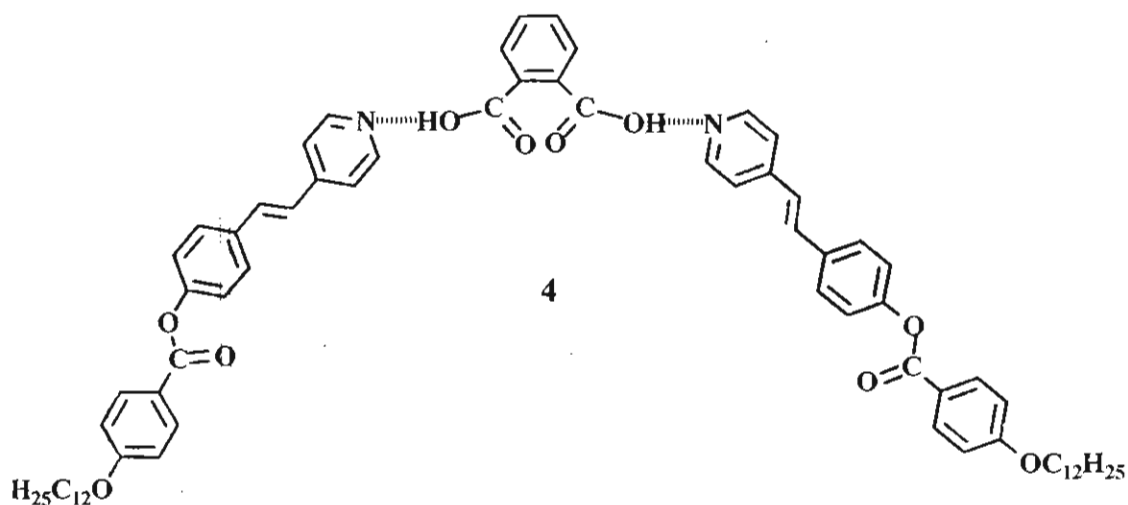
Chart 1.4.

In an analogous fashion, the interaction of two stilbazole units linked by a triethyleneglycol spacer, also yields an LC material.[30]

Kreese *et al.* have shown that materials obtained from the monocarboxylic acids and alkyl pyridine derivatives show mesomorphic properties which are highly dependent upon the length of the molecule.[31] It has been shown that amines

and alcohols can also be used as hydrogen bond donors. instead of pyridine for generating LC materials. Early examples of complexes not bearing a central pyridyl-carboxyl unit are shown in Chart 1.5. wherein the diacylhydrazines (**5, 6,** Chart 1.5.) self organize through multiple hydrogen bonds. These compounds exhibit broad S phases.[12]

5

6
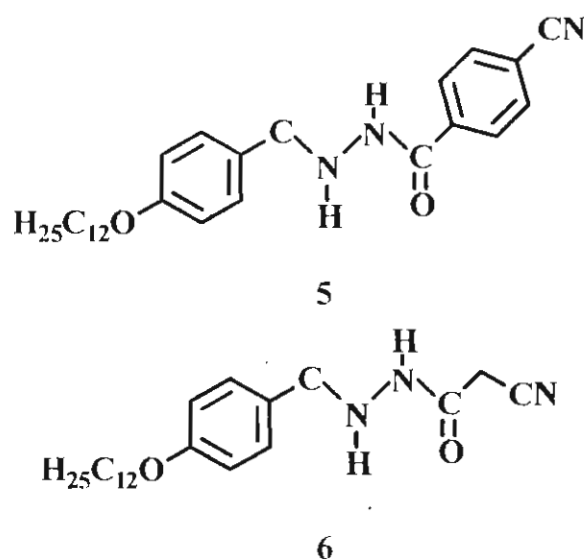
Chart 1.5.

The chiral carbonylbis(amino acid esters) which bear a urea moiety were also found to exhibit S mesophases. Formation of hydrogen bonds between the urea moieties results in parallel stacked layers, explaining the appearance of smectic mesophases in such materials.

Recently, it was reported that S_G phases could be generated *via* intermolecular hydrogen bonding between *p-n*-alkylbenzoic acids and *p*-hydroxybutyl benzoate.[32]

1.3.2. Hydrogen Bonded Liquid Crystalline Polymers

Hydrogen bonding has also been used for the synthesis of polymeric systems. In the case of LC polymers, new types of supramolecular materials have been built through specific intermolecular interactions. Supramolecular side chain mesogenic polymers, main chain polymeric and low molecular weight complexes have been prepared through intermolecular hydrogen bonds. Whereas conventional LC polymers consist of only covalent bonds, the supramolecular polymeric LC complexes may contain hydrogen bonded mesogenic cores or hydrogen bonded moieties that connect mesogenic molecules to the polymers.

LC phases in polymers can be stabilized or induced by hydrogen bonding interaction between carboxyl and pyridyl moieties.[24] LC polymers bearing a carboxyl group in the side chain were mixed with 4-*trans*-stilbazole derivatives bearing a pyridyl group and the mesomorphic properties of the resultant polymers were investigated. Polymer **7** (Chart 1.6.) was formed by the interaction of a poly(acrylic acid) derivative with a *trans*-stilbazole ester,[24] both of which exhibit mesomorphic behaviour. This polymer has a mesomorphic range between 140 °C

and 155 °C, whereas, the *trans*-stilbazole is liquid crystalline between 168 °C and
216 °C.

7
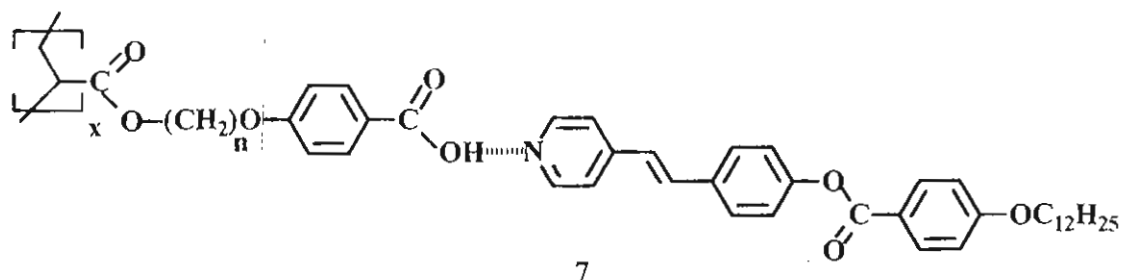
Chart 1.6.

Similar polymers were complexed with various *trans*-4-alkoxy-4'-
stilbazoles possessing a linear alkyl chain spacer to afford thermally stable
smectic A LCs.[33] The isotropization and melting temperatures of these
supramolecular polymeric assemblies depend on the number of carbon atoms in
the terminal alkoxy group. Hydrogen bonded polymers **8**, (Chart 1.7.) of
poly(acrylic acid) containing both the bifunctional hydrogen bond acceptor
4,4'-bipyridine and the monofunctional acceptor *trans*-4-hexyloxy-4'-stilbazole
also exhibit LC behaviour. An increase in proportion of the bifunctional acceptor
is accompanied by an increase in glass transition temperature and decrease in the
melting point of the polymer.[28]

8
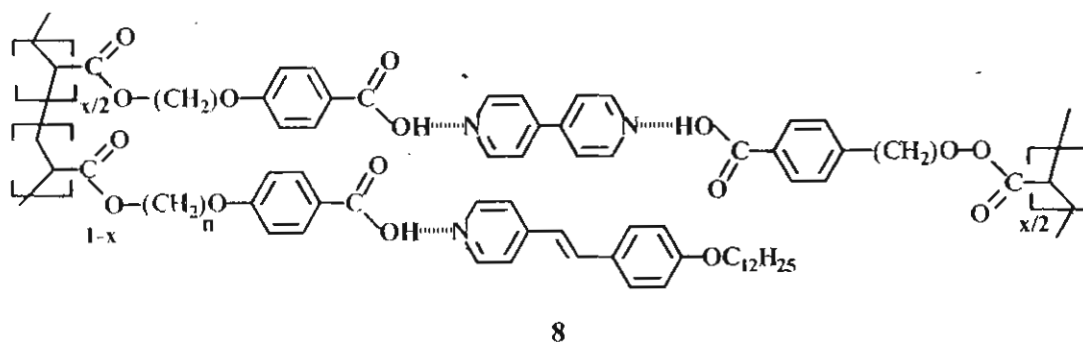
Chart 1.7.

Polysiloxanes, specifically poly(methylsiloxanes) and poly-(methyl-*co*-dimethylsiloxanes) containing a benzoic acid moiety in their side chain, themselves exhibit LC properties. These polymers hydrogen bond with mesogenic *trans*-4-ethoxy-4'-stilbazole and the non-mesogenic *trans*-4-ethoxy-4'-stilbazole, to give LC polymers.[34] Stilbazoles are used frequently as hydrogen bond acceptors because of the high enthalpy value for the formation of complexes between carboxyl and pyridyl groups.[35] Thus, polysiloxane donors bearing a pendant propyloxybenzoic acid group mixed with stilbazole-*N*-oxide yields polymers,[36] that exhibit S_A or S_C phases above their glass transition temperature, whereas neither of the components of the complexes exhibit LC behaviour.

The interactions of 4-polyvinylpyridine with mesogenic biphenyl derivatives bearing a carboxyl group have recently been investigated.[37] The monotropic LC phase observed for the mesogenic compound alone disappears and

the mesophases of the resulting complexes are dependent on the ratio of the interacting components. The resultant polymers exhibit good thermal stabililty.

1.3.3. Hydrogen Bonded Chiral Liquid Crystals

LCs containing chiral centers have attracted considerable attention due to the unique nature of such molecules which can give rise to cholesteric or chiral LCs either in the pure form or when doped in nematic LC.[38] The characteristic helical structure (Figure 1.2.b) of the cholesteric LCs impart unique optical properties such as selective reflection of light, thermochromism and circular dichroism. Cholesteric LCs have also been used to generate coloured glassy materials.[38-40]

The first hydrogen bonded chiral liquid crystal was prepared using a polysiloxane carboxylic acid as hydrogen bond donor and an optically active (S)(–)*trans*-4-(2-methoxypropyloxy)-4'-stilbazole.[41] These complexes form chiral smectic (S_C*) phases over an extended temperature range as a result of the formation of linear structures such as **9** (Chart 1.8.) which possesses a large length to breadth ratio.

9
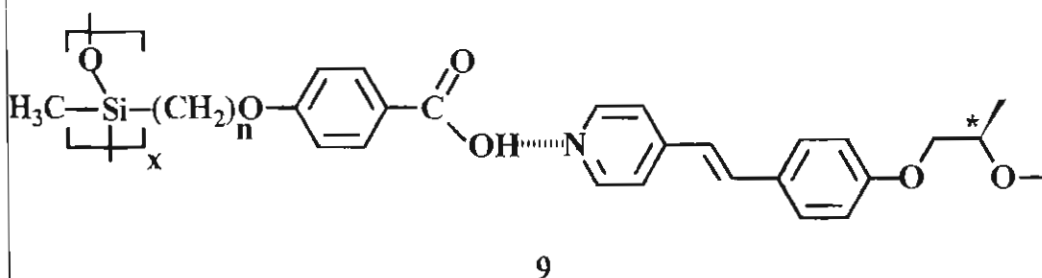
Chart 1.8.

As in LCs of low molecular mass, the presence of a strong terminal lateral dipole and a polarizable core in **9** (Chart 1.8.) should aid in the formation of tilted smectic phases. In another study, a non-mesogenic chiral proton donor, i.e., the mono-(2-methylbutyl)ester of terephthalic acid was prepared and mixed with 4-alkoxy-4'-stilbazoles in a 1:1 ratio. Depending upon the alkoxy chain length for these complexes, blue phases, chiral nematic (N*) and chiral smectic (S$_C$*) phases were observed.[42] Chiral LC phases were also generated *via* the complexation between 4-*n*-alkyloxybenzoic acids and chiral stilabazoles. These supramolecular assemblies exhibited N* and S$_C$* phases. The hydrogen bonded complex between 4,4'-bipyridine and 4-[(S)(–)2-methylbutyloxy]benzoic acid exhibits chiral LC phases with a wide range of temperatures.[43] Hydrogen bonding between 3-cholesteryloxycarbonyl propanoic acid and 4-(4-alkoxybenzoyloxy)-4'-stilbazoles or *N*-(4-pyridylmethylidiene)anilines also result in the formation of chiral LCs.[44] These complexes show S$_A$ and cholesteric LC phases. Supramolecular chiral networks using optically active stilbazole dimer (**10**, Chart 1.9.) and trifunctional hydrogen bond donor units have also been constructed.[45]

10
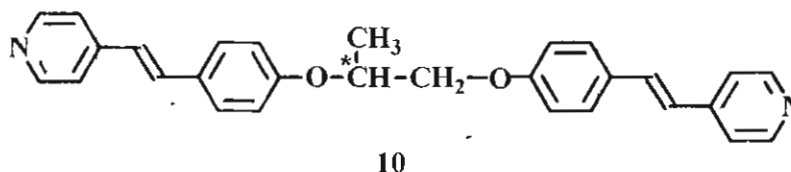
Chart 1.9.

These supramolecular networks exhibit cholesteric mesophases in the heating and cooling cycles.

Ferroelectric LCs (FLC) have attracted much attention since it has been reported that FLC devices are capable of switching on short time scales.[46-49] Ferroelectric LCs can be generated in liquid crystalline systems by attaching or doping a chiral molecule. The concept of inducing ferroelectric properties through hydrogen bonding was first realized by Frechet *et al.*.[41] Polysiloxanes with pendant 4-*n*-alkyloxybenzoic acid groups have been complexed with an optically active (S)(–)*trans*-4-(2-methoxypropyloxy)-4'-stilbazole. In yet another study hydrogen bonded FLCs were prepared using non mesogenic mono-(2-methylbutyl)ester of terephthalic acid and *n*-alkyloxystilbazoles.[42] The dielectric properties of hydrogen bonded LCs are also important because they provide much information on the physical properties of the polymers. Supramolecular complexes built between 4-*n*-octyloxybenzoic acid and chiral stilbazoles also forms stable FLCs.[50]

1.3.4. Hydrogen Bonded Discotic Liquid Crystals

Reports on hydrogen bonded discotic LCs are relatively few. Self assembly of non-disc like molecules to form columnar mesophases was first observed for

neat soaps.[2] Hydrogen bonding in 6(*5H*)-phenanthridones results in the formation of a discotic liquid crystalline phase (**11**, Chart 1.10.).[51,52]
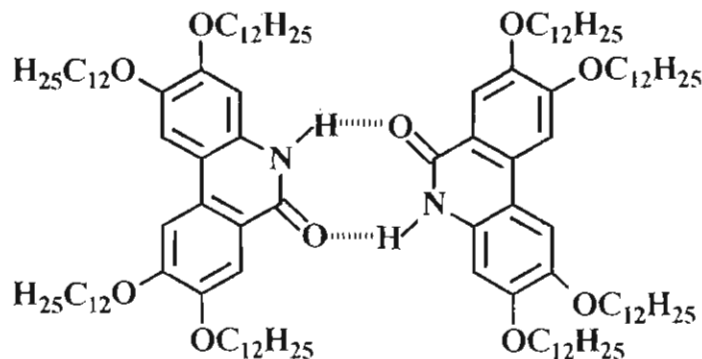
11

Chart 1.10.

A columnar mesophase is also formed in the hydrogen bonded supramolecular assembly between (3,4,5-tri-*n*-dodecyloxy)benzoyloxy-pyridine and hexafluoroglutaric acid.[53] The strong intermolecular hydrogen bonding present in *N*-acelated 2,2'-bipyridine-3,3'-diamines generates discotic liquid crystallinity. The columnar LC behaviour of sheet shaped 2,4,6-triarylamino-1,3,5-triazine bearing six peripheral decyloxy chains, which hydrogen bonds to two-fold alkoxy substituted non-mesomorphic benzoic acids is also reported.[54] Recent studies suggest that tris-imidazole base (**12**, Chart 1.11.) with substituted alkyloxybenzoic acids forms columnar LCs.[55,56]
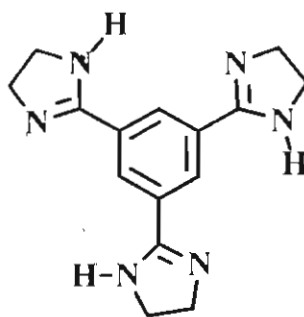
12

Chart 1.11.

1.3.5. Hydrogen Bonded Liquid Crystalline Compounds Derived from Amphiphilic Moieties

Hydrogen bonding has also been employed for the formation of LCs derived from amphiphilic mesogens consisting of two distinct segregated units, one hydrophobic and the other hydrophilic. In hydrogen bonded amphiphiles segregation occurs between the polar groups which become the driving force for the formation of LC phases.

The structural versatility of carbohydrate moieties provides the basis for the synthesis of a great variety of amphiphilic carbohydrates. The first reported example of an amphiphilic LC carbohydrate is a β-hexadecyl-D-glucoside prepared more than eighty years ago.[13.] Carbohydrate LCs are formed by the functionalisation of carbohydrate moieties with one or more long aliphatic chains. Generally carbohydrate amphiphiles with one lipophilic chain form smectic

phases. while carbohydrates with more than one lipophilic chains form columnar

mesophases.[15-17]
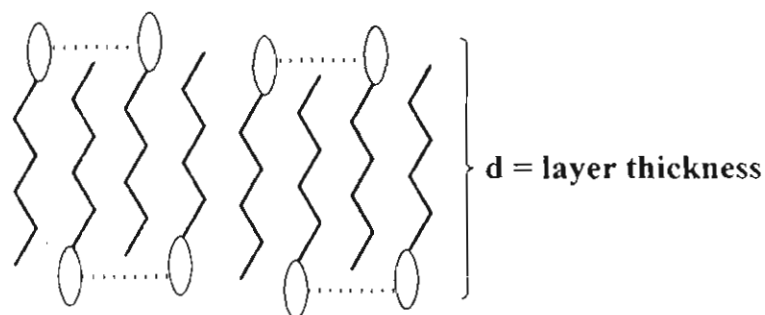
Figure 1.5. (Adapted from reference 57)

The *n*-alkyl-β-D-glucopyranosides exhibit S_A LC phases because of the

bilayer structure, which is stabilized by hydrogen bonding (**1**, Chart 1.1.).[16] These

smectic phases are found to be identical to the lyotropic lamellar phase and the d

spacing in these phases is equal to twice the length of the aliphatic chain plus the

length of the carbohydrate moiety.[58] Homologous series of D-glucose and 2-

deoxy-D-glucose derivatives with an amino-linked alkyl chain show S_{Ad} phases

(the layer spacing is found to be less than twice the length of the alkyl chain and

the carbohydrate moiety, Figure 1.5.). This can be explained by a model in which

carbohydrate moieties constitute the core, held together in a dynamic hydrogen

bonded net work and the aliphatic chains are in the interior of the supramolecular

structure (Figure 1.5.).

Compounds like dithioacetals, which have two aliphatic chains, exhibit a hexagonal columnar LC phase.[59] The supramolecular structure for these molecules is depicted in Figure 1.6.[60] In a similar fashion, 6,6-dialkyl-D-galactopyranoses which possess two alkyl chains also form columnar supramolecular structures due to the formation multimers held together by hydrogen bonding.
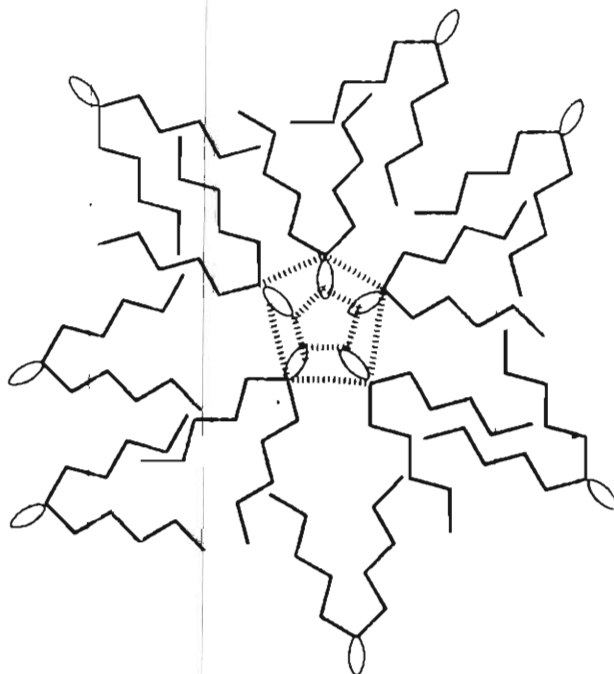
Figure 1.6. Schematic representation of the molecular arrangement for the formation of hexagonal columnar mesophase in diacetals having two aliphatic chains (adapted from reference 60).

The crucial factors for the formation of LCs from amphiphiles containing multiple hydroxyl groups are the tendency of the hydroxyl groups to form a dynamic network of cooperative hydrogen bonds and also their location at the ends of lipophilic chains. Diols and polyols with one polar head exhibit

thermotropic LC behaviour.[61] Examples of such polyols are shown in Chart 1.12. These polyols are structurally related to carbohydrate LCs and can be regarded as the simplest members of this large class of materials.

13

14
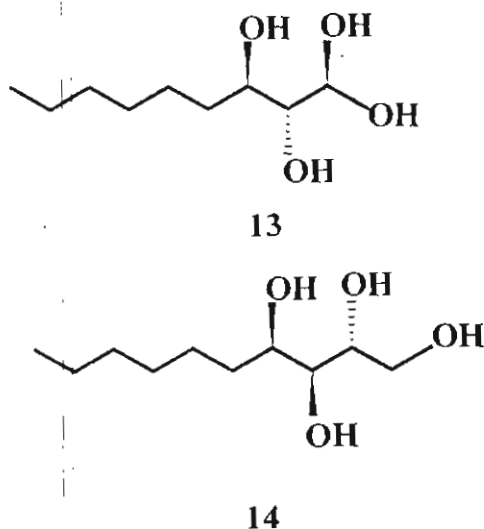
Chart 1.12.

Introduction of a rod like moiety in these compounds stabilizes the LC phases. For example, 1,3-cyclohexanediols and 1,2-cyclohexanediols which are linked through an ester group to a benzene ring with two and three alkyl chains give rise to columnar discotic phases. The mesogen is not a disc like unit, but six molecules assembled through hydrogen bonding give rise to a hexagonal structure.[62]

Amphiphiles bearing complementary functional groups can also show LC properties. The first reported examples of this type are the LCs formed *via*

hydrogen bonding between 2,6-diaminopyridines and uracil derivatives with long aliphatic chains (15, Chart 1.13).[63] In these systems three hydrogen bonds formed between the interacting heterocyclic bases stabilize the observed mesophase. LC phases are also obtained by the interaction of a component containing two recognition sites and a second component containing one recognition site, in a 1:2 molar ratio.
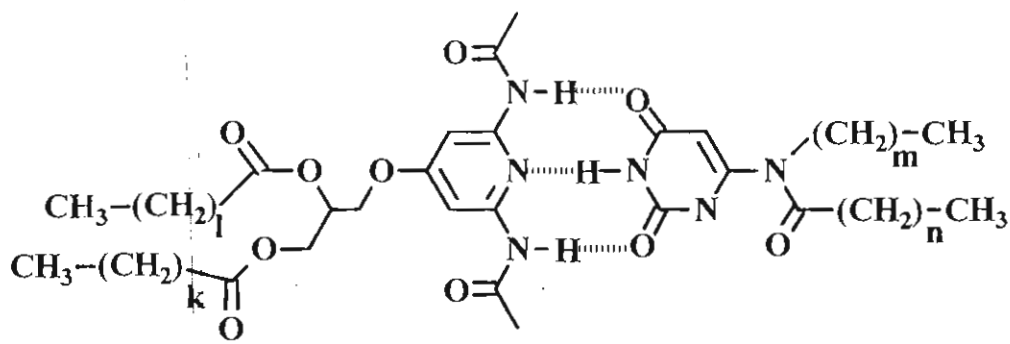
15

Chart 1.13.

1.3.6. Characterization of the Hydrogen Bonded Assemblies

After the report of Kato *et al.* in 1989,[23,24] which describes the formation of LC materials between a pyridyl moiety and a carboxylic acid, hydrogen bonded LCs have been extensively studied.[10-12,15-18,20-31,33-35,37,41,42,44,45,50-54,56-58,62-117] These complexes are prepared by melting equimolar concentrations of a hydrogen bond donor and a hydrogen bond acceptor above the melting point of the mixture,

followed by slow cooling to room temperature. In the case of high melting compounds, hydrogen bond donors and acceptors are dissolved in suitable hydrogen bonding solvents like pyridine, tetrahydrofuran, ethanol and slow evaporation of the solvent under reduced pressure generates the supramolecular assemblies. These complexes were characterized by FTIR measurements and by studying the phase diagram of binary mixtures of the hydrogen bond donor and acceptor.

Hydrogen bonding between a proton donor and pyridine can be classified into three types (Scheme 1.1.), which depend upon the intermolecular distance between different potential curves.[35]
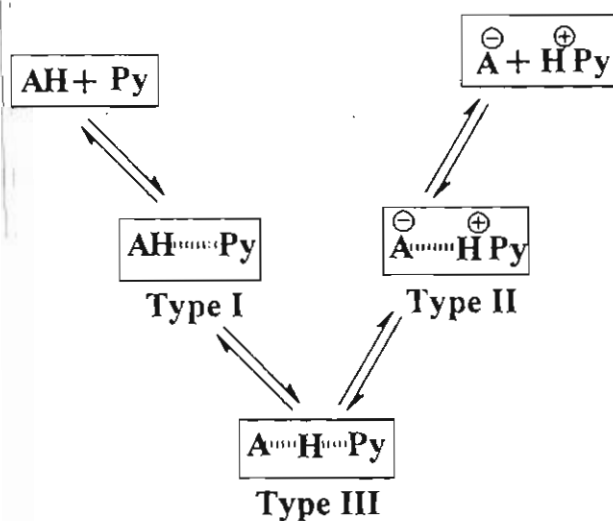
Scheme 1.1.

For weak or moderately strong hydrogen bonds the hydrogen atom is located closer to one as shown in Type I (Scheme 1.1.). The potential energy is correspondingly unsymmetrical with a double minimum potential. As the strength

of the hydrogen bond increases and the A---B length decreases the hydrogen atom is not so clearly identified as more strongly associated with one atom or the other (Type III, Scheme 1.1.). Thus, for strongly hydrogen bonded materials the potential energy diagram will possess two equal potential minima with a low potential barrier between the two. Alternatively, a single symmetric potential energy curve with a truly broad minimum may be observed. It has been reported that in the case of phenols, and benzoic acids complexed with pyridine, Type I complexes are formed, and in the case of hydrochloric acid in pyridine, Type II complexes are observed (Scheme 1.1.). For weak hydrogen bonds, usually a broad structureless band centered around 3300 cm^{-1} is observed. As we progress to hydrogen bonds of intermediate strength, as in carboxylic acid dimers or phenol-pyridine complexes, the stretching mode shifts to 3100-2800 cm^{-1}.[78] For strong hydrogen bonded systems, for example in the case of acid base complexes, intense broad bands around 2800, 2500 and 1800 cm^{-1} are observed and the proton becomes increasingly delocalized.

The nature of the supramolecular assembly obtained in hydrogen bonded LCs can be analysed using FTIR. For example, formation of a hydrogen bonded complex between 4-*n*-butyloxybenzoic acid and *trans*-4-[4-ethoxybenzoyloxy]-4'-stilbazole has been supported by FTIR measurements. In a simple 1:1 mixture of the acid and stilbazole, a band at 1681 cm^{-1} due to the carbonyl group of the

carboxylic acid dimer (C=O---HO-) is observed.[23] In contrast, a 1:1 mixture of these compounds prepared by slow evaporation of a pyridine solution shows a new band at 1704 cm^{-1}, replacing the band at 1681 cm^{-1} and indicating the existence of the carbonyl group of the carboxylic acid complexed with the pyridyl moiety of the stilbazole derivative. Also, the O-H bands observed at 2500 and 1920 cm^{-1} are indicative of strong hydrogen bonding.

The heterointermolecular hydrogen bonding observed in the complexes between a hydrogen bond donor and acceptor can also be confirmed by investigating the thermal properties of their binary mixtures. When a non-nematic solute is mixed with a nematic LC, nematic-isotropic phase transition temperature (T_{N-I}) usually decreases. In some cases however, addition of carboxylic acid and phenol derivatives of biphenyl to 4-pentyl-4'-cyanobiphenyl result in the increase in T_{N-I}. This behaviour has been ascribed to intermolecular hydrogen bonding between the solutes and the cyanobiphenyl. Recent studies on binary mixtures have shown the importance of pyridine moiety and carboxylic acid interaction for the stabilization of the LC range in a binary system of the non liquid crystalline 4,4'-bipyridine and 4-*n*-butylbenzoic acid or on *cis-s-cis* enaminoketones, respectively.[103] For the binary mixtures of 4-*n*-decylbenzoic acid and *trans*-4,4'-bipyridylethylene, in which hydrogen bond donor

as well as acceptor are non mesogenic, a N phase is observed for the mixture containing between 10 and 50% of the bipyridylethylene (Figure 1.7.).[27]
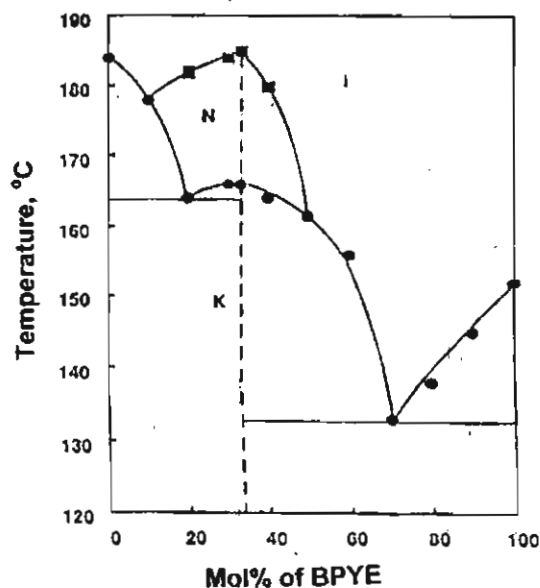
Figure 1.7. Binary phase diagram of *trans*-4,4'-bipyridylethylene and 4-*n*-decylbenzoic acid (adapted from reference 27).

This can be ascribed to hydrogen bonding interaction between the two components. The maximum isotropization temperature observed for the binary mixture of 33 mol% of bipyridylethylene and 4-*n*-decylbenzoic acid can be interpreted as being due to the formation of a unique material by complexation of the acid with *trans*-4,4'-bipyridylethylene in a 1:2 stoichiometry (Figure 1.7.).

Also, the binary phase analysis of 4-*n*-pentyloxybenzoic acid and *N*-(*p*-methoxy-o-hydroxybenzylidene)-*p*-aminopyridine (MHBAP) shows clearly the existence of S_C and N phases in the mixtures (Figure 1.8.).[107]
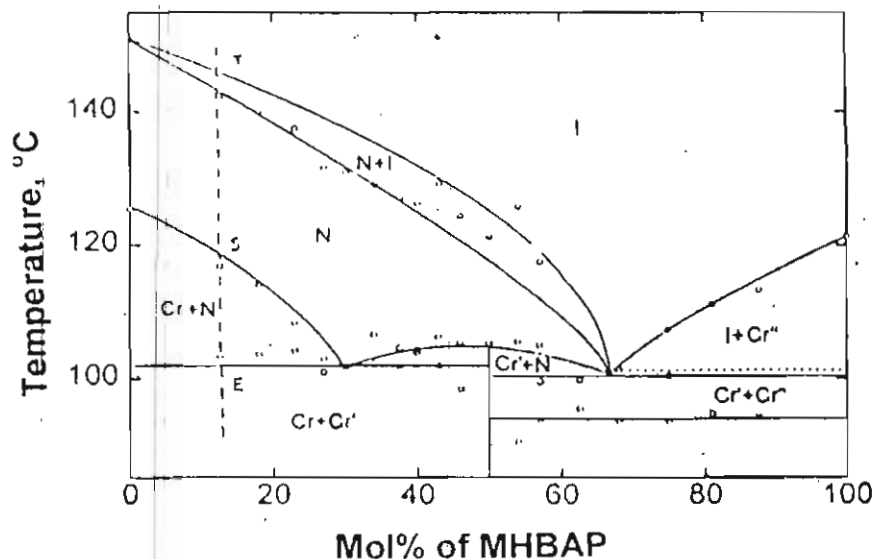
Figure 1.8. Binary phase diagram of 4-*n*-pentyloxybenzoic acid and a MHBAP (adapted from reference 107).

The presence of a melting maximum for the crystalline mixtures containing 50 mol% of MHBAP proves without doubt that a well defined 1:1 stoichiometric compound is formed (Figure 1.8.). However in these mixtures an azeotropic maximum was not seen, which indicates that the interaction between the dimerized alkoxybenzoic acid and the hydrogen bonded 1:1 stoichiometric compound are not particularly stronger in the mesomorphic state than they are in the isotropic state. The IR spectra of these mixtures were not weighed superposition of the spectra of the pure components, but instead presented distinct features and changes depending on the compositions. With increase in the MHBAP concentration, two additional broad bands (at ~1935 and 2450 cm^{-1}) appear in the spectra, indicating strong hydrogen bonding of the pyridine rings with the carboxyl groups of the acids.[107] Their intensity passes through a

maximum for concentrations of 50 mol% of MHBAP, pointing to the formation of a 1:1 complex between the MHBAP and the benzoic acid. At the same time, the two bands at 2665 and ~2560 cm^{-1}, along with the very broad and strong OH band at ~3000 cm^{-1}, all three of which characterize the acid dimers, decrease in intensity and vanish completely beyond 50 mol% of MHBAP. For the 50 mol% mixture, the C-O stretching band of the pure acid dimer at 1678 cm^{-1} is replaced by a doublet (at 1685 and 1695 cm^{-1}). suggesting the formation of hydrogen bonds with a double minimum energy potential.

1.4. Optical and Electrooptical Properties of Liquid Crystals

LCs show large optical anisotropy, which can be switched by changing the alignment of the LC molecules with an electric field.[1] In view of this LCs have been widely used as an active media in display devices.[2,118,119] The twisted nematic, which is most commonly used is essentially based on the electrooptic properties of the LCs (Figure 1.9.). In this device the 90° twist in the arrangement of the LC molecules across the cell results in a twist of plane polarized light by 90°. Such cells therefore appear bright when placed between crossed polarizers. On application of an electric field above a threshold voltage (V_t), the LC molecules align perpendicular to the cell surface, and the inability of the cell to twist the plane of polarization of light, under these conditions makes them appear dark between crossed polarizers. Although this type of switching is used in

numerous commercial devices, their switching times are very slow, being greater than several milliseconds. This is due to the slower response of LCs to electric fields.[120]
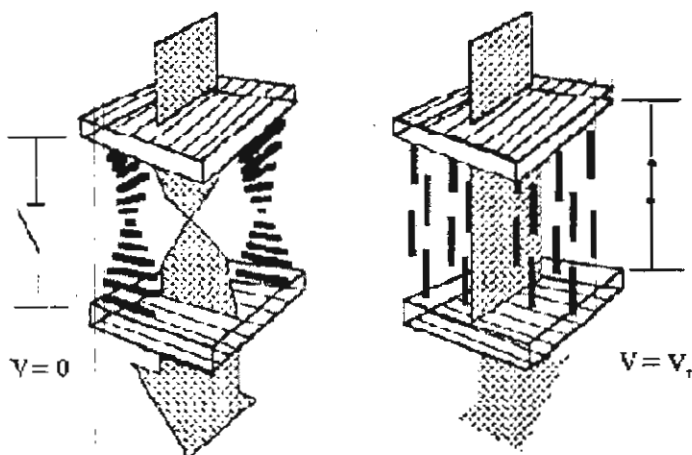
Figure 1.9. Schematic view of a twisted N display (adapted from reference 2).

If the response times for the switching of LCs can be enhanced, apart from display devices LCs can also be used for various photonic applications such as optical computing and real time holography. Photochemical transformations in LCs can bring about both alignment changes as well as phase transitions. Using light as stimulus the switching response times of LCs can be enhanced by several orders of magnitude.[48,120]

1.5. Photochemical Studies in Liquid Crystalline Media

In most of the studies on photochemistry in organized media, the role of the medium has been to try and control or modify in some way the

photochemical or photophysical property of guest molecules. The use of LC media to control photochemical and/or photophysical properties of guest molecules have also been extensively explored. Most of such studies have however met with only limited success.

A far more interesting aspect of the study of photochemical processes of guest molecules in LC media is that the photochemical transformations can modify the alignment or phase transition properties of the LC host. The cooperative behaviour of LC molecules and their long-range order can help to amplify relatively weak photochemical processes occurring at the molecular level, to macroscopic phenomena. Such processes have immense potential for application in optical switching of LCs.

Photolysis can bring about both alignment changes as well as phase transitions in LCs. In addition light has properties such as intensity, polarization and wavelength which can be selectively used for such improved information processing. In view of this, development of photoactive LCs is being intensively pursued the world over.

Shibaev *et al.* have demonstrated the use of laser induced phase transition in LCs in display systems.[121] In these types of devices the write in process includes photolysis of aligned LC cells with a laser beam. Increase in temperature along the laser beam trace results in phase transition from the LC

state to the isotropic state. Removal of the laser beam leads to rapid cooling of the isotropic state to an unaligned LC state, producing light scattering centers such as focal conic textures. These light scattering centers remain in the LC cells as static figures. The stability of the stored information is not high in such devices and the contrast will be lost after some period of time. In such devices the heat content of photon is used for bringing about phase transitions.

In contrast, photon induced chemical transformation of LC molecules or guest molecules dissolved in LCs can also bring about changes in the alignment or phase transition properties of LCs. These effects have been termed as photon-mode switching as opposed to heat-mode switching caused by photolysis.

Studies on the photon-mode response of LCs started in the late 1960's when Haas *et al.* reported a change in selective reflectivity of a cholesteric LC mixture composed of cholesteryl bromide and other cholesteryl derivatives on photolysis. This change in the reflectivity arose from a change in the helical pitch of the cholesteric LC resulting from a photochemical reaction of cholesteryl bromide in the LC mixture.[39] They also reported that the *photolysis of a mixture of cholesteric compounds doped with stilbene chromophores causes a N to isotropic phase transition due to the trans-cis isomerization of stilbene.*

In the photon-mode-switching processes polymeric LC (PLC) materials have also been widely used as supporting materials. Some of the advantages of polymeric materials are that below its glass transition temperature, the segmental motion of the polymer chains is frozen-in, and thus the stored information can be kept stable over longer periods. Photon-mode image storage was first demonstrated in polymeric LCs by Wendorff *et al.*.[122,123] In their system, photolysis caused isomerization of photochromic groups incorporated into the PLCs resulting in grating formation in the material. The grating arises due to a change in the refractive index resulting from photoisomerization. The advantage of the photon-mode recording over the heat-mode recording lies in its superior resolution and possibility of multiplex recording.[122,123] First reports on the photon-mode process in PLCs were based on the photochemical phase transition behaviour of PLCs with side chain phenyl benzoate mesogens.[124,125]

Photon-mode process can be subdivided into (a) photoinduced phase transition and (b) photoinduced changes in the alignment of LCs.

1.5.1. Photoinduced Phase Transitions

Phase transition can be triggered by photochemical reactions of guest molecules doped in LC matrices. There have been several reports on such

photoinduced phase transitions of LCs containing guest molecules such as azobenzene and spiropyran derivatives. In LC containing azobenzene derivatives, the rod like shape of the *trans* form of the azobenzenes tend to stabilize the LC phase while the *cis* form tend to destabilize it. Thus, *trans-cis* photoisomerization of the azobenzene derivatives can lead to lowering of the LC to isotropic (I) phase transition temperature of the mixture.[124-128] Time-resolved studies using lasers have shown that light induced phase transition in such systems usually occur in the time scale of 200-500 ms, although the photochemical transformation of the guest molecule is usually complete within the laser pulse duration (< 10 ns). These studies indicate that the response of the LC host material to photochemical transformation of the guest is very slow.[129]

Recently, it has been shown that LC materials that are inherently photoactive can respond much faster resulting in faster switching times.[120,130-132] Thus, optical switching in low molecular weight photoactive LCs (Chart 1.14.) have been reported to occur with response times of 100 μs.

16

17
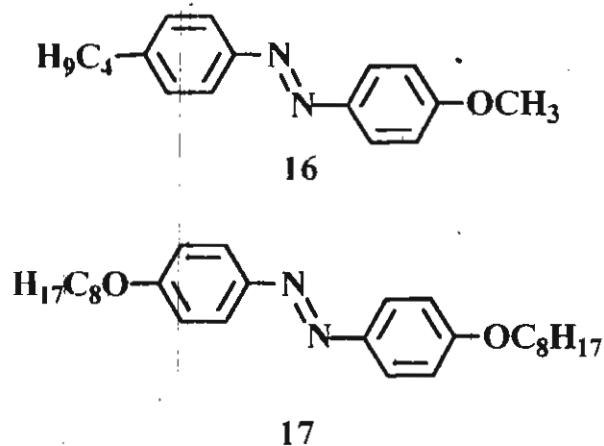
Chart 1.14.

Ikeda and coworkers have reported the behaviour of photoisomerization

of a PLC (Chart 1.15).[120,132]

18
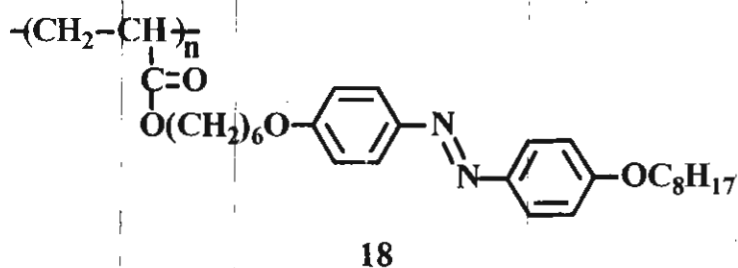
Chart 1.15.

This compound shows a N phase from 55 °C to 155 °C. On photolysis,

trans-cis isomerization of the azo moiety results in a N to isotropic phase

transition. Following this, thermal *cis-trans* isomerization can occur resulting

in randomly oriented molecules of the *trans* form. Due to random orientation,

the material at this stage will possess optical properties similar to that of the
isotropic phase. This process is followed by realignment of the azo
chromophores leading to the recovery of the original N phase (Figure 1.10.).
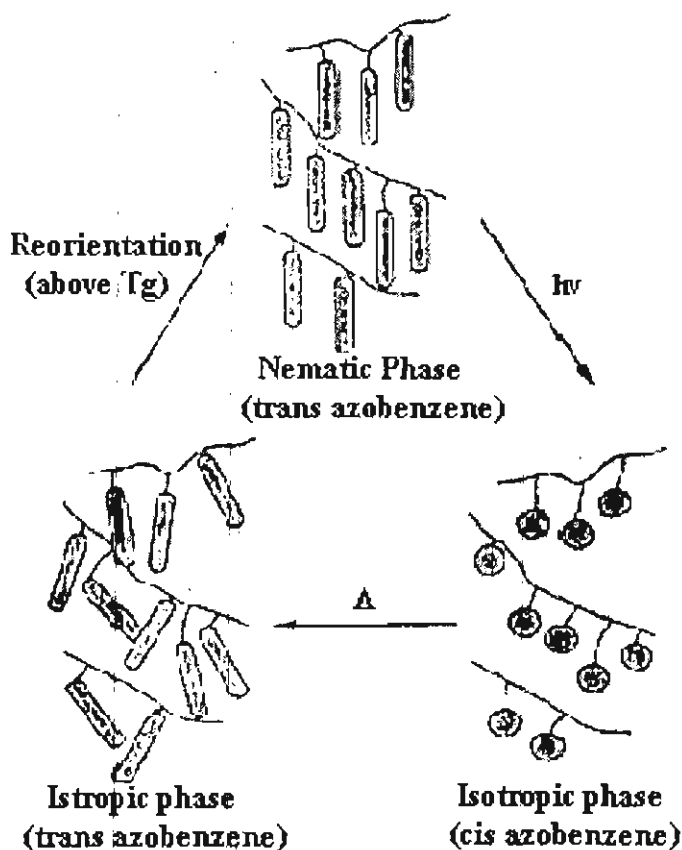
Figure 1.10. **Schematic illustration of the orientation of *trans* azobenzene mesogens (adapted from reference 132).**

Ikeda *et al.* have also shown that such polymeric materials can be used for
long term storage of information when operated below their glass transition
temperatures (T_g).[132] When the photoinduced N to isotropic phase transition is

performed below the T_g of the polymer, the unaligned isotropic phase is maintained even after the thermal *cis-trans* isomerization is complete. Using such materials, Ikeda *et al.* have stored the information for more than 1 year. Erasure of the information is then effected by heating the polymeric material above its T_g, whereby reorientation of the azo chromophores results in the recovery of the N phase (Figure 1.10.). Another major advantage of polymeric LCs over low molecular weight LCs is that they show a much wider temperature range under which optical transformation can be induced.

In another study, Lansac *et al.* have reported the photocontrolled nanophase segregation in cyanobiphenyl LCs containing azo derivatives (Chart 1.16.).[133] In this the photoactive molecules are driven from within the S layers to locations between the layers by *trans-cis* photoisomerizations, which increase reversibly the S layer spacing of a mixture of cyanobiphenyl and azobenzene. This effect can be used for low-power, high-resolution optical data storage, and more generally for the manipulation of organic materials at the nanometric scale.

20

19

$\Delta \bigg\Vert \lambda_1$

21
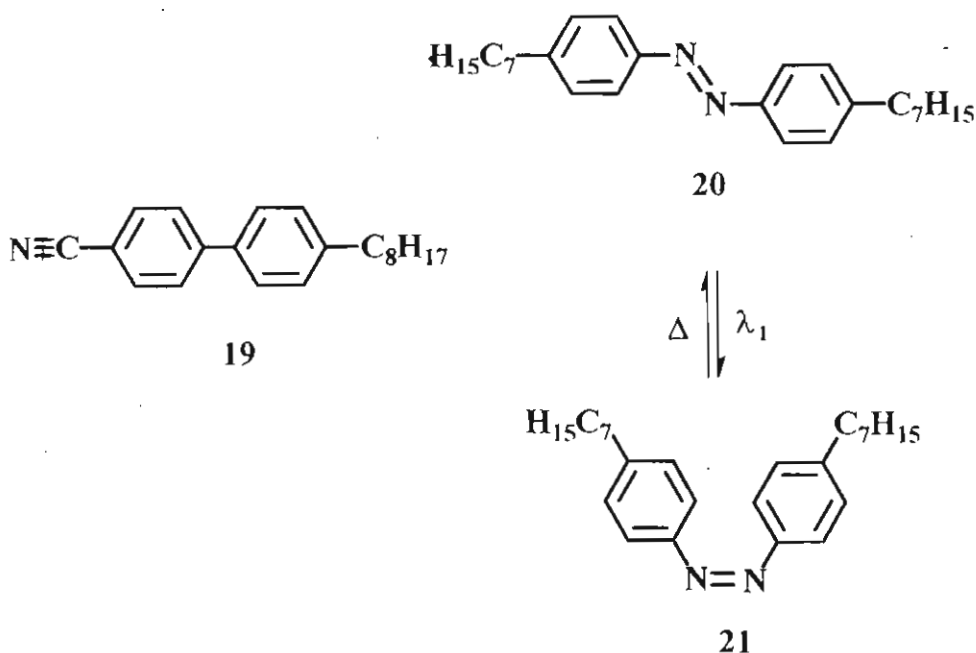
Chart 1.16.

Kato *et al.* have reported the sequential photolysis of the polymeric hydrogen complex between **22** and the azobenzenecarboxylic acid **23** (Chart 1.17.).[81] In this, the hydrogen bonded complex exhibits N phase from 47 °C to 93 °C. The photoresponsivity has been tested for this hydrogen bonded mesogen. The absorption maximum of **23** used as the photochromic guest in the present study is 350 nm in chloroform solution, at room temperature. Upon exposure of **23** to UV light (365 nm) in chloroform at room temperature, more than 90% of **23** is converted to the *cis* form. Irradiation with visible light (> 400 nm) causes the reverse *cis-trans* photoisomerization.
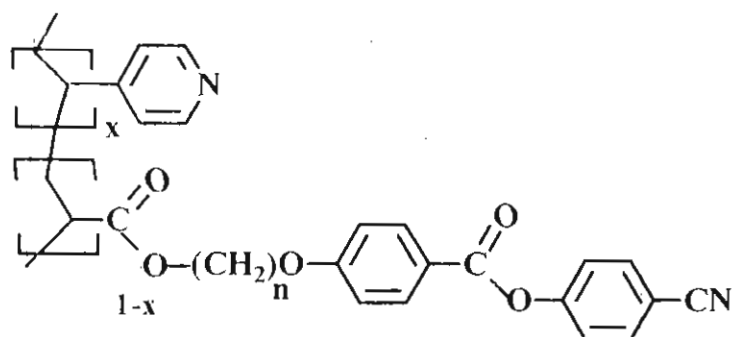
22
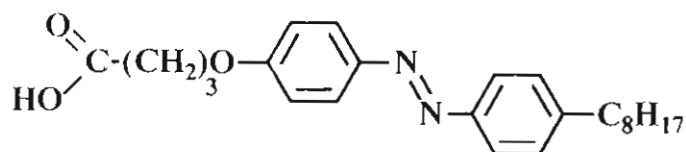
23

Chart 1.17.

1.5.2. Photoinduced Alignment Changes in Liquid Crystals

In photoalignment of LCs the orientational direction of the LC molecules is controlled or manipulated by photolysis of photochromic molecules doped into the LC matrix.[134] The photoreorientation of the photochromic guest molecules induces cooperative reorientation of non-photoactive LC molecules.[135,136] This cooperative effect in NLCs provides a convenient method for translating molecular phenomena into a macroscopic

phenomenon. The mechanism of polarized light induced reorientation of LC

molecules doped with photochromic molecules is depicted in Figure 1.11.[134]
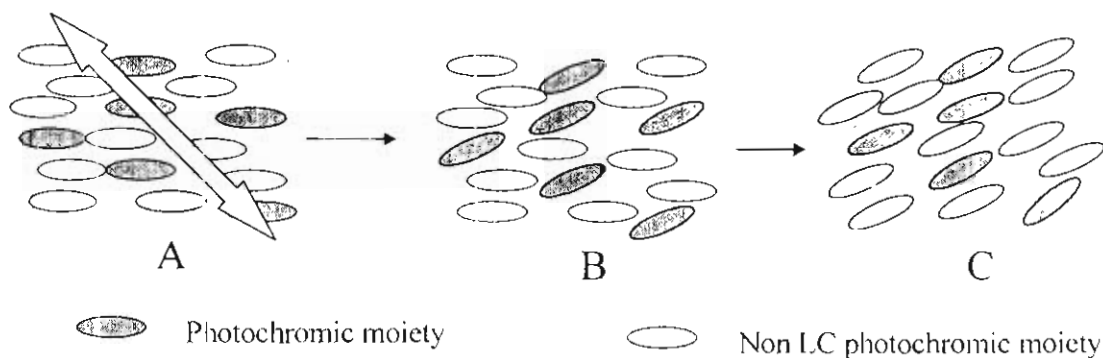
Figure 1.11. Molecular reorientation of photochromic LCs irradiatated with linearly polarized light. (A) before photolysis; (B) photo-reorientation of photochromic guests; (C) cooperative photo-reorientation of LC molecules (adapted from reference 134).

When irradiated by linearly polarized light, photochromic molecules, possessing shape anisotropy, undergo photoisomerization cycles, such as *trans-cis-trans* photoisomerization of azo derivatives, and change their orientation, with the molecule tending to line up in a direction perpendicular to the direction of polarization of the excitation beam.

Apart from doping LCs with photochromic molecules, the alignment of LCs can also be altered by using modified cell surfaces in which the photochromic material is either covalently linked to the surface or deposited on it using

polymeric binders.[134,137-142] Such surfaces are called command surfaces, which can bring about photoinduced changes in the alignment of bulk LCs as shown in Figure 1.12.
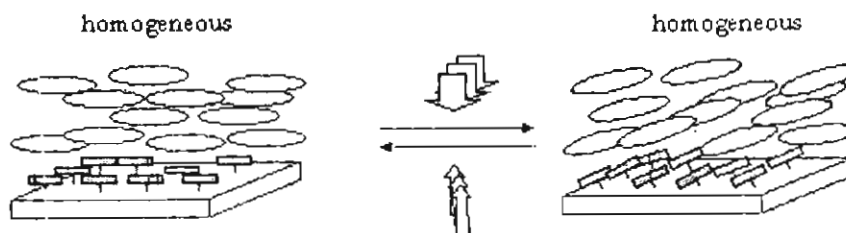
Figure 1.12. Illustrative representation of surface-assisted photo-alignment control of liquid crystal molecules tethered to a substrate surface (adapted from reference 134).

1.6. References

1. H. Kelker, R. Hatz, *Handbook of Liquid Crystals*, Verlag Chemie, Weinheim, **1980.**

2. B. Bahadur, *Liquid Crystals-Applications and Uses*, *(Vol. 1-3)*, World Scientific, Singapore, **1995.**

3. G. Friedel, *Ann. Physique.* **1922**, *18*, 273.

4. A. J. Leadbetter, *Thermotropic Liquid Crystals*, (Ed.: G. W. Gray), Wiley, Chichester, **1987.**

5. P. S. Pershan, *Structure of Liquid Crystal Phases*, World Scientific, Singapore, *1988.*

6. S. Chandrasekhar, B. K. Sadashiva, K. A. Suresh, *Pramana* **1977**, *9*, 471.

7. J. Billard, J. C. Dubois, Nguyen Huu Tinh, A. Zann, *Nouveau. J. Chim.* **1978**, *2*, 535.

8. D. Demus, L. Richter, *Texture of Liquid Crystals*, Weinheim, New York, **1978**.

9. F. Reinitzer, *Monatsh* **1888**, *9*, 421.

10. D. S. Lawrence, T. Jiang, M. Levett, *Chem. Rev.* **1995**, *95*, 2229.

11. J-M. Lehn, *Angew. Chem. Int. Ed. Engl.* **1990**, *29*, 1304.

12. C. M. Paleos, D. Tsiourvas, *Angew. Chem. Int. Ed. Engl.* **1995**, *34*, 1696.

13. E. Fisher, B. Helferich, *Justus Liebigs Ann. Chem.* **1911**, *383*, 68.

14. C. R. Noller, W. C. Rockwell, *J. Am. Chem. Soc.* **1938**, *60*, 2076.

15. G. A. Jeffrey, *Acc. Chem. Res.* **1986**, *19*, 168.

16. J. W. Goodby, *Mol. Cryst. Liq. Cryst.* **1984**, *110*, 205.

17. G. A. Jeffrey, *Mol Cryst. Liq. Cryst.* **1984**, *110*, 221.

18. G. W. Gray, B. Jones, *J. Chem. Soc.* **1954**, 1467.

19. G. W. Gray, B. Jones, *J. Chem. Soc.* **1953**, 4179.

20. V. V. Krasnogholovets, G. A. Puchkovskaya, A. A. Yakubov, *Mol. Cryst. Liq. Cryst.* **1995**, *265*, 143.

21. A. Mori, H. Takeshita, R. Nimura, M. Isobe, *Liq. Cryst.* **1993**, *14*, 821.

22. U. Beginn, G. Lattermann, *Mol. Cryst. Liq. Cryst.* **1994**, *241*, 215.

23.   T. Kato, J. M. J. Frechet, *J. Am. Chem. Soc.* **1989**, *111*, 8533.

24.   T. Kato, J. M. J. Frechet, *Macromolecules* **1989**, *22*, 3818.

25.   T. Kato, H. Adachi, A. Fujishima, J. M. J. Frechet, *Chem. Lett.* **1992**, 265.

26.   T. Kato, A. Fujishima, J. M. J. Frechet, *Chem. Lett.* **1990**, 919.

27.   T. Kato, J. M. J. Frechet, P. G. Wilson, T. Saito, T. Uryu, A. Fujishima, C. Jin, F. Kaneuchi, *Chem. Mater.* **1993**, *5*, 1094.

28.   T. Kato, H. Kihara, U. Kumar, A. Fujishima, T. Uryu, J. M. J. Frechet, *Polym. Prepr.* **1993**, *34*, 722.

29.   T. Kato, P. G. Wilson, A. Fujishima, J. M. J. Frechet, *Chem. Lett.* **1990**, 2003.

30.   L. J. Yu, J. S. Pan, *Liq. Cryst.* **1993**, *14*, 829.

31.   H. Kreese, I. Szulzewsky, S. Diele, R. Paschke, *Mol. Cryst. Liq. Cryst.* **1994**, *238*, 13.

32.   P. A. Kumar, M. Srinivasulu, V. G. K. M. Pisipati, *Liq. Cryst.* **1999**, *26*, 1339.

33.   T. Kato, H. Kihara, T. Uryu, A. Fujishima, J. M. J. Frechet, *Macromolecules* **1992**, *25*, 6836.

34.   U. Kumar, T. Kato, J. M. J. Frechet, *J. Am. Chem. Soc.* **1992**, *114*, 6630.

35.   S. E. Odinokov, A. A. Mashkovsky, V. P. Glazunov, A. V. Iogansen, B. V. Rassadin, *Spectrochemica Acta* **1976**, *32A*, 1355.

36. U. Kumar. J. M. J. Frechet. *Adv. Mater.* **1992**, *4*, 665.

37. F. A. Brandys, C. G. Bazulin, *Polym. Prepr.* **1993**, *34*, 186.

38. J. L. Fergason, *Mol. Cryst.* **1966**, *1*, 293.

39. W. E. Haas, J. Adams, J. Wysocki, *Mol. Cryst. Liq. Cryst.* **1969**, 7, 371.

40. N. Tamaoki, A. V. Parfenov, A. Masaki, H. Matsuda, *Adv. Mater.* **1997**, *9*, 1102.

41. U. Kumar, J. M. J. Frechet, T. Kato, S. Ujiie, K. Timura, *Angew. Chem. Int. Ed. Engl.* **1992**, *31*, 1531.

42. L. J. Yu, *Liq. Cryst.* **1993**, *14*, 1303.

43. M. Grunert, R. Alan Howie, A. Kaeding, C. T. Imrie, *J. Mater. Chem.* **1997**, 211.

44. Y. Tian, X. Xu, Y. Zhao, X. Tang, T. Li, *Liq. Cryst.* **1997**, *22*, 87.

45. H. Kihara, T. Kato, T. Uryu, J. M. J. Frechet, *Liq. Cryst.* **1998**, *24*, 413.

46. K. Skarp, M. A. Handschy, *Mol. Cryst. Liq. Cryst.* **1988**, *165*, 439.

47. N. A. Clark, S. T. Lagerwall, *Appl. Phys. Lett.* **1980**, *36*, 899.

48. T. Ikeda, T. Sasaki, K. Ichimura, *Nature* **1993**, *361*, 428.

49. T. Sasaki, T. Ikeda, K. Ichimura, *J. Am. Chem. Soc.* **1994**, *116*, 625.

50. H. Kihara, T. Kato, Y. Uryu, S. Ujiie, U. Kumar, J. M. J. Frechet, D. W. Bruce, D. J. Price, *Liq. Cryst.* **1996**, *21*, 25.

51.   R. Kleppinger, C. P. Lillya, C. Yang, *Angew. Chem. Int. Ed. Engl.* **1995**, *34*, 1637.

52.   R. Kleppinger, C. P. Lillya, C. Yang, *J. Am. Chem. Soc.* **1997**, *119*, 4097.

53.   H. Bernhardt, W Weissflog, H. Kresse, *Chem. Lett.* **1997**, 151.

54   A. R. A. Palmans, J. A. J. M. Vekemans, H. Fischer, *Chem. Eur. J.* **1997**, *3*, 300.

55   A. Kraft, A. Reichert, R. Kleppinger, *Chem. Commun.* **2000**, 1015.

56.   A. Kraft, A. Reichert, *Tetrahedron* **1999**, *55*, 3923.

57.   H. A. V. Doren, L. M. Wingert, *Mol. Cryst. Liq. Cryst.* **1991**, *198*, 381.

58.   D. B-Volant, R. Fornasier, E. Szalai, C. David, *Mol. Cryst. Liq. Cryst.* **1986**, *135*, 93.

59.   H. A. Van Doren, T. J. Burma, R. M. Kellogg, H. Wynberg, *J. Chem. Soc. Chem. Commun* **1988**, 460.

60.   G. A. Jeffrey, L. M. Wingert, *Liq. Cryst.* **1992**, *12*, 179.

61.   F. Hentrich, C. Tschierske, H. Zaschke, *Angew. Chem. Int. Ed. Engl.* **1991**, *30*, 440.

62.   G. Lattermann, G. Staufer, *Liq. Cryst.* **1989**, *4*, 347.

63.   M-J. Brienne, J. Galard, J-M. Lehn, I. Stibor, *J. Chem. Soc. Chem. Commun.* **1989**, 1868.

64. C. Alexander, C. P. Jariwala, C-M. Lee, A. C. Griffin, *Polym. Prepr.* **1993**, *34*, 168.

65. K. Antonova, M. Petrov, N. Kirov, T. Tenev, H. Ratajczak, J. Baran, *Mol. Cryst. Liq. Cryst.* **1995**, *261*, 63.

66. K. Araki, T. Kato, U. Kumar, J. M. J. Frechet, *Macromol. Rapid. Commun.* **1995**, *16*, 733.

67. K. Asaba, A. S. T. Kubota, H. F. Tanaka, A. Igarashi, S. Kobinasta, *Mol. Cryst. Liq. Cryst.* **1998**, *318*, 243.

68. E. B. Barmatov, D. A. Pebalk, M. V. Barmatova, V. P. Shibaev, *Liq. Cryst.* **1997**, *23*, 447.

69. C. G. Bazulin, A. Tork, *Macromolecules* **1995**, *28*, 8877.

70. H. Bernhardt, W. Weissflog, H. Kreese, *Angew. Chem. Int. Ed. Engl.* **1996**, *35*, 874.

71. P. Bladdon, A. C. Griffin, *Macromolecules* **1993**, *26*, 6604.

72. J. Clauss, M. J. Duer, L. F. Gladden, A. C. Griffin, C. P. Jariwala, C. Stourton, *J. Chem. Soc. Faraday Trans.* **1996**, *92*, 893.

73. J. Clauss, M. J. Duer, L. F. Gladden, A. C. Griffin, C. P. Jariwala, C. Stourton, *J. Chem. Soc. Faraday Trans.* **1996**, *92*, 811.

74. N. Feeder, W. Jones, *Mol. Cryst. Liq. Cryst.* **1992**, *211*, 111.

75. S. J. Geib, C. Vicent, E. Fan, A. D. Hamilton, *Angew. Chem. Int. Ed. Engl.* **1993**, *32*, 119.

76. D. Goldman, R. Dietel, D. Janietz, C. Schmidt, J. H. Wendorff, *Liq. Cryst.* **1998**, *24*, 413.

77. G. A. Jeffrey, *Mol. Cryst. Liq. Cryst.* **1990**, *185*, 209.

78. S. L. Johnson, K. A. Rumon, *J. Phys. Chem.* **1965**, *69*, 74.

79. T. Kato, T. Uryu, F. Kaneuchi, C. Jin, J. M. J. Frechet, *Liq. Cryst.* **1993**, *14*, 1311.

80. T. Kato, H. Kihara, U. Kumar, T. Uryu, J. M. J. Frechet, *Angew. Chem. Int. Ed. Engl.* **1994**, *33*, 1644.

81. T. Kato, N. Hirota, A. Fujishima, J. M. J. Frechet, *J. Polym. Sci. A. Polym. Chem.* **1996**, *34*, 57.

82. T. Kato, H. Kihara, S. Ujiie, T. Uryu, J. M. J. Frechet, *Macromolecules* **1996**, *29*, 8734.

83. T. Kato, G. Kondo, H. Kihara, *Chem. Lett.* **1997**, 1143.

84. T. Kato, T. Kawakami, *Chem. Lett.* **1997**, 211.

85. T. Kato, Y. Kubota, T. Uryu, S. Ujiie, *Angew. Chem. Int. Ed. Engl.* **1997**, *36*, 1617.

86. T. Kato, O. Ihata, S. Ujilile, M. Tokita, J. Watanabe, *Macromolecules* **1998**, *31*, 3551.

87. T. Kato, G. Kondo, D. Hanabusa, *Chem. Lett.* **1998**, 193.

88. H. Kihara, T. Kato, T. Uryu, J. M. J. Frechet, *Chem. Mater.* **1996**, *8*, 961.

89. Y. Kobayashi. Y. Matsunaga, *Bull. Chem. Soc. Jpn.* **1987**, *60*, 3515.

90. T. Koga, H. Ohba, A. Takase, S. Sakagami, *Chem. Lett.* **1994**, 2071.

91. K. Koh, K. Araki, S. Shinkai. *Tetrahedron Lett.* **1994**, *35*, 8255.

92. K. N. Koh, K. Araki, T. Komori, S. Shinkai, *Tetrahedron Lett.* **1995**, *36*, 5191.

93. H. Kreese, I. Szulzewski, P. Mandt, R. Frach, *Mol. Cryst. Liq. Cryst.* **1994**, *257*, 19.

94. J. Y. Lee, P. C. Painter, M. M. Coleman, *Macromolecules* **1988**, *21*, 954.

95. H-C. Lin, Y-S. Lin, Y-T. Chen, I. Chao, T-W. Li, *Macromolecules* **1998**, *31*, 7298.

96. H. Lochmuller, R. W. Souter, *J. Phys. Chem.* **1973**, *77*, 3016.

97. S. Malik, P. K. Dhal, R. A. Mashelkar, *Macromolecules* **1995**, *28*, 2159.

98. J. L. M. V. Nunen, B. F. B. Folmer, R. J. M. Nolte, *J. Am. Chem. Soc.* **1997**, *119*, 283.

99. M. Paleos, *Mol. Cryst. Liq. Cryst.* **1994**, *243*, 159.

100. C. B. St. Pourcain, A. C. Griffin, *Macromolecules* **1995**, *28*, 4116.

101. D. J. Price, T. Richardson, D. W. Bruce, *J. Chem. Soc. Chem. Commun.* **1995**, 1911.

102. D. J. Price, H. Adams, D. W. Bruce, *Mol. Cryst. Liq. Cryst.* **1996**, *289*, 127.

103. W. Pyzuk, E. Gorecka, A. Krowczynski, D. Pociecha, J. Szydlowska, J. Przedmojski, *Liq. Cryst.* **1996**, *21*, 885.

104. A. Sato, T. Kato, T. Uryu, *J. Polym. Sci. A. Polym. Chem.* **1996**, *34*, 503.

105. M. Schellhorn, G. Lattermann, *Macromol. Chem. Phys.* **1995**, *196*, 211.

106. Z. Sideratou, C. M. Paleos, *Mol. Cryst. Liq. Cryst.* **1995**, *265*, 19.

107. Z. Sideratou, D. Tsiourvas, C. M. Paleos, A. Skoulios, *Liq. Cryst.* **1997**, *22*, 51.

108. V. Tal'roze, S. A. Kuptsov, I. Sycheva, V. S. Bezborodov, A. Plate, *Macromolecules* **1995**, *28*, 8689.

109. Y. Tian, X. Xu, Y. Zhao, X. Tang, T. Li, J. Sun, C. Li, A. Pan, *Thin Solid Films* **1996**, *284-285*, 603.

110. A. Treybig, H. Bernhardt, S. Diele, W. Weissflog, H. Kreese, *Mol. Cryst. Liq. Cryst.* **1997**, *293*, 7.

111. C. Tschierske, G. Brezesinski, F. Kuschel, H. Zaschke, *Mol. Cryst. Liq. Cryst. Lett.* **1989**, *6*, 139.

112. C. Tschierske, A. Lunow, H. Zaschke, *Liq. Cryst.* **1990**, *8*, 885.

113. H-H. Tso, J-S. Wang, C-Y. Wu, H-C Lin, *New J. Chem.* **1998**, 771.

114. S. U. Vallerien, M. Werth, F. Kremer, H. W. Spiess, *Liq. Cryst.* **1990**, *8*, 889.

115. K. Willis, J. E. Luckhurst, D. J. Price, J. M. J. Frechet, H. Kihara, T. Kato, G. Ungar, D. W. Bruce, *Liq. Cryst.* **1997**, *21*, 585.

116. B. Xu, T. M. Swager, *J. Am. Chem. Soc.* **1995**, *117*, 5011.

117. F-S. Yen, J-L. Hong, *Macromolecules* **1997**, *30*, 7927.

118. W. E. Haas, *Mol. Cryst. Liq. Cryst.* **1983**, *94*, 1.   G/2018

119. B. Bahadur, *Mol. Cryst. Liq. Cryst.* **1984**, *109*, 3.

120. T. Ikeda, O. Tsutsumi, *Science* **1995**, *268*, 1873.

121. V. P. Shibaev, S. G. Kostromin, N. A. Plate, S. A. Ivanov, V. Yu Vetrov, I. A. Yakovlev, *Polym. Commun.* **1983**, *24*, 364.

122. M. Eich, J. H. Wendorff, *Makromol. Chem. Rapid Commun.* **1987**, *8*, 467.

123. M. Eich, J. H. Wendorff, B. Reck, H. Ringsdorf, *Makromol. Chem. Rapid Commun* **1987**, *8*, 59.

124. T. Ikeda, S. Horiuchi, D. B. Karanjit, S. Kurihara, S. Tazuke, *Macromolecules* **1990**, *23*, 36.

125. T. Ikeda, S. Horiuchi, D. B. Karanjit, S. Kurihara, S. Tazuke, *Macromolecules* **1990**, *23*, 42.

126. T. Ikeda, S. Kurihara, D. B. Karanjit, S. Tazuke, *Macromolecules* **1990**, *23*, 3938.

127. S. Kurihara, T. Ikeda, T. Sasaki, H-B. Kim, S. Tazuke, *Mol. Cryst. Liq. Cryst.* **1991**, *195*, 251.

128. S. Kurihara, T. Ikeda, T. Sasaki, H-B. Kim, S. Tazuke, *J. Chem. Soc. Chem. Commun.* **1990**, 1751.

129. T. Ikeda, T. Sasaki, H-B. Kim, *J. Phys. Chem.* **1991**, *95*, 509.

130. A. Shishido, O. Tsutsumi, A. Kanazawa, T. Shiono, T. Ikeda, N. Tamai, *J. Am. Chem. Soc.* **1997**, *119*, 7791.

131. A. Shishido, O. Tsutsumi, A. Kanazawa, T. Shiono, T. Ikeda, *J. Phys. Chem. B* **1997**, *101*, 2806.

132. O. Tsutsumi, T. Shiono, T. Ikeda, G. Galli, *J. Phys. Chem. B* **1997**, *101*, 1332.

133. Y. Lansac, M. A. Glaser, N. A. Clark, O. D. Lavrentovich, *Nature* **1999**, *398*, 54.

134. K. Ichimura, *Chem. Rev.* **2000**, *100*, 1847.

135. M. Gibbons, P. J. Shannon, S-T. Sun, B. J. Swetlin, *Nature* **1991**, *351*, 49.

136. P. J. Shannon, W. M. Gibbons, S-T. Sun, *Nature* **1994**, *368*, 532.

137. M. Schadt, H. Seiberle, A. Schuster, S. M. Kelly, *Jpn. J. Appl. Phys.* **1995**, *34*, 3240.

138. S-T. Sun, W. M. Gibbons, P. J. Shannon, *Liq. Cryst.* **1992**, *12*, 869.

139. M. Schadt, H. Seiberle, A. Schuster, *Nature* **1996**, *381*, 212.

140. N. Kawatsuki, K. Matsuyoshi, T. Yamamoto, *Macromolecules* **2000**, *33*, 1698.

141. N. Kawatsuki, C. Suehiro, T. Yamamoto, *Macromolecules* **1998**, *31*, 5984.

142. N. Kawatsuki, H. Ono, H. Takatsuka, T. Yamamoto, O. Sangen, *Macromolecules* **1997**, *30*, 6680.

CHAPTER 2

SYNTHESIS AND STUDIES OF SOME HYDROGEN BONDED SUPRAMOLECULAR LIQUID CRYSTALLINE ASSEMBLIES CONTAINING AZOPYRIDYL CHROMOPHORES

2.1. Abstract

The synthesis and characterization of some supramolecular hydrogen bonded mesomorphic materials containing azopyridyl moieties are described. These assemblies were prepared by the combination of hydrogen bond acceptors such as 4-*n*-alkyloxyphenyl,4'-azopyridines (**3a-e**), 4-pyridylazo,4'-phenyl-*n*-alkanoates (**9a, b**) and 4,4'-azobipyridine (**11**) with hydrogen bond donors such as 4-*n*-alkyloxybenzoic acids (**4a-e**). Thermal properties of these supramolecular complexes were examined by polarizing optical microscopy (POM) and differential scanning calorimetry (DSC). It has been observed that these compounds exhibit well defined liquid crystalline phases over a wide range of temperatures in the heating as well as in the cooling cycles which are distinctly different from those of the parent compounds. The mesogenic behaviour of

materials containing varying proportions of hydrogen bond donors and acceptors were also investigated in detail. The binary phase diagram of these mixtures and IR spectroscopy of the supramolecular hydrogen bonded complexes indicate that, at stoichiometric ratios, heterointermolecular hydrogen bonding results in the formation of unique mesomorphic materials. The effect of the photochromic behaviour of the azo moiety, present in these systems, on their liquid crystalline behaviour has been investigated. The hydrogen bonded assembly formed between 4-*n*-dodecyloxybenzoic acid (**4e**) and 4,4'-azobipyridine (**11**) showed a marked change in its phase transition temperatures on illumination by 320 nm UV light. Similar effects were not observed for the hydrogen bonded assemblies containing **3a-e** and **9a, b**. This has been attributed to rapid thermal *cis-trans* isomerization of the azo moiety in the hydrogen bonded assemblies. The effect of hydrogen bonding on the thermal *cis-trans* isomerization process was investigated in hydrogen bonding solvents. The rate constant for this process was observed to increase with the hydrogen bonding ability of the solvent.

2.2. Introduction

In photonics, increasing attention is being paid to the study of molecules or molecular systems whose chemical or physical properties can be reversibly controlled using light as a stimulus, due to the importance of such systems in

erasable direct read after write devices (EDRAW).[1-8] Research in this area has been directed towards the development of materials that can respond in a unique manner to the different properties of light such as wavelength, intensity and polarization. Liquid crystalline (LC) materials are particularly suited for such applications since their liquid like nature provides the possibility of molecular motion in response to the properties of light.[6,9-43] Also their long-range order arising from the cooperative behaviour of LC molecules can help to amplify relatively weak chemical or physical effects arising on photon absorption. At present, LCs are mainly used in electrooptic devices, where the optical properties are controlled by an externally applied voltage.[44] The response times of such materials are usually very slow, being of the order of milliseconds. LC materials that can respond to light (optical switching) can potentially have much faster switching times of the order of microseconds. Such devices can find use in advanced photonic applications such as optical computing and real time holography.[7]

Earlier studies related to the design of such photosensitive LC dealt with systems containing photochromic guest molecules such as azobenzenes or *spiropyrans dissolved in LC host materials.[11,13,15] Photochemical transition of the guest* materials in such systems result in the physical transformation of the guest.

Recent studies have shown however that LC materials that are inherently photoactive have much faster switching times.[6-8,26,27,30]

As discussed in the introductory Chapter 1, mesomorphism in materials arises from the proper combination of molecular shape anisotropy and intermolecular interactions. In conventional LC materials these structural requirements are incorporated into the molecule *via* covalent linkage. Recently it has been reported that LC materials can be designed *via* non-covalent linkages between molecules containing the required structural features.[45] Thus, LC materials have been constructed using intermolecular hydrogen bonding, van der Walls interaction and ionic interactions. Hydrogen bonding has been used as a means for the preparation of a large variety of self assembled materials.[16,46-59]

In this Chapter, the preparation of mesomorphic materials *via* hydrogen bonding of molecules containing the azopyridyl moieties such as 4-*n*-alkyloxyphenyl,4'-azopyridine (**3a-e**), 4-pyridylazo,4'-phenyl-*n*-alkanoates (**9a, b**) and 4,4'-azobipyridine (**11**) with a series of 4-*n*-alkyloxybenzoic acids (**4a-e**) are described.[60] The photoisomerization of the azo derivatives has been examined in hydrogen bonding solvents. The ability of the azo chromophore to impart photoswitching properties to these materials has also been investigated.

2.3. Results and Discussion

2.3.1. Hydrogen Bonded Assemblies Containing 4-*n*-Alkyloxyphenyl,4'-azopyridine

2.3.1.1. Synthesis and Characterization

The hydrogen bonded supramolecular mesogens described in this section were prepared according to Scheme 2.1.
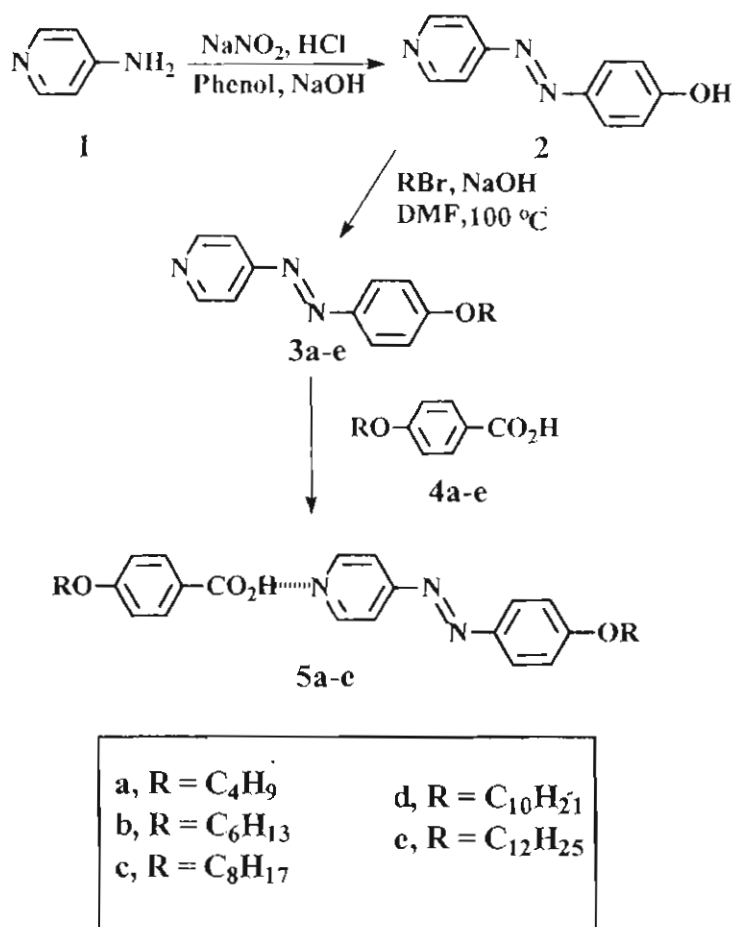
Scheme 2.1.

4-Hydroxyphenylazopyridine. **2** was synthesized by the diazotization of 4-aminopyridine followed by coupling with phenol. Alkylation of **2** by *n*-alkyl bromides in presence of sodium hydroxide and dimethylformamide gave **3a-e** in 60-70% yields. The 4-*n*-alkyloxybenzoic acids (**4a-e**) were prepared from 4-hydroxybenzoic acid using a reported procedure.[61,62]

All the compounds under investigation were characterized on the basis of their spectral data and the details are provided in the Experimental Section (2.4.). The hydrogen bonded assemblies (**5a-e**) were synthesized by heating equimolar quantities of 4-*n*-alkyloxyphenyl,4'-azopyridines (**3a-e**) and 4-*n*-alkyloxybenzoic acids (**4a-e**). These compounds were mixed thoroughly above the melting point of the mixture for a few minutes. The mixture was then allowed to cool slowly to yield the LC materials **5a-e**.[63]

2.3.1.2. Liquid Crystalline Properties

The pyridyl group is known to strongly hydrogen bond with carboxylic acids, and the supramolecular materials formed *via* hydrogen bonding between **3a-e** and **4a-e** showed interesting LC properties. Phase transition characteristics of the complexes studied by polarizing optical microscopy (POM) and differential scanning calorimetry (DSC) are clearly indicative of the selective formation of new mesogenic materials, **5a-e** (Scheme 2.1.). POM of **5a** exhibited a nematic (N) phase as identified from its N schlieren

texture (Figure 2.1.), from 110 °C to 143 °C in the heating cycle and from 135 °C to 100 °C in the cooling cycle.[64] The phase transition temperatures obtained for these assemblies are summarized in Table 2.1. The supramolecular assemblies **5b** and **5c** showed both S_A and N phases in the heating and cooling cycle, whereas only a S_A phase was observed for **5d** and **5e** (Figure 2.2.). The phase transition temperatures were reproducible over several heating and cooling cycles for all the supramolecular assemblies.

Table 2.1. Phase transition temperatures of 4-alkyloxyphenyl,4'-azopyridyl assemblies.

Compound	Phase transition temperature, °C[†]	
	Heating	Cooling
5a	K 110 N 143 I	I 135 N 100 K
5b	K 79 S_A 110 N 141 I	I 138 N 95 S_A 73 K
5c	K 104 S_A 123 N 131 I	I 130 N 121 S_A 101 K
5d	K 92 S_A 126 I	I 120 S_A 85 K
5e	K 99 S_A 129 I	I 124 S_A 84 K

[†] K = crystalline, N = nematic, S_A = smectic A and I = isotropic phase.
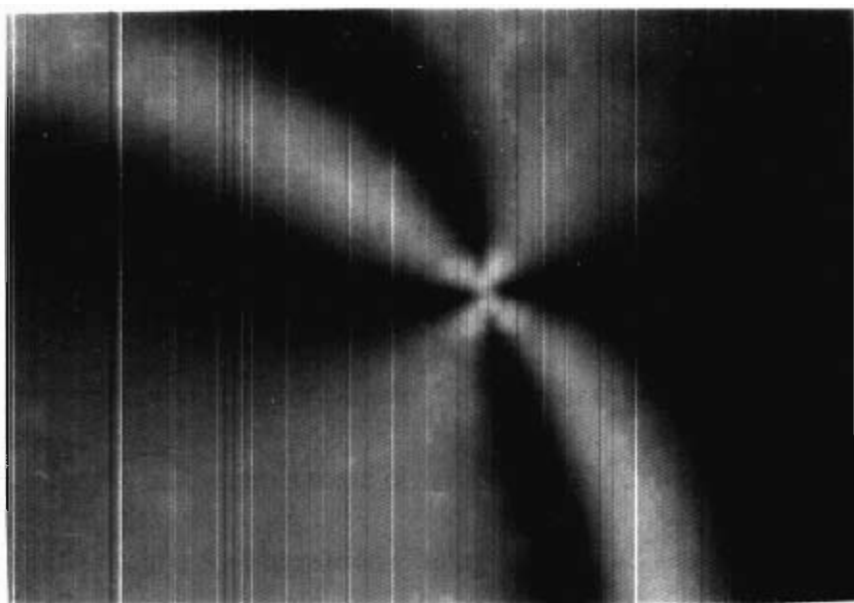
Figure 2.1. Optical photomicrograph of nematic schlileren texture observed for 5a, at 120 °C, in the cooling cycle.

Figure 2.2. Optical photomicrograph of focal conic texture observed for 5e, at 115 °C, in the cooling cycle.

DSC curves obtained for the above assemblies confirm the LC phases observed under the POM. The temperatures at which the transition was observed using DSC were similar to those observed by POM. The DSC curves of **5d** and **5e** are shown in Figures 2.3. and 2.4., respectively. For example, in the heating cycle **5d** show endotherms at 81 °C due to the crystal to crystal transition, at 97 °C due to a K-S_A transition and at 125 °C due to the S_A to isotropic phase transition (Figure 2.3.). Similarly for **5e**, endotherms were observed at 100 °C for K-S_A transition and 128 °C corresponding to the S_A-I transition (Figure 2.4.).
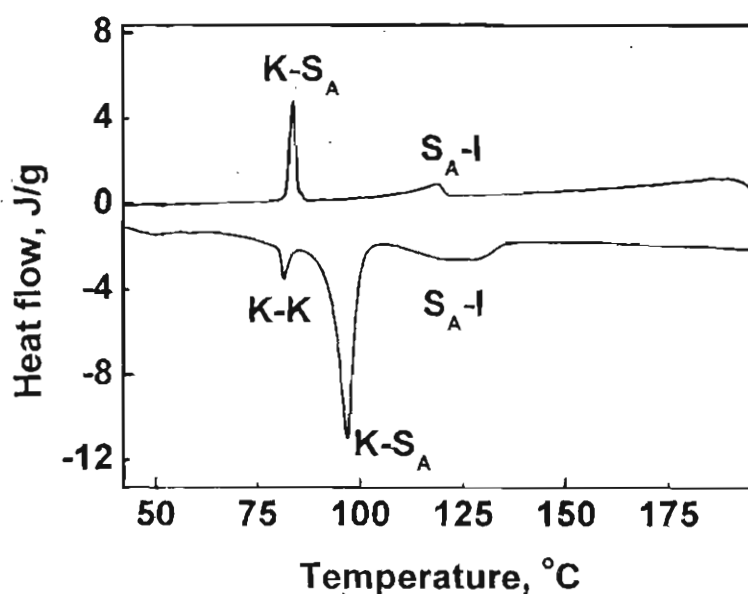
Figure 2.3. DSC trace obtained for 5d in the heating and cooling cycles.
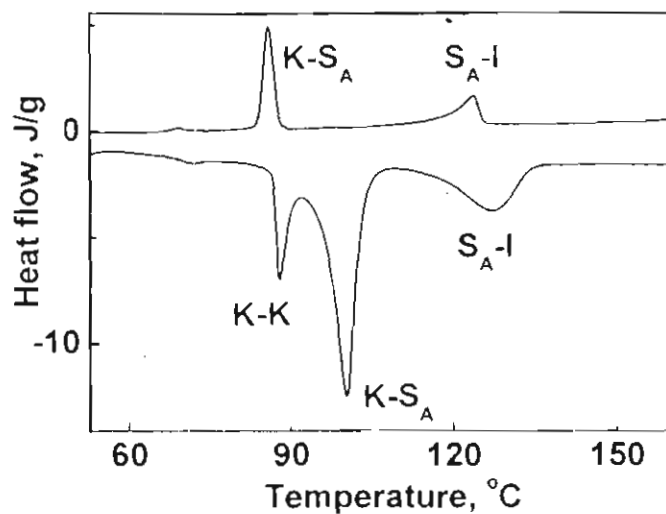
Figure 2.4. DSC trace obtained for 5e in the heating and cooling cycles.

The dependence of the transition temperatures of the complexes on chain

length of the alkyl groups is shown in Figure 2.5.
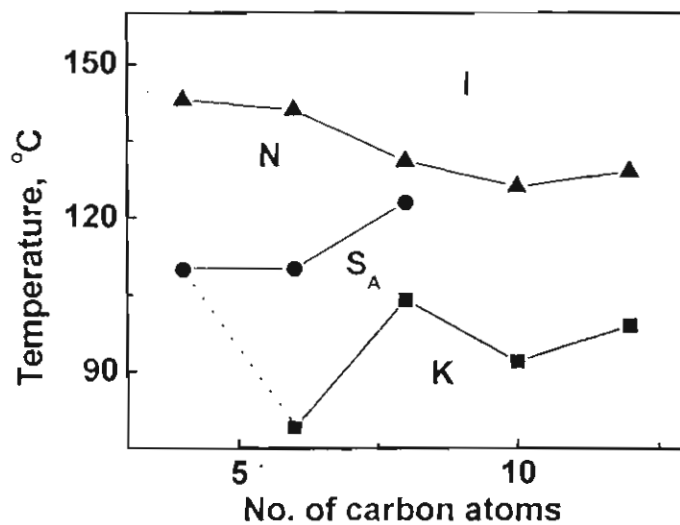
Figure 2.5. Plot of transition temperature against the number of carbon atoms
(n) in the alkyl chain for the 1:1 hydrogen bonded complexes, 5a-e.

With increasing chain length of the alkyl groups in hydrogen bonded assemblies the isotropization temperature decreases. Also for the assembly containing the lowest alkyl chain length (n = 4), the S_A liquid crystalline phase was not observed. The observed dependence on alkyl chain length is similar to that reported for LC molecules obtained *via* covalent linkages.[65]

The LC properties of materials are highly sensitive to substituent effects. In hydrogen bonded LCs, these properties are generally related to the strength of the hydrogen bonds involved. In the pyridine/acid complexes the association constant will be primarily affected by the acidity of the acid (H donor) and the basicity of the pyridine derivative.[66] We have investigated the effect of substituent on the mesomorphic properties by studying the supramolecular assemblies, **6a-e** (Chart 2.1.), formed between 4-*n*-hexyloxyphenyl,4'-azopyridine **(3b)** and benzoic acid derivatives. The phase transition temperatures of **6a-e** during the heating and cooling cycle are listed in Table 2.2. The phase transition temperatures of **5b** are also included for comparison.

6a-e

| a, R =H | c, R = NO$_2$ |
| b, R =Cl | d, R = CN |
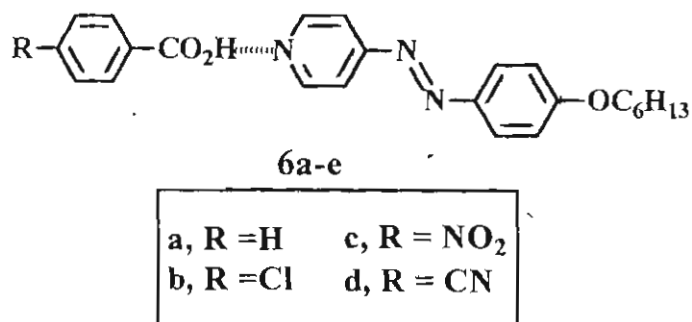
Chart 2.1.

Table 2.2. Phase transition temperatures of 6a-e.

Compound	Phase transition temperature, °C†	
	Heating	Cooling
5b	K 79 S$_A$ 110 N 141 I	I 138 N 95 S$_A$ 73 K
6a	K 95 I	
6b	K 124 S$_A$ 127 I	I 126 S$_A$ 112 K
6c	K 151 S$_A$ 156 N 170 I	I 168 N 156 S$_A$ 156 K
6d	K 135 N 171 I	I 169 N 131 K

† K = crystalline. N = nematic, S$_A$ = smectic A and I = isotropic phase.

The unsubstituted benzoic acid complex (**6a**) melts directly from the crystalline to the isotropic phase without the formation of an intervening LC phase, whereas the supramolecular assembly **6b** exhibits a focal conic texture, characteristic of a S$_A$ for a short range from 124 °C to 127 °C in the heating cycle. Compound **6c**, where R = NO$_2$ showed S$_A$ and N phases, whereas **6d** showed a threaded texture characteristic of a N phase from 135 °C to 171 °C (Table 2.2.). Comparison of these values with those of **5b** suggests that an electron donating *para* substituent on the benzoic acid results in

stabilization of the LC phase. for these assemblies. •

2.3.1.3. Thermal Properties of Binary Mixtures

Studies on the LC properties of stoichiometric complexes formed between 3a-e and 4a-e indicated the formation of unique materials and the phase transition temperatures for these materials are sharp and highly reproducible. Further confirmation for the formation of unique materials was obtained by studying the thermal properties of binary mixtures of the hydrogen bond donor and acceptor in varying proportions. We have investigated the binary phase diagram for two representative mixtures containing 4-*n*-hexyloxyphenyl,4'-azopyridine (3b) and 4-*n*-hexyloxybenzoic acid (4b) and 4-*n*-dodecyloxyphenyl,4'-azopyridine (3e) and 4-*n*-dodecyloxybenzoic acid (4e).

The LC properties of the binary mixtures were examined by POM using a heating/cooling rate of 5 °Cmin^{-1}. 4-*n*-Hexyloxybenzoic acid shows a NLC phase from 101 °C to 161 °C whereas compound 3b melts sharply at 56.9 °C. The binary mixtures mainly exhibited a N phase. In addition a S_A phase was also observed in mixtures containing 30-60 mol% of 3b. Some of the key features noticeable in the phase diagram (Figure 2.6.) are discussed below.
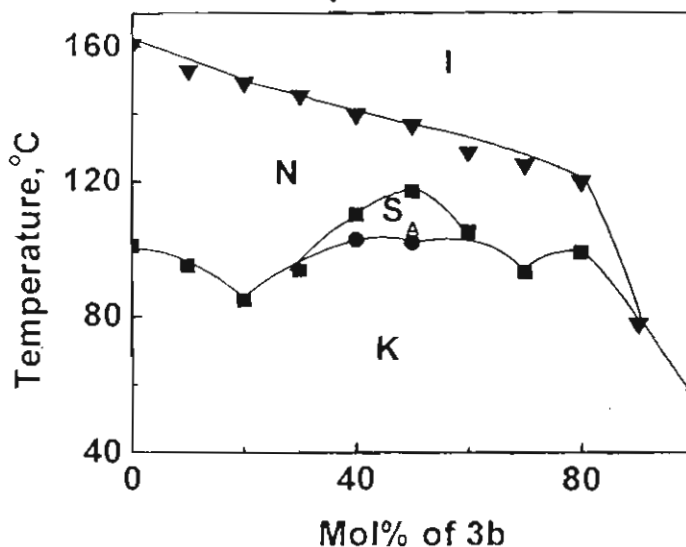
Figure 2.6. The binary phase diagram of 3b and 4-*n*-hexyloxybenzoic acid.

The presence of two eutectic points around 20 and 60 mol% of **3b** strongly supports the formation of pure liquid crystalline material in the 1:1 ratio. However, the absence of an azeotropic maximum for the S and N mixtures suggest that the interactions between the dimerized alkyloxybenzoic acid and the hydrogen bonded 1:1 stoichiometric compound are not particularly stronger in the mesomorphic state than they are in the isotropic liquid state. The presence of a melting maximum for the crystalline mixtures containing 50 mol% of **3b** proves conclusively that a well defined material is formed at a 1:1 stoichiometric ratio resulting from the hydrogen bonding of one molecule of **3b** and one molecule of 4-*n*-alkyloxybenzoic acid (Figure 2.6.).

Phase diagrams for **3e** and **4e** also show similar type of behaviour. Eutectic

points observed for 30 and 70 mol% of **3e** and melting maximum at 50 mol%

confirms the formation of hydrogen bonded supramolecular assembly. For the 10

and 20 mol% mixtures a N phase was observed near the isotropic temperature. The

four-brush schlieren texture and fan shaped texture observed for 10-40 mol%

mixtures confirms the formation of a S_C LC phase. Formation of S_A phase was

confirmed by the focal conic texture, which transforms to a homeotropic phase

for the binary mixtures containing 40-90 mol% of **3e** (Figure 2.7.).
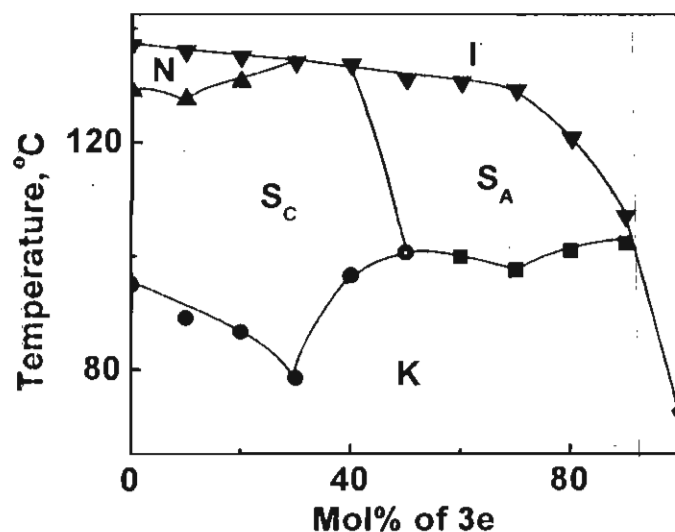
Figure 2.7. The binary phase diagram of 3e and 4-*n*-dodecyloxybenzoic acid.

2.3.1.4. Isomerization Studies

The azo chromophore present in the hydrogen bonded assemblies **3a-e** can

undergo photoisomerization. Since the *trans* form of azo derivatives is generally

more stable, thermal *cis-trans* isomerization is usually observed. Compounds **3a-e** possess a strong band around 360 nm due to the π-π* transition. Photoisomerization of **3c** in toluene was examined by steady state photolysis, using a 200 W high-pressure mercury lamp equipped with a 360 nm band-pass filter, as light source. On photolysis, the absorption at 360 nm decreases while that at 450 nm, due to the n-π* transition of the *cis* form increases. The photostationary state was reached within 3 minutes of photolysis. In the photostatioinary state the *cis:trans* ratio was observed to be 2:3. The quantum yields of *trans-cis* isomerization for all these hydrogen bond acceptors (**3a-e**), determined using azobenzene as actinometer was around 0.2 in toluene. The rate of thermal *cis* to *trans* isomerization following photolysis was determined spectrophotometrically, by monitoring the increase in absorbance of π-π* absorption at 360 nm, which is accompanied by a decrease in absorbance at 450 nm. The *cis-trans* isomerization, which occurs in the dark follows first order kinetics and the rate constant, was estimated using equation 2.1.

$$k = [1/t] \ln (OD^{\infty} - OD^{0})/(OD^{\infty} - OD^{t}) \qquad \textbf{2.1.}$$

Where, 't' is the time in seconds, 'OD^{∞}' and 'OD^{0}' are the final and initial absorbances and 'OD^{t}' is the absorbance at the time 't'. Figure 2.8. shows typical plots for equation 2.1. at two different temperatures and the rate constants

obtained at different temperatures are summarized in Table 2.3.
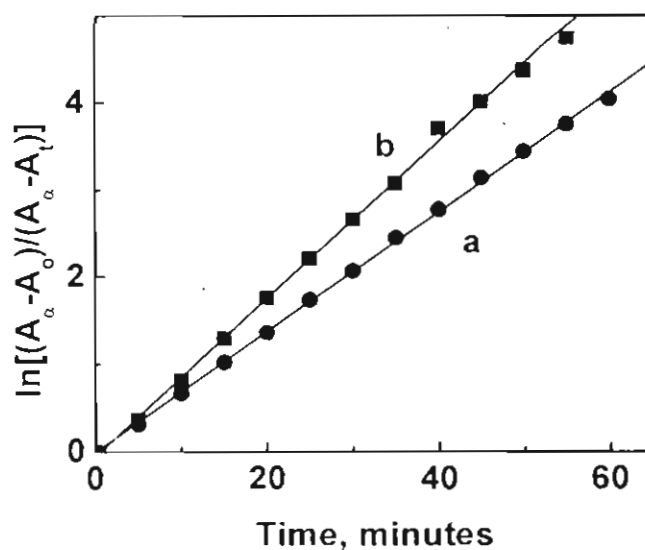
Figure 2.8. **Kinetic plots of 3e in toluene, showing the rate of formation of** *trans* **isomer after photolysis at: (a) 40 °C and (b) 50 °C.**

Table 2.3. **Rate constants of the** *cis-trans* **isomerization of 3e in toluene.**

Temperature (K)	$k \times 10^2 \ s^{-1}$
303	3.6
308	6.3
313	7.6
318	18.5

From the plot of ln *k* versus 1/T, (Figure 2.9.) the activation energy of the

process calculated using Arrhenius equation was 93 kJmol^{-1}. There was no

significant effect of the variation of alkyl chain length on the rates of thermal

isomerization or on the activation energy.
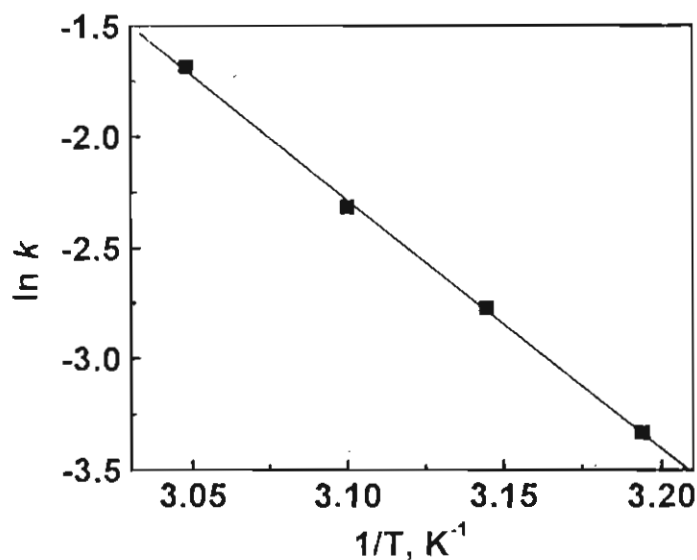
**Figure 2.9. Arrhenius plot obtained for the *cis-trans* thermal isomerization of
3e in toluene.**

In order to study the effect of hydrogen bonding on the isomerization

rates, photoisomerization was also investigated in hydrogen bonding solvents. The

absorption maximum and rate of *cis-trans* isomerization in different solvents are

shown in Table 2.4.

Table 2.4. Rate constants of *cis-trans* isomerization and lifetimes of 3e in hydrogen bonding solvents.

Solvent	λ_{max}, nm	k, s^{-1}	Lifetime, s
Methanol	358	6.6×10^{-3}	150.6
Ethanol	358	7.7×10^{-2}	12. 9
Trifluoroethanol	355	3.1	0.32
Acetic acid	400	1.1×10^{3}	8.0×10^{-4}
Methanolic hydrochloric acid (10 μM)	400	2.0×10^{3}	5.0×10^{-4}

In alcoholic solvents a slight hypsochromic shift in the π-π* absorption of 3e was observed. In acetic acid solution, however, a bathochromic shift was observed. In order to examine whether this shift could arise due to protonation of the pyridyl moiety the absorption spectrum of 3e was measured in methanol solution containing hydrochloric acid (> 10 μM). Under these conditions, the pyridyl moiety will exist in its protonated form. The absorption maximum was observed to be 400 nm, which is same as that observed in acetic acid indicating

that in acetic acid also the pyridyl moiety exists in its protonated form. Although the pyridyl derivatives exists in its protonated form when acetic acid is used as a solvent, in the 1:1 stoichiometric ratios present in the assemblies the pyridyl moiety will exist in the hydrogen bonded form with the benzoic acid derivatives. The IR data of the assemblies strongly support this view. For example the O-H bands around 2500 and 1920 cm^{-1} observed for the hydrogen bonded assemblies in the IR spectra are indicative of strong hydrogen bonding between pyridyl moiety and benzoic acid derivatives.[67,68] These bands replace the O-H band around 3000 cm^{-1} observed for the weakly hydrogen bonded acid dimers in the pure acid.

Cis-trans isomerizations of **3e** in alcoholic solvents were studied by steady state photolysis. The rate constants and lifetimes of the process are summarized in Table 2.4. It is evident that *cis-trans* isomerization increases with hydrogen bond donating strength of the solvent.

In acetic acid and trifluoroethanol solution however no change could be observed in the absorption spectrum of **3e** on steady state photolysis, due to rapid thermal *cis-trans* isomerization. In these cases, the rate constants were determined using nanosecond flash photolysis experiments. The third harmonic (355 nm) of a Quanta-Ray GCR-12 Nd:YAG laser (pulse duration 10 ns, energy 60 mJ/pulse) was used to excite **3e** and optical changes were monitored using a laser spectrometer (Applied photophysics model LKS-20). Figure 2.10. shows absorption-time profile at 360 nm following laser pulse excitation of a solution of

3e in trifluoroethanol. A 360 nm band-pass filter was placed between the sample and analyzer lamp to prevent secondary photolysis of the *cis* isomer formed in the photoisomerization. A bleach is observed at 355 nm due to the conversion of *trans* 3e to its *cis* form. The recovery of the bleach corresponds to the thermal *cis-trans* isomerization. The lifetime and rate constant of this process measured in different solvents are given in the Table 2.4.
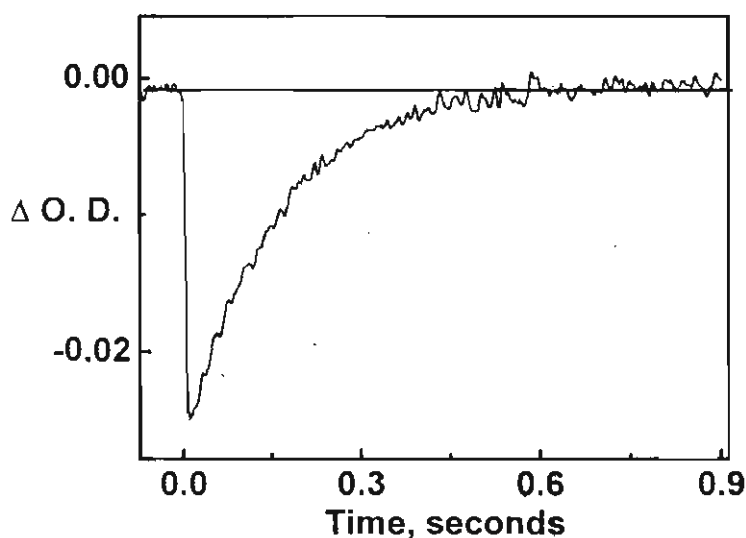
Figure 2.10. Transient absorption-time profile recorded at 360 nm, following 355 nm laser pulse excitation of 3e in trifluoroethanol.

Figure 2.11. shows the absorption-time profile obtained after excitation of 3e in acetic acid using the 355 nm laser pulse and observed at 400 nm (a 400 nm band-pass filter was placed between the sample and analyzer lamp). The rate constant for isomerization is two orders of magnitude higher in acetic acid, compared to that in trifluoroethanol.
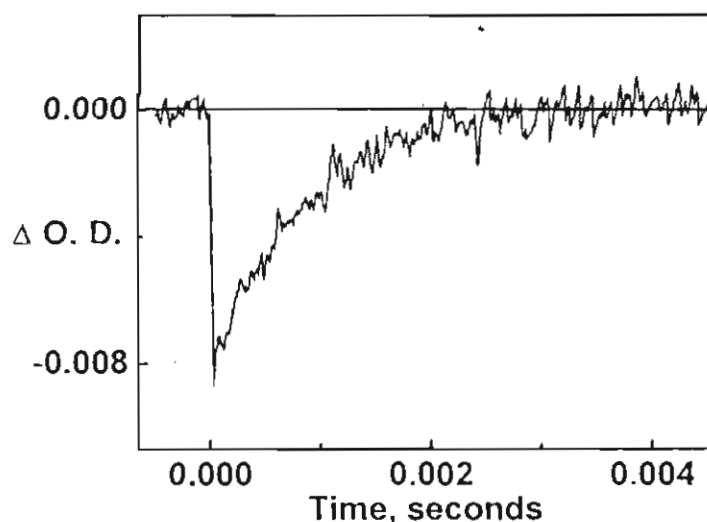
Figure 2.11. Transient absorption-time profile recorded at 400 nm, following 355 nm laser pulse excitation of 3e in acetic acid.

These studies indicate that both hydrogen bonding as well as protonation of the pyridyl moiety brings about a substantial enhancement in the rate of *cis* to *trans* isomerization. Hydrogen bonding as well as protonation of the pyridyl group will lead to an increase in its electron withdrawing ability. This would lead to an enhancement in the donor-acceptor nature of the 4-*n*-alkyloxyphenyl,4'-azopyridine. Donor-acceptor-substituted azobenzene derivatives have been reported to undergo very fast *cis* to *trans* thermal isomerization reactions.[69]

Attempts were made to observe photoinduced phase changes in the hydrogen bonded materials, by photolysing their LC phases using 360 nm light. POM studies did not show any changes in the LC phases on photolysis. Two

probable reasons for this could be that at the high temperatures required to observe

the LC phases for these materials, the thermal *cis* to *trans* isomerization would be

very rapid. Moreover, hydrogen bonding would also result in an enhancement in

the rate of thermal isomerization.

2.3.2. Hydrogen Bonded Assemblies of 4-Pyridylazo,4'-phenyl-*n*-alkanoate

The 4-*n*-alkyloxyphenyl,4'-azopyridine hydrogen bonded assemblies

undergo rapid *cis-trans* isomerization due to the donor-acceptor nature of the azo

chromophore. In an effort to circumvent this problem, the LC and

photoisomerization behaviour of hydrogen bonded assemblies of 4-pyridylazo,4'-

phenyl-*n*-alkanoate (**9a, b**) with substituted benzoic acids have been investigated.

Due to the presence of the electron withdrawing ester group the thermal *cis-trans*

isomerization in the systems is expected to be much slower for these materials.

2.3.2.1. Synthesis and Characterization

The hydrogen bonded supramolecular assemblies **10a-j** were prepared as

per Scheme 2.2. Reaction of *n*-alkyl acids (**7a-b**) with thionyl chloride afforded

the respective *n*-alkyl acid chlorides (**8a-b**), which on subsequent reaction with

4-hydroxyphenyl,4'-azopyridine in dry dichloromethane and triethylamine gave

9a-b (72% yield). Compounds **9a-b** were characterized on the basis of their

spectral data. Complexation with hydrogen bond donors was carried out by

thorough mixing of a melt of equimolar amounts of **9a-b** and **4a-e**, followed by slow cooling. Details of the synthetic procedures are described in the Experimental Section (2.4.).
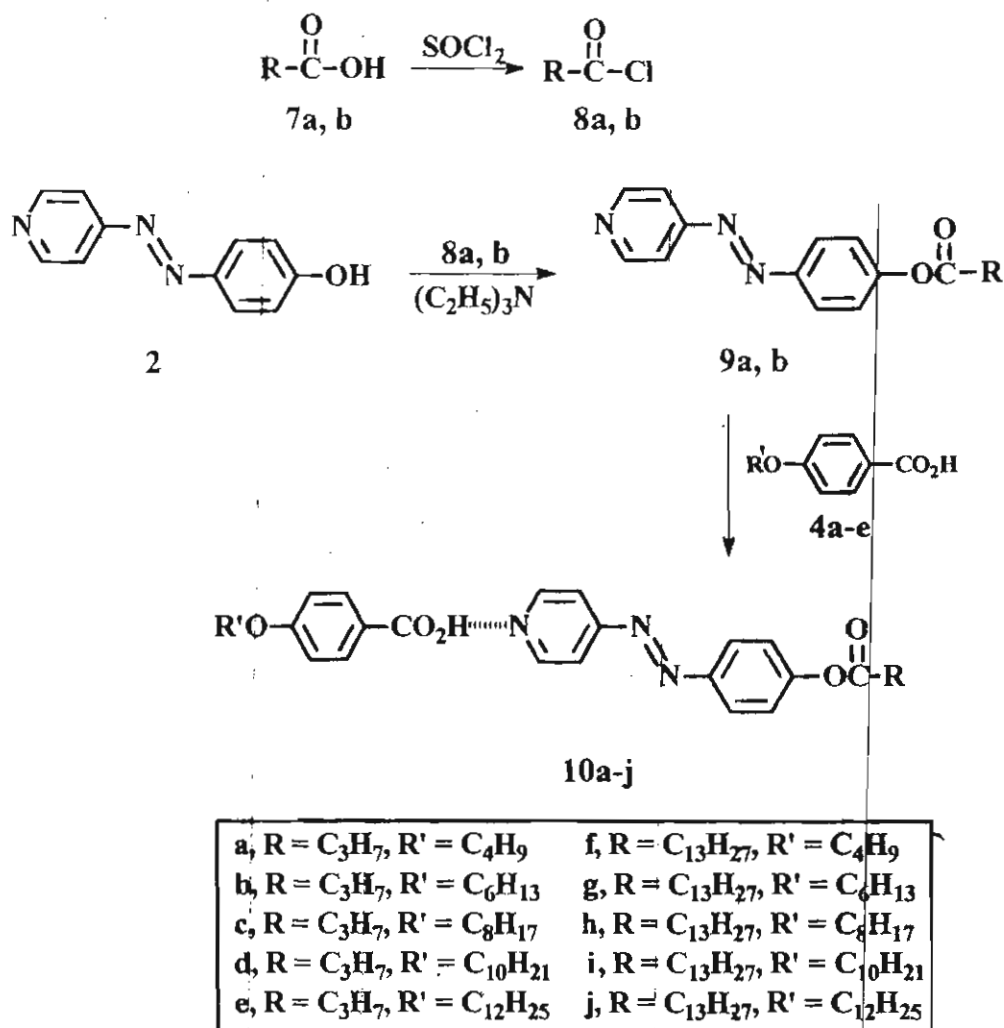
Scheme 2.2.

2.3.2.2. Liquid Crystalline Properties

Supramolecular assemblies of the hydrogen bond acceptors 4-pyridylazo,4'-phenyl-*n*-butanoate (**9a**) and 4-pyriylazo,4'-phenyl-*n*-tetradecanoate (**9b**) with 4-*n*-alkyloxybenzoic acids (n = 4, 6, 8, 10 and 12) as hydrogen bond donors were prepared as described above. The complexes behave as single LC materials and show clear phase transitions. The thermal properties of the mixtures are different from those of the individual components. In the hydrogen bonded assemblies containing 4-pyridylazo,4'-phenyl-*n*-butanoate a N phase was observed, except for **10e** which exhibited a S_A phase at lower temperatures and a N phase at higher temperatures. This behaviour is similar to those reported generally for nematogenic compounds, containing oxygen atom in the branched chain, in which increasing chain length stabilizes the S_A phases.[65] The phase transition temperatures observed by POM are summarized in Table 2.5.

A plot of the dependence of the phase transition temperatures on alkyl chain length for the **10a-e** is shown in Figure 2.12. With increasing chain length a decrease in the isotropization temperature is observed which is in accordance with the normal mesomorphic behaviour of NLCs.[65]

Table 2.5. Phase transition temperatures of 10a-j.

Compound	Phase transition temperature, °C†	
	Heating	Cooling
10a	K 85.9 N 135.7 I	I 133.7 N 83.2 K
10b	K 100.5 N 131.1 I	I 128.9 N 81.8 K
10c	K 82.9 N 128.2 I	I 126.5 N 68.4 K
10d	K 86.8 N 119.4 I	I 118.2 N 71.4 K
10e	K 108.9 S_A 112.5 N 121.2 I	I 119.1 N 111.5 S_A 62.3 K
10f	K 76.2 S_A 126.0 I	I 123. 3 S_A 50.0 K
10g	K 74.8 S_C 128.2 I	I 125.9 S_C 46.4 K
10h	K 71.2 S_C 128.8 I	I 126.5 S_C 45 K
10i	K 80.1 S_C 130.0 I	I 125.2 S_C 74.3 K
10j	K 91.9 S_C 129.2 I	·I 126.2 S_C 62.3 K

†K = crystalline, N = nematic, S_A = smectic A, S_C = smectic C and I = isotropic phase.
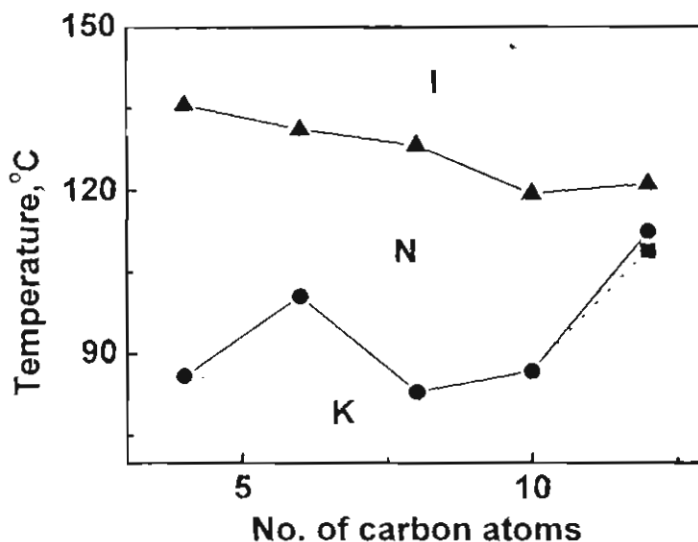
Figure 2.12. **Plot of transition temperature against the number of carbon atoms (n) in the alkyl chain for the 1:1 hydrogen bonded complexes, 10a-e.**

The hydrogen bonded assemblies **10f-j** were found to be smectogenic; **10f** shows a fan shaped texture at 76.2 °C which confirms the formation of a S_A phase. It isotropizes at 126.0 °C. In the cooling cycle S_A phase was observed between 123.3 °C to 50.0 °C. The compounds **10g-j** show S_C LC phases. Figure 2.13. shows the dependence of phase transition temperatures of **10f-j** on the alkyl chain length. While in the case of hydrogen bonded assemblies containing of 4-pyridylazo,4'-phenyl-*n*-butanoate (**10a-e**) the clearing temperatures of the materials is independent on the alkyl chain length. In this series the lowest crystal to mesophase transition was observed for **10h** (Table 2.5.).
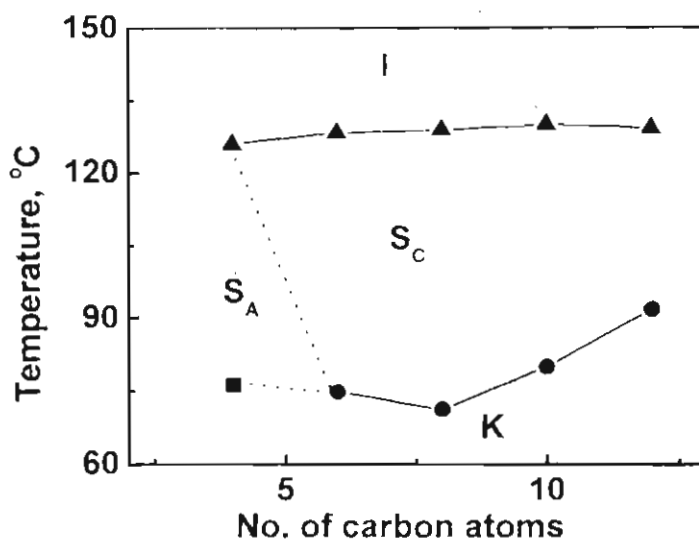
Figure 2.13. **Plot of transition temperature against the number of carbon atoms (n) in the alkyl chain for the 1:1 hydrogen bonded complexes, 10f-j.**

2.3.2.3. Thermal Properties of the Binary Mixtures

The phase transition behaviour of binary mixtures containing varying mol% of 4-pyridylazo,4'-phenyl-n-tetradecanoate (**9b**) and 4-n-octyloxybenzoic acid (**4c**) was studied using POM with a heating and cooling rate of 5 °Cmin⁻¹. 4-n-Octyloxybenzoic acid shows a S_C LC phase from 101 °C to 117 °C and a N phases from 117 °C to 143 °C. The binary mixture of 10-40 mol% of **9b** exhibited S_C and N LC phases, whereas only S_C phases were observed for the 50 and 60 mol% mixture of **9b**. Above 60 mol% S_A phase was seen. The eutectic points observed at 40 and 70 mol% of **9b** and a melting maxima observed at 50 mol% of

the binary mixture supports the formation of a 1:1 **4c/9b** hydrogen bonded

assembly. The absence of the isotropization maxima at 50 mol% indicates that the

strength of the hydrogen bonding in the acid dimer is much more stable than for

acid/pyridine complex in the mesomorphic state (Figure 2.14.).
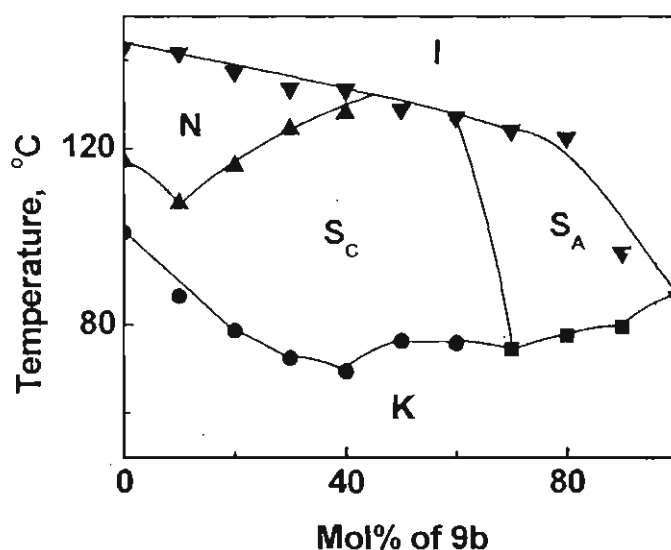
Figure 2.14. The binary phase diagram of 9b and 4-*n*-octyloxybenzoic acid.

2.3.2.4. Isomerization Studies

The azo compound **9b** in the ground state absorbs at 323 nm in toluene.

Photolysis using a 320 nm band-pass filter from a 200 W high-pressure mercury

lamp causes *trans-cis* isomerization of **9b** and a photostationary state is reached

within 75 seconds. The ratio of *cis* to *trans* in the steady state was determined to

be 2:3 as in the cases of **3a-e**. The rate constants for the reverse reactions were

also determined at different temperatures and are summarized in Table 2.6. From

the dependence of the rate constants on inverse of temperature, the activation

energy for this process was estimated as 90 kJM^{-1}, using the Arrhenius equation.

Table 2.6. Rate constants of *cis-trans* isomerization of 9b in toluene.

Temperature (K)	$k \times 10^3 \text{ s}^{-1}$
303	12.9
308	25.9
313	44.9
318	70.2

The rate constants for the thermal *cis-trans* isomerization was studied using

steady state photolysis or flash photolysis experiments and the data are

summarized in Table 2.7.

A clear trend in increase in the rate constants with increasing hydrogen

bond donating strength of the solvent becomes evident (Table 2.7.). The rate

constants for this process were about an order of magnitude slower for **9b**

compared to that of **3e** in the corresponding solvents.

Table 2.7. Rate constants for *cis-trans*. isomerization and lifetimes of 9b in different hydrogen bonding solvents.

Solvent	$\lambda_{max,}$ nm	k, s^{-1}	Lifetime, s
Methanol	321	3.2×10^{-4}	3.2×10^{3}
Ethanol	321	4.1×10^{-3}	242.4
Trifluoroethanol	314	9.4×10^{-2}	10.0
Acetic acid	340	105.6	9.5×10^{-3}
Methanolic hydrochloric acid (10 μM)	346	132.8	7.7×10^{-3}

2.3.3. Hydrogen Bonded Assemblies of 4,4'-Azobipyridine

The thermal *cis* to *trans* isomerization was considerably slower for the 4-pyridylazo,4'-phenyl-*n*-alkanoate (**9a**, **b**) derivatives compared to the 4-*n*-alkyloxyphenyl,4'-azopyridine (**3a-e**) derivatives. For observing photoinduced phase changes in the LC phase however the reverse isomerization rates have to be even slower. In this Section we have explored the LC and photochemical properties of supramolecular hydrogen bonded assemblies formed between 4,4'-azobipyridine (**11**) and 4-*n*-alkyloxybenzoic acids. The reverse isomerization of the 4,4'-azobipyridine (**11**) was observed to be much slower than those of the azopyridine derivatives reported in the previous sections.

2.3.3.1. Synthesis and Characterization

4,4'-Azobipyridine (**11**) was synthesized from 4-aminopyridine according to a reported procedure (Scheme 2.3.).[70] Oxidation of 4-aminopyridine in presence of sodium hypochlorite (4%) gave 4,4'-azopyridine in a 44% yield. The hydrogen bonded assemblies were prepared by the slow heating of 2:1 molar ratios of acids and **11** up to the melting temperature and slow cooling (Scheme 2.3.). All compounds were characterized on the basis of their spectral data. The detailed synthetic procedures for these compounds are provided in the Experimental Section (2.4.).

a, R = C_4H_9	d, R = $C_{10}H_{21}$
b, R = C_6H_{13}	e, R = $C_{12}H_{25}$
c, R = C_8H_{17}	
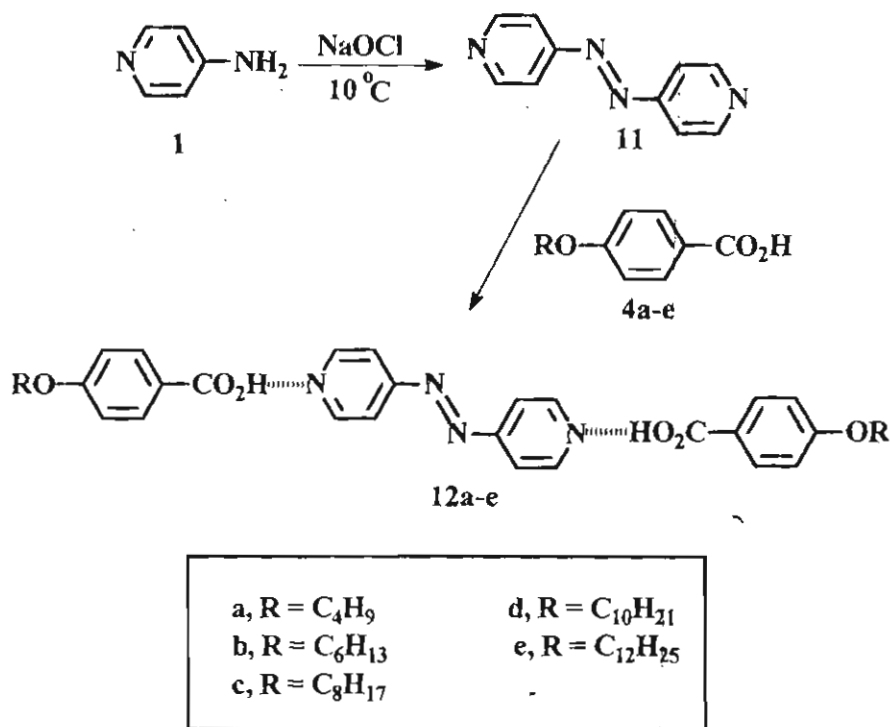
Scheme 2. 3.

2.3.3.2. Liquid Crystalline Properties

The thermal behaviour of these complexes **12a-e**, studied using POM indicated sharp phase transitions and formation of homogeneous mesophases. The thermal properties of the complexes were distinctly different from those of the individual components. Homogeneous phases with a fan shaped texture, characteristic of smectic phase were observed for all the complexes. The phase transition temperatures of these assemblies are summarized in Table 2.8.

Table 2.8. Phase transition behaviour of 12a-e.

Compound	Phase transition behaviour, °C†	
	Heating	Cooling
12a	K 140 S 161 I	I 159 S 119 K
12b	K 95 S 148 I	I 146 S 78 K
12c	K 104 S 156 I	I 156 S 85 K
12d	K 90 S 144 I	I 141 S 74 K
12e	K 86 S 143 I	I 142 S 79 K
12e*	K 133 S 140 I	I 137 S 90 K

†K = crystalline, S = smectic and I = isotropic phase.
*Phase transition behaviour of **12e**, after photolysis using 320 nm light in the first heating and cooling cycles.

The dependence of phase transition temperatures of the hydrogen bonded assemblies with the chain length of alkyl chain is shown in Figure 2.15.
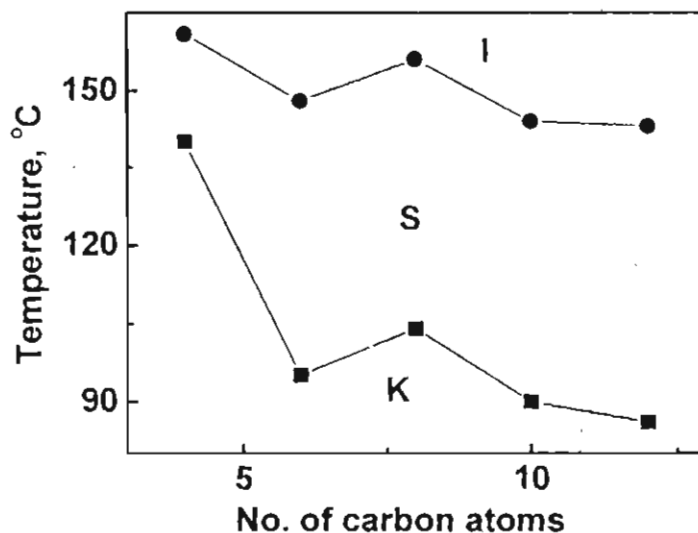
Figure 2.15. Plot of transition temperature against the number of carbon atoms (n) in the alkyl chain for the hydrogen bonded complexes, 12a-e.

The DSC curves obtained for these supramolecular assemblies supports the LC phases observed under POM. The endotherm and exotherm obtained for **12b** are shown in Figure 2.16. In the heating cycle **12b** show a peak at 93 °C due to the K-S transition and a peak at 148 °C due to the S-I transition (Figure 2.16.).
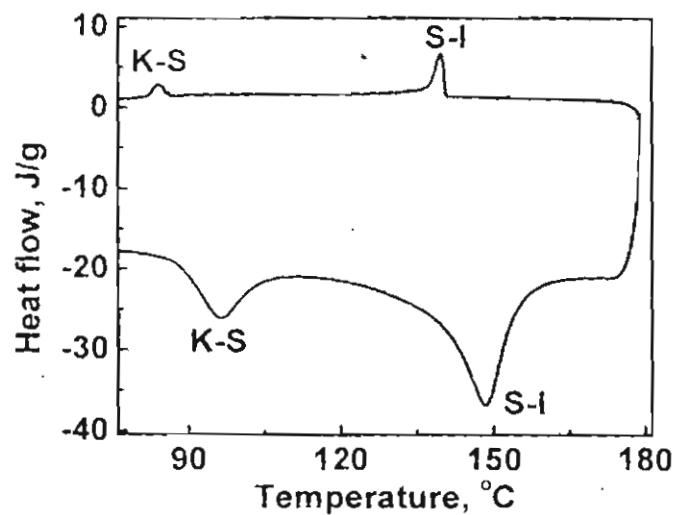
Figure 2.16. DSC curve obtained for 12b in the heating and cooling cycles.

2.3.4.3. Thermal Properties of the Binary Mixtures

The phase diagram for the mixtures of 4,4'-azopyridine (11) and 4-*n*-dodecyloxybenzoic acid (4e) were as shown in the Figure 2.17.
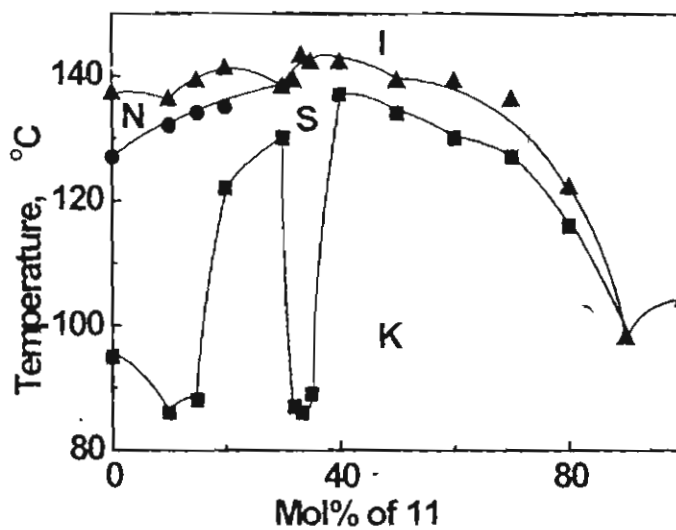
Figure 2.17. The binary phase diagram of 11 and 4-*n*-dodecyloxybenzoic acid.

The binary mixture of 10 mol% of **11** shows a depression in the N-I melting temperature indicative of the destabilization of the nematic phase. The mixture containing 10-20 mol% of **11** exhibited mainly S_C LC phase and in the mixtures containing 30-80 mol% of **11**, S_A was observed (Figure 2.17.). From the phase diagram the formation of hydrogen bonded supramolecular assembly at 2:1 ratios of **11** and **4e** can be confirmed by the eutectic points observed at 86 °C and 116 °C. Further confirmation is provided by the observation of an isotropization maximum for the mixture containing 33.3 mol% of **11** and **4e**. The presence of hydrogen bonding was also confirmed from their infrared spectra. The O-H stretching frequency of **12e** for example, at 2437 cm^{-1} and 1941 cm^{-1} is indicative of strong hydrogen bonding between pyridyl moiety and carboxylic group.[67,68]

2.3.3.4. Isomerization Studies

Photolysis of *trans*-**11** would lead to partial isomerization to its *cis* form. The quantum yield ($\Phi_{trans-cis}$) of *trans* to *cis* photoisomerization of **11** in benzene was determined as 0.025, using azobenzene as the actinometer. The quantum yield was slightly lower in trifluoroethanol ($\Phi_{trans-cis}$ = 0.016), suggesting that hydrogen bonding could lead to some reduction in the photoisomerization efficiency of **11**. Conversion of **11** in the supramolecular assembly from *trans* to *cis* leads to destabilization of the liquid crystalline phase (Scheme 2.4.).
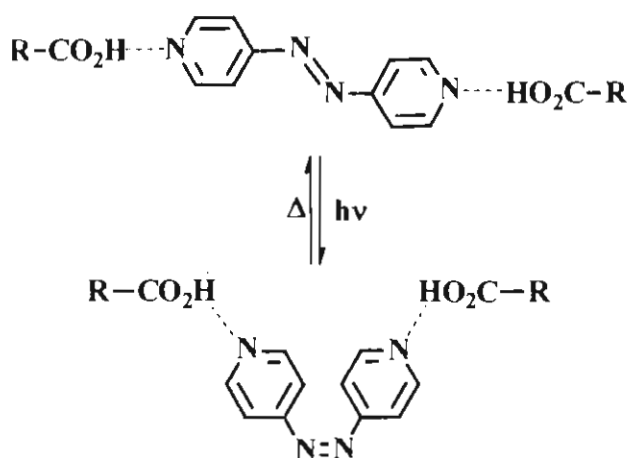
Scheme 2.4.

Photoinduced phase changes were studied for **12e**. Thin films of **12e** were prepared by slow cooling of the isotropic liquid to 110 °C. At this temperature the film showed the fan shaped texture with narrow and elongated ellipse texture, characteristic of S_A (Figure 2.18.a).[64]

(a)   (b)   (c)
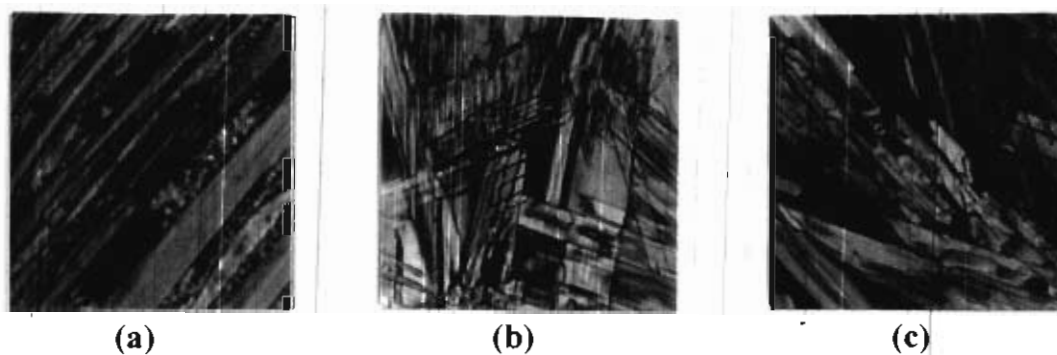
Figure 2.18; Optical photomicrographs of 12e (a) before photolysis at 110 °C, S_A phase (b) after photolysis using 320 nm light at 110 °C, crystalline phase and (c) after photolysis, at 135 °C, S_B phase.

The film turned crystalline on photolysis with light from a 200 W medium pressure mercury lamp, filtered through a 320 nm band-pass filter (Figure 2.18.b). After photolysis, the film was cooled to 79 °C and subsequently subjected to heating and cooling cycle and the associated phase changes are shown in Table 2.8 (**12e***). In the heating cycle (K-S) the phase transition of the photolysed film occurred at a much higher temperature (133 °C) than for the unphotolysed sample, which can be attributed to the destabilizing effect of the *cis* form of **12e** on the LC properties of the assembly. Interestingly, in the cooling cycle the photolysed film shows a stable homogeneous S phase up to 90 °C. Besides the change in the phase transition temperatures, photolysis of these films also brings about a clear change in the nature of the liquid crystalline phase. For the photolysed films rod-like and rounded grains typical of smectic B (S$_B$) LCs was observed (Figure 2.18.c).[64]

On subsequent heating and cooling cycles, additional phase transitions were observed to that reported in Table 2.8. (**12e***), suggesting partial thermal reversal of *cis* form of **12e** back to its *trans* form. The photoinduced effects were thermally fully reversible within three hours of photolysis and could be repeated over several cycles.

2.4. Experimental Section

Melting points are uncorrected and were recorded on a Mel-temp II melting point apparatus. Phase transitions were observed using a Nikon HFX 35A Optiphot-2 polarized light microscope, equipped with Linkam THMS 600 heating and freezing stage connected to Linkam TP92 temperature programmer. DSC scans were performed using Du Pont DSC 2010 Differential Scanning Calorimeter attached to Thermal Analyst 2100 data station under air. IR spectra were recorded on a Perkin Elmer Model 882 infrared spectrophotometer. The electronic spectra were recorded on a Shimadzu Model UV-3101PC UV-Vis-NIR scanning spectrophotometer. The ^{1}H and ^{13}C NMR spectra were recorded on a Bruker DPX 300 MHz FTNMR spectrometer using tetramethylsilane (TMS) as the internal standard. Steady state photolysis experiments were carried out using a 200 W high-pressure mercury lamp. Monochromatic light (intensity = 9.3 x 10^{-8} Einsteins min^{-1}) obtained by using a 320 nm or 360 nm band-pass filter was used for photolysis experiments. Nanosecond laser flash photolysis experiments were carried out by employing an Applied Photophysics Model LKS-20 laser kinetic spectrometer using GCR-12 series Quanta Ray Nd:YAG laser. The third harmonic of the laser (355 nm, 60mJ /pulse, pulse width 10 ns) was used for exciting the azo compounds.

2.4.1. Materials

Reagent grade reactants and solvents were used as received from suppliers. Extremely dry solvents were prepared as per standard procedures. Spectroscopic grade solvents were used for all measurements.

2.4.2. 4-Hydroxyphenyl,4'-azopyridine (2)

To an aqueous concentrated hydrochloric acid solution of 4-aminopyridine (2g. 20 mmol), a 20% aqueous sodium nitrite solution was added at −5 °C, followed by the addition of phenol (1.88 g, 20 mmol) in sodium hydroxide (10%, aqueous solution). The precipitate obtained was recrystallized from ethyl acetate to give 2.4 g (62%) of the compound, mp. 268 °C (dec.).

IR v_{max} (KBr): 3106, 2597, 2377, 1707, 1588, 1409 cm^{-1}; UV λ_{max} (toluene): 347 nm (ε = 2,844 M^{-1}cm^{-1}); ^{1}H NMR (300 MHz, DMSOd$_6$): δ 6.9 (2H, d, aromatic), 7.6 (2H, d, aromatic), 7.8 (2H, d, aromatic), 8.7 (2H, d, aromatic), 10.6 (1H, s, phenolic); ^{13}C NMR (75 MHz, DMSOd$_6$): δ 116.32, 116.73, 126.33, 145.79, 151.85, 157.37, 162.85.

2.4.3. General Procedure for the Preparation of 4-*n*-Alkyloxyphenyl,4'-azopyridine (3a-e)

4-Hydroxyphenyl,4'-azopyridine (2), *n*-alkyl bromide and sodium hydroxide were dissolved in dimethylformamide and the reaction mixture was heated at 100 °C

for 24 h. It was cooled to room temperature and added to water and extracted with benzene. The solvent was evaporated and the compound was purified by column chromatography using benzene as eluent. The compound was recrystallized from a mixture of ethyl acetate and petroleum ether (1:19), to give a pure sample.

4-*n*-Butyloxyphenyl,4'-azopyridine (3a)

Mp. 82 °C (yield 60%); IR ν_{max} (KBr): 2963, 2934, 1598, 1463, 1402, 1311, 1266, 1140, 1068, 973, 830 cm^{-1}; UV λ_{max} (toluene): 360 nm (ε = 20,287 M^{-1}cm^{-1}); ^{1}H NMR (300 MHz, CDCl$_3$): δ 0.9 (3H, t, CH$_3$), 1.4-1.5 (2H, m, OCH$_2$-CH$_2$-CH$_2$), 1.7-1.8 (2H, m, OCH$_2$-CH$_2$), 4.0 (2H, t, OCH$_2$), 7.0 (2H, d, aromatic), 7.7 (2H, d, aromatic), 8.0 (2H, d, aromatic), 8.8 (2H, d, aromatic); ^{13}C NMR (75 MHz, CDCl$_3$): δ 13.79, 19.18, 31.14, 68.16, 114.84, 116.14, 125.57, 146.65 151.15, 157.72, 163.46.

4-*n*-Hexyloxyphenyl,4'-azopyridine (3b)

Mp. 57 °C (yield 62%); IR ν_{max} (KBr): 2935, 2868, 1604, 1467, 1404, 1312, 1259, 1140, 1025, 841cm^{-1}; UV λ_{max} (toluene): 360 nm (ε = 21,620 M^{-1}cm^{-1}); ^{1}H NMR (300 MHz, CDCl$_3$): δ 0.9 (3H, t, CH$_3$), 1.4-1.5 (6H, m, OCH$_2$-CH$_2$-CH$_2$), 1.7-1.8 (2H, m, OCH$_2$-CH$_2$), 4.0 (2H, t, OCH$_2$), 7.0 (2H, d, aromatic), 7.7 (2H, d, aromatic), 8.0 (2H, d, aromatic), 8.8 (2H, d, aromatic); ^{13}C NMR

(75 MHz. CDCl₃): δ 14.01, 22.57, 25.65, 29.68, 31.53, 68.50, 114.86, 116.14, 125.58, 146.68, 151.20, 157.46, 162.90.

4-*n*-Octyloxyphenyl,4'-azopyridine (3c)

Mp. 67 °C (yield 66%); IR v_{max} (KBr): 2932, 2864, 1599, 1471, 1414, 1320, 1261, 1137. 1017, 843 cm⁻¹; UV λ_{max} (toluene): 360 nm (ε = 19,258 M⁻¹cm⁻¹); ¹H NMR (300 MHz, CDCl₃): δ 0.9 (3H, t, CH₃), 1.4-1.5 (10H, m, OCH₂-CH₂-CH₂), 1.7-1.9 (2H, m. OCH₂-CH₂), 4.0 (2H, t, OCH₂), 7.0 (2H, d, aromatic), 7.7 (2H, d, aromatic), 8.0 (2H, d, aromatic), 8.8 (2H, d, aromatic); ¹³C NMR (75 MHz, CDCl₃): δ 14.15, 22.70, 26.04, 29.17, 29.27, 29.37, 31.84, 68.56, 114.92, 116.21, 125.64, 146.85, 151.23, 156.96, 162.79.

4-*n*-Decyloxyphenyl,4'-azopyridine (3d)

Mp. 63 °C (yield 64%); IR v_{max} (KBr): 2929, 2862, 1598, 1507, 1420, 1413, 1253, 1139, 1014, 841 cm⁻¹; UV λ_{max} (toluene): 360 nm (ε = 20,600 M⁻¹cm⁻¹); ¹H NMR (300 MHz, CDCl₃): δ 0.9 (3H, t, CH₃), 1.3-1.5 (14H, m, OCH₂-CH₂-CH₂), 1.7-1.9 (2H, m, OCH₂-CH₂), 4.0 (2H, t, OCH₂), 7.0 (2H, d, aromatic), 7.7 (2H, d, aromatic), 8.0 (2H, d, aromatic), 8.8 (2H, d, aromatic); ¹³C NMR (75 MHz, CDCl₃): δ 14.63, 23.18, 26.51, 29.64, 29.72, 29.85, 30.08, 30.13, 32.41, 68.89, 115.29, 116.66, 126.10, 147.18, 151.55, 157.45, 163.30.

4-*n*-Dodecyloxyphenyl,4'-azopyridine (3e)

Mp. 71 °C (yield 60%); IR v_{max} (KBr): 2927, 2856, 1597, 1497, 1468, 1409, 1313, 1253, 1139, 1006, 921, 844 cm^{-1}; UV λ_{max} (toluene): 360 nm (ε = 21,454 M^{-1}cm^{-1}); ^{1}H NMR (300 MHz, CDCl$_3$) δ 0.9 (3H, t, CH$_3$), 1.3-1.5 (18H, m, OCH$_2$-CH$_2$-CH$_2$), 1.7-1.9 (2H, m, OCH$_2$-CH$_2$), 4.0 (2H, t, OCH$_2$), 7.0 (2H, d, aromatic), 7.7 (2H, d, aromatic), 8.0 (2H, d, aromatic), 8.8 (2H, d, aromatic); ^{13}C NMR (75 MHz, CDCl$_3$): δ 14.56, 23.23, 26.51, 29.64, 29.70, 29.85, 29.95, 30.08, 30.15 30.23, 32.41, 68.89, 115.29, 116.66, 126.10, 147.17, 151.55, 157.89, 163.35.

2.4.4. 4-*n*-Alkyloxybenzoic acids (4a-e)

These compounds (4a-e) were prepared from 4-hydroxybenzoic acid by a reported procedure and characterized by spectral analyses and their phase transition temperatures. These acids exhibited the following phases.

4a (n = 4), K 147 N 160 I; 4b (n = 6), K 101 N 161 I; 4c (n = 8), K 101 S$_C$ 117 N 143 I; 4d (n = 10), K 97 S$_C$ 122 N 142 I; 4e (n = 12), K 95 S$_C$ 129 N 137 I.

2.4.5. General Procedure for the Preparation of 4-Pyridylazo,4'-phenyl-*n*-alkanoates (9a, b)

A mixture of 4-hydroxyphenyl,4'-azopyridine (2) and triethylamine was dissolved in dichloromethane. To this reaction mixture *n*-alkyl acid chloride was

added dropwise and heated at 40 °C for 36 h.. The reaction mixture was cooled to room temperature and added to cold water. It was extracted with dichloromethane. The organic layer was washed with sodium hydroxide (10%, aqueous). The solvent was evaporated off and the crude product was purified by column chromatography using a mixture of ethyl acetate and petroleum ether (1:19) as eluent to give a pure sample.

4-Pyridylazo,4'-phenyl-*n*-butanoate (9a)

Mp. 68 °C (yield 72%); IR ν_{max} (KBr): 2970, 2936, 1760, 1588, 1487, 1408, 1298, 1213, 1138, 930, 838 cm^{-1}; UV λ_{max} (toluene): 323 nm (ε = 12,027 M^{-1}cm^{-1}); ^{1}H NMR (300 MHz, CDCl$_3$): δ 0.9 (3H, t, CH$_3$), 1.7-1.8 (2H, m, CH$_2$-CH$_2$-CO), 2.5-2.6 (2H, t, CH$_2$-CO), 7.3-7.5 (2H, d, aromatic), 7.7 (2H, d, aromatic), 8.0 (2H, d, aromatic), 8.8 (2H, d, aromatic); ^{13}C NMR (75 MHz, CDCl$_3$): δ 13.61, 18.37, 36.23, 116.47, 122.49, 124.79, 150.76, 154.03.

4-Pyridylazo,4'-phenyl-*n*-tetradecanoate (9b)

Mp. 86 °C (72%); IR ν_{max} (KBr): 2924, 2858, 1755, 1587, 1487, 1409, 1220, 1150, 925, 848 cm^{-1}; UV λ_{max} (toluene): 323 nm (ε = 16,353 M^{-1}cm^{-1}); ^{1}H NMR (300 MHz, CDCl$_3$): δ 0.9 (3H, t, CH$_3$), 1.2-1.4 (20H, m, CH$_2$-CH$_2$-CH$_2$-CO),

1.7-1.8 (2H, m, CH$_2$-CH$_2$-CO) 2.5-2.6 (2H, t, CH$_2$-CO), 7.3-7.5 (2H, d, aromatic), 7.7 (2H, d, aromatic), 8.0 (2H, d, aromatic), 8.8 (2H, d, aromatic); ^{13}C NMR (75 MHz, CDCl$_3$): δ 14.10, 22.67, 24.83, 29.07, 29.22, 29.33, 29.42, 29.57, 29.62, 29.66, 31.90, 34.41, 116.88, 122.56, 124.97, 149.82, 154.32, 157.97, 171.77.

2.4.5. Preparation of 4,4'-Azobipyridine (11)

To a cold aqueous solution of 4-aminopyridine (1g, 10 mmol), dissolved in water (5 mL), sodium hypochlorite solution (4%, 100 mL) was added dropwise over a period of 45 min, maintaining the temperature at 5-10 °C range. The compound that precipitated was filtered and washed with cold water. The filtrate was extracted with ether and the ether layer was concentrated. The solid material obtained was recrystallized from hexane to give 0.8 g (44%) of 11, mp. 104 °C.

IR ν$_{max}$ (KBr): 1595, 1571, 1417, 1225, 835 cm^{-1}; UV λ$_{max}$ (toluene): 270 nm (ε = 16,000 M^{-1}cm^{-1}); ^{1}H NMR (300 MHz, CDCl$_3$): δ 7.6-7.8 (4H, d, aromatic), 8.8-9.0 (4H, d, aromatic); ^{13}C NMR (75 MHz, CDCl$_3$): δ 151.00, 116.29.

2.5. Conclusions

Hydrogen bonded mesomorphic materials were prepared from azopyridine containing hydrogen bond acceptors (**3a-e**, **9a**, **b** and **11**) with hydrogen bond donors such as 4-*n*-alkyloxybenzoic acids. These supramolecular materials (**5a-e**, **10a-j** and **12a-e**) exhibit LC properties over a range of temperatures. Binary phase diagram analysis of the representative examples of hydrogen bond donors and acceptors in each series confirmed the selective formation of a novel supramolecular material at stoichiometric ratio. The effect of the photochromic behaviour of the azo moiety, present in these systems, on the LC properties of the hydrogen bonded assemblies was also examined. The supramolecular assembly formed between 4,4'-azobipyridine and 4-*n*-dodecyloxybenzoic acid showed a marked change in its LC properties after photolysis with UV light. Similar effects were not observed for the hydrogen bonded assemblies of other azopyridyl moieties. This can be attributed to the rapid *cis-trans* isomerization of the azo derivative. The effect of hydrogen bonding on the rate of thermal isomerization of azopyridyl derivatives was examined. The rate constant of *cis-trans* isomerization increases with increase in the hydrogen bonding strength of the solvent.

2.6. References

1. M. Emmelius, G. Pawlowski, H. W. Vollman, *Angew. Chem. Int. Ed. Engl.* **1989**, *28*, 1445.

2. I. Cabrera, M. Engel, L. Haübling, C. Mertisdorf, H. Ringsdorf, *Photoinduced Structural Changes in Organized Supramolecular Systems: Frontiers in Supramolecular Organic Chemistry and Photochemistry* (Ed.: H. Schneider, H. Dürr), Weinheim, New York, **1991**.

3. H. Ringsdorf, I. Carbrera, A. Dittrich, *Angew. Chem. Int. Ed. Engl.* **1991**, *30*, 76.

4. M. Suarez, G. B. Schuster, *J. Am. Chem. Soc.* **1995**, *117*, 6732.

5. M. Zhang, G. B. Schuster, *J. Org. Chem.* **1994**, *59*, 1855.

6. T. Ikeda, O. Tsutsumi, *Science* **1995**, *268*, 1873.

7. K. Ichimura, *Chem. Rev.* **2000**, *100*, 1847.

8. Y. Lansac, M. A. Glaser, N. A. Clark, O. D. Lavrentovich, *Nature* **1999**, *398*, 54.

9. S. Kurihara, T. Ikeda, S. Tazuke, *Jpn. J. Appl. Phys.* **1988**, *22*, L1791.

10. S. Kurihara, T. Ikeda, T. Sasaki, H-B. Kim, S. Tazuke, *J. Chem. Soc. Chem. Commun.* **1990**, 1751.

11. T. Ikeda, S. Kurihara, D. B. Karanjit, S. Tazuke, *Macromolecules* **1990**, *23*, 3938.

12. T. Ikeda, S. Horiuchi, D. B. Karanjit, S. Kurihara, S. Tazuke, *Macromolecules* **1990**, *23*, 36.

13. T. Ikeda, S. Horiuchi, D. B. Karanjit, S. Kurihara, S. Tazuke, *Macromolecules* **1990**, *23*, 42.

14. T. Ikeda, T. Miyamoto, S. Kurihara, M. Tsukada, S. Tazuke, *Mol. Cryst. Liq. Cryst.* **1990**, *182B*, 357.

15. T. Ikeda, T. Sasaki, H-B. Kim, *J. Phys. Chem.* **1991**, *95*, 509.

16. S. Kurihara, T. Ikeda, T. Sasaki, H-B. Kim, S. Tazuke, *Mol. Cryst. Liq. Cryst.* **1991**, *195*, 251.

17. T. Sasaki, T. Ikeda, K. Ichimura, *Macromolecules* **1992**, *25*, 3807.

18. T. Ikeda, T. Sasaki, K. Ichimura, *Nature* **1993**, *361*, 428.

19. T. Sasaki, T. Ikeda, K. Ichimura, *Macromolecules* **1993**, *26*, 151.

20. T. Sasaki, T. Ikeda, K. Ichimura, *J. Am. Chem. Soc.* **1994**, *116*, 625.

21. T. Sasaki, T. Ikeda, *J. Phys. Chem.* **1995**, *99*, 13002.

22. T. Sasaki, T. Ikeda, *J. Phys. Chem.* **1995**, *99*, 13008.

23. T. Sasaki, T. Ikeda, *J. Phys. Chem.* **1995**, *99*, 13013.

24. M. Negishi, O. Tsutsumi, T. Ikeda, T. Hiyama, J. Kawamura, M. Aizawa, S. Takehara, *Chem. Lett.* **1996**, 319.

25. M. Negishi, K. Kanie, T. Ikeda, T. Hiyama, *Chem. Lett.* **1996**, 583.

26. A. Shishido, O. Tsutsumi, A. Kanazawa, T. Shiono, T. Ikeda, N. Tamai, *J. Am. Chem. Soc.* **1997**, *119*, 7791.

27. O. Tsutsumi, T. Shiono, T. Ikeda, G. Galli, *J. Phys. Chem. B* **1997**, *101*, 1332.

28. A. Shishido, O. Tsutsumi, A. Kanazawa, T. Shiono, T. Ikeda, *J. Phys. Chem. B* **1997**, *101*, 2806.

29. A. Kanazawa, S. Hirano, A. Shishido, M. Hasegawa, O. Tsutsumi, T. Shiono, T. Ikeda, Y. Nagase, E. Akiyama, Y. Takamura, *Liq. Cryst.* **1997**, *23*, 293.

30. O. Tsutsumi, Y. Demachi, A. Kanazawa, T. Shiono, T. Ikeda, Y. Nagase, *J. Phys. Chem. B* **1998**, *102*, 2869.

31. Y. Wu, Y. Demachi, O. Tsutsumi, A. Kanazawa, T. Shiono, T. Ikeda, *Macromolecules* **1998**, *31*, 4457.

32. Y. Wu, Y. Demachi, O. Tsutsumi, A. Kanazawa, T. Shiono, T. Ikeda, *Macromolecules* **1998**, *31*, 1104.

33. Y. Yu, Y. Demachi, O. Tsutsumi, A. Kanazawa, T. Shiono, T. Ikeda, *Macromolecules* **1998**, *31*, 349.

34. S. Ogiri, A. Kanazawa, T. Shiono, T. Ikeda, *Macromolecules* **1998**, *31*, 1728.

35. O. Tsutsumi, T. Kitsunai, A. Kanazawa, T. Shiono, T. Ikeda, *Macromolecules* **1998**, *31*, 355.

36. Y. Wu, T. Ikeda, Q. Zhang, *Adv. Maer.* **1999**, *11*, 300.

37. S. Ogiri, H. Nakamura, A. Kanazawa, T. Shiono, T. Ikeda, *Macromolecules* **1999**, *32*, 4806.

38. T. Yamamoto, M. Hasegawa, A. Kanazawa, T. Shiono, T. Ikeda, *J. Phys. Chem. B* **1999**, *103*, 9873.

39. Y. Wu, J. Mamiya, A. Kanazawa, T. Shiono, T. Ikeda, Q. Zhang, *Macromolecules* **1999**, *32*, 8829.

40. Y. Wu, Q. Zhang, A. Kanazawa, T. Shiono, T. Ikeda, Y. Nagase, *Macromolecules* **1999**, *32*, 3951.

41. H-K. Lee, K. Doi, A. Kanazawa, T. Shiono, T. Ikeda, T. Fujisawa, M. Aizawa, B. Lee, *Polymer* **2000**, *41*, 1757.

42. T. Yamamoto, M. Hasegawa, A. Kanazawa, T. Shiono, T. Ikeda, *J. Mater. Chem.* **2000**, *10*, 337.

43. A. Kanazawa, T. Ikeda, J. Abe, *Angew. Chem. Int. Ed. Engl.* **2000**, *39*, 612.

44. B. Bahadur, *Liquid Crystals-Applications and Uses*, (*Vol. 1-3)*, World Scientific, Singapore, **1995**,

45. C. M. Paleos, D. Tsiourvas, *Angew. Chem. Int. Ed. Engl.* **1995**, *34*, 1696.

46. T. Kato, J. M. J. Frechet, *Macromolecules* **1989**, *22*, 3818.

47. T. Kato. J. M. J. Frechet, *J. Am. Chem. Soc.* **1989**, *111*, 8533.

48. T. Kato, P. G. Wilson, A. Fujishima, J. M. J. Frechet, *Chem. Lett.* **1990**, 2003.

49. T. Kato, H. Kihara, U. Kumar, A. Fujishima, T. Uryu, J. M. J. Frechet, *Polym. Prepr.* **1993**, *34*, 722.

50. T. Kato, H. Kihara, U. Kumar, T. Uryu, J. M. J. Frechet, *Angew. Chem. Int. Ed. Engl.* **1994**, *33*, 1644.

51. T. Kato, H. Kihara, S. Ujiie, T. Uryu, J. M. J. Frechet, *Macromolecules* **1996**, *29*, 8734.

52. T. Kato, Y. Kubota, T. Uryu, S. Ujiie, *Angew. Chem. Int. Ed. Engl.* **1997**, *36*, 1617.

53. T. Kato, G. Kondo, D. Hanabusa, *Chem. Lett.* **1998**, 193.

54. H. Kihara, T. Kato, Y. Uryu, S. Ujiie, U. Kumar, J. M. J. Frechet, D. W. Bruce, D. J. Price, *Liq. Cryst.* **1996**, *21*, 25.

55. R. Kleppinger, C. P. Lillya, C. Yang, *Angew. Chem. Int. Ed. Engl.* **1995**, *34*, 1637.

56. R. Kleppinger, C. P. Lillya, C. Yang, *J. Am. Chem. Soc.* **1997**, *119*, 4097.

57. A. Kraft, A. Reichert, R. Kleppinger, *Chem. Commun.* **2000**, 1015.

58. H. Kreese, I. Szulzewski, P. Mandt, R. Frach, *Mol. Cryst. Liq. Cryst.* **1994**, 257, 19.

59. U. Kumar, J. M. J. Frechet, T. Kato, S. Ujiie, K. Timura, *Angew. Chem. Int. Ed. Engl.* **1992**, *31*, 1531.

60. V. A. Mallia, M. George, S. Das, *Chem. Mater.* **1999**, *11*, 207.

61. G. W. Gray, B. Jones, *J. Chem. Soc.* **1953**, 4179.

62. G. W. Gray, B. Jones, *J. Chem. Soc.* **1954**, 1467.

63. Z. Sideratou, C. M. Paleos, *Mol. Cryst. Liq. Cryst.* **1995**, *265*, 19.

64. D. Demus, L. Richter, *Texture of Liquid Crystals*, Weinheim, New York, **1978**.

65. H. Kelker, R. Hatz, *Handbook of Liquid Crystals*, Verlag Chemie, Weinheim, **1980**.

66. H. Bernhardt, W. Weissflog, H. Kreese, *Angew. Chem. Int. Ed. Engl.* **1996**, *35*, 874.

67. S. L. Johnson, K. A. Rumon, *J. Phys. Chem.* **1965**, *69*, 74.

68. S. E. Odinokov, A. A. Mashkovsky, V. P. Glazunov, A. V. Iogansen, B. V. Rassadin, *Spectrochemica Acta* **1976**, *32A*, 1355.

69. T. Asano, T. Okada, *J. Org. Chem.* **1984**, *49*, 4387.

70. E. V. Brown, G. R. Granneman, *J. Am. Chem. Soc.* **1975**, *97*, 621.

CHAPTER 3

SYNTHESIS AND STUDIES OF SOME CHOLESTEROL CONTAINING HYDROGEN BONDED SUPRAMOLECULAR MESOGENS

3.1. Abstract

Supramolecular hydrogen bonded liquid crystalline (LC) materials containing cholesterol groups have been synthesized and characterized. These assemblies were prepared by complexing cholest-5-en-3-ol-(3β)[4-phenyl,4'-pyridylazo]carbonate (4) with a series of hydrogen bond donors such as 4-*n*-alkyloxybenzoic acids (5a-e) and 4-*n*-alkyloxycinnamic acids (9a-e). These heterointermolecular hydrogen bonded complexes (6a-e, 10a-e) exhibit LC phases, which were confirmed using POM and DSC. Binary phase diagram of mixtures of the hydrogen bond donor and acceptor indicate the formation of pure intermolecular hydrogen bonded assemblies in 50 mol% mixtures. Attempts were also made to preserve the cholesteric super-structure pitch in the solid state of the cholesteric LCs. This has been achieved by sudden cooling of the complexes (10a-d) from their cholesteric phase temperatures to 0 °C. The glassy

phases thus formed show the characteristic iridescent colours of cholesteric LCs. These glasses are highly stable at room temperature and their colours could be erased by heating the films above the LC temperatures of the respective assemblies. Photochemical and thermal isomerization of cholest-5-en-3-ol-(3β)[4-phenyl,4'-pyridylazo]carbonate (**4**) have also been investigated. In protic solvents the rate of the thermal *cis-trans* isomerization was observed to increase with the hydrogen bonding ability of the solvent.

3.2. Introduction

Cholesteric colours have fascinated people since the discovery of cholesteric LCs by F. Reinzer in 1888.[1] The unique optical properties of cholesteric phases are due to the presence of a helical super-structure. Classically, isotropic liquids containing chiral molecules, e.g., sugar solutions, are described as optically active, since the right- and left-handed components of plane polarized light propagate at different velocities, causing the plane of propagation of the emerging beam to be rotated. These properties are often referred to as circular birefringence and give rise to rotations of about 10 °/mm. In the case of cholesteric LCs, there is therefore a two-fold optical activity: (i) molecular and (ii) macromolecular, associated with the helical super-structure (Figure 3.1.). When plane polarized light propagates through this structure its right-handed and

left-handed components see different refractive indices, resulting in phase retardation between them and rotation of the plane of the polarized light. The important difference compared to optical rotation in solutions containing optically active materials is that the rotation is much greater in cholesteric LCs (~ 1000 °/mm).

A unique feature of the helical structure is the selective light reflection, which is the origin of brilliant colours that are displayed under certain conditions. The reflected wavelength (Figure 3.1.) is related to the pitch length (p) and refractive index (n) of the film as shown in equation 3.1.

$$\lambda = n\, p \, \cos\theta \qquad\qquad \textbf{3.1.}$$

pitch length (p),
$360°$ rotation
of director
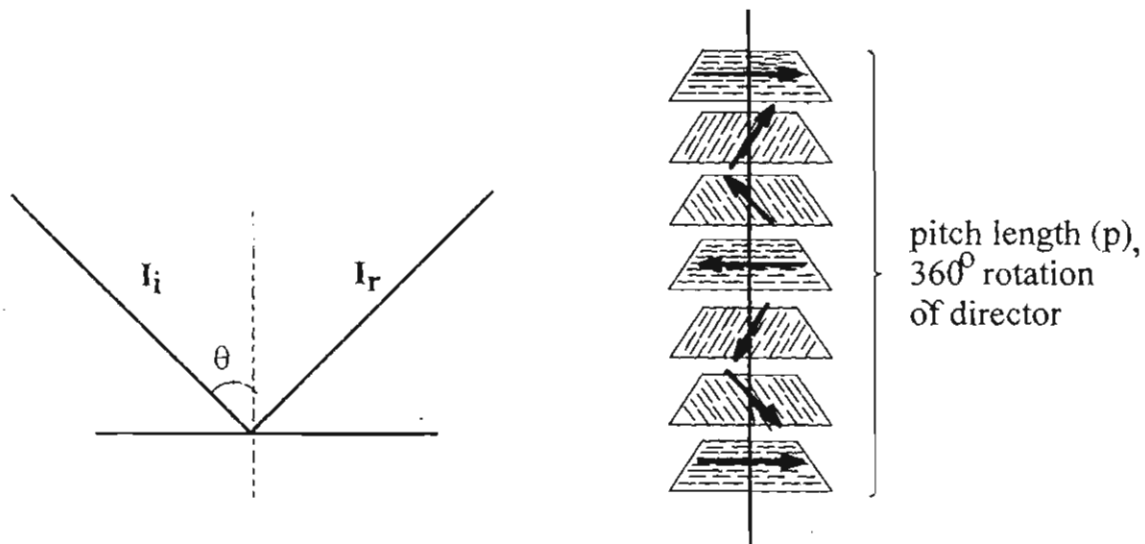
Figure 3.1.

This selective reflection is analogous to Bragg X-ray diffraction.[2,3] This can be explained by considering Figure 3.1. Each layer represents the orientation of director. Therefore for each layer or sheet, two refractive indices may be defined; namely n_c which is parallel to the director and n_o which is right angles to it in the same plane. If a plane polarized beam with nearly the same wavelength as the pitch of the helix and plane of polarization parallel to the director, is incident on a cholesteric LC film with a right handed helix, then the left circularly polarized component will be transmitted, seeing some average refractive index. However the right circularly polarized component will see a sinusoidal variation in refractive index along the helix axis with n_c repeat at every 180° rotation or $p/2$ spacing and be scattered. The scattered light from each $p/2$ plane constructively interferes and is reflected as right handed circularly polarized light, whose wavelength is given by equation 3.2.

$$\lambda = n_c p \qquad\qquad \textbf{3.2.}$$

By the same process, incident plane polarized light with its plane orthogonal to the director will have 50% of its intensity reflected at a wavelength given by equation 3.3.

$$\lambda' = n_o p \qquad\qquad \textbf{3.3.}$$

When ordinary white light is incident on the helix, all wavelengths between λ and λ' is reflected and the bandwidth is given by equation 3.4.

$$\Delta\lambda = p(n_c - n_o) \qquad \qquad \textbf{3.4.}$$

where,

$$n = n_c - n_o \qquad \qquad \textbf{3.5.}$$

As a consequence of this circular dichroism cholesteric LCs show an anomalous dispersion in their rotatory power at the selective reflection wavelength. This is analogous to the Cotton effect shown by optically active isotropic liquids containing a chromophore.[4]

The pitch (*p*) of cholesteric LCs is sensitive to weak external physical perturbations such as temperature, pressure, electrical and magnetic fields,[5-7] as well as to dissolved molecules. Fergason has reported on the colour change of cholesteric phases induced by traces of dissolved gases.[8,9] In the late 1960's, Haas *et al.* reported a change in the selective reflectivity of the cholesteric LC mixture composed of cholesteryl bromide and other cholesteryl derivatives on photolysis.[10] This change in the reflectivity arose from a change in the helical pitch of the cholesteric LC resulting from the photochemical reaction of cholesteryl bromide in the LC mixture.[11] They also observed that photolysis with UV light of LC cells

containing mesogens with stilbene units in the molecules brought about *trans-cis* isomerization of the stilbene units, causing simultaneously a nematic (N) to isotropic (I) phase transition of the host LC. Irreversible change in the selective reflectivity of cholesteric pitch was also reported by Haas *et al.*.[11] Reversible photoinduced changes in the reflectance band (> 100 nm) have been recently reported in the eutectic mixtures of cholesteric liquid crystals containing chiral azobenzene derivatives.[12,13]

In most pure cholesteric materials, the pitch is a decreasing function of temperature. An elementary picture of the temperature dependence of the pitch can be given in analogy with the theory of thermal expansion in crystals.[14] The strong temperature dependence of the pitch has practical applications in thermography, as was first demonstrated by Fergason.[8,15] The material has to be so chosen that the pitch (p) is of the order of the wavelength of visible light in the temperature range of interest. This is achieved by preparing suitable mixtures. Small variations of temperature are shown up as changes in the colour of the scattered light and this phenomenon can be used for a number of applications such as measurement and visual display of surface temperatures,[16,17] as well as imaging of infrared[18,19] and microwave patterns.[20]

Pollmann and Stegemeyer investigated the effect of pressure on the pitch of cholesteryl oleyl carbonate (COC) mixed with cholesteryl chloride and found that the pitch increases very rapidly with pressure,[6] the effect being more pronounced, the greater the concentration of COC. This is attributed to the increase in the transition temperature with increasing pressure,[21-23] causing the pitch at room temperature to rise accordingly.

The dependence of pitch on composition was first described by Friedel.[24] For a given composition there is an inversion of the rotatory power as the temperature is varied, indicating a change in the handedness of the helix. The inverse pitch exhibits a linear dependence on temperature, passing through zero at the nematic point where there is an exact compensation of the right- and left-handed forms. A similar reversal of handedness takes place as the composition is varied.[25] The inverse pitch shows a linear relationship with composition around the nematic point, but there are significant departures when one of the components has a smectic phase at a lower temperature.[26] It is well known that a nematic LC readily adopts a helical configuration if a small amount of a cholesteric is added to it. For low concentrations of the cholesteric, the inverse pitch is a linear function of the concentration, but at higher concentrations, the linear law is not obeyed.[27] A small quantity of a non-mesomorphic optically active compound may also

transform a nematic into a cholesteric.[28] However, the handedness of the helix does not seem to be directly related to the absolute configuration of the solute as has been shown by Saeva.[29]

The specific colour displayed by cholesteric LC films disappear on solidification due to crystallization. Solid materials wherein the helical super-structure of cholesteric LCs has been maintained can be obtained however by inducing polymerization in the cholesteric phase. Polymeric solid materials, in which the super-structure of cholesteric phase is fixed, display the characteristic iridescent colours of cholesterics. However, these colours are generally insensitive to external influences such as pressure and temperature.[30] The high viscosity of the three-dimensional networks of polymer chains practically fixes the pitch of the helical configuration of polymers.[31-34] It has been also shown that the colours of such solids can be tuned by changing the monomer ratio in the copolymers, by changing the temperature of photopolymerization reaction. It is however not possible to obtain colour switching using such polymeric materials. Such reversible and fast switching is essential for developing rewritable full colour recording devices. Tamaoki *et al.*,[35-37] have shown recently that glasses obtained from low molecular weight cholesterol derivatives (Chart 3.1.) exhibit stable and rapidly changeable colours of cholesteric films in the solid state (Figure 3.2.).

Coloured images can be recorded and erased repeatedly on such films by thermal
and photochemical treatment.
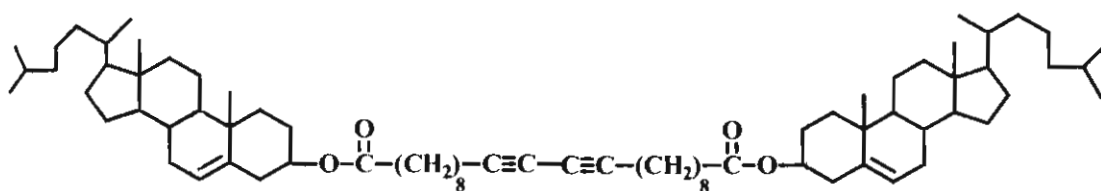
1

Chart 3.1.
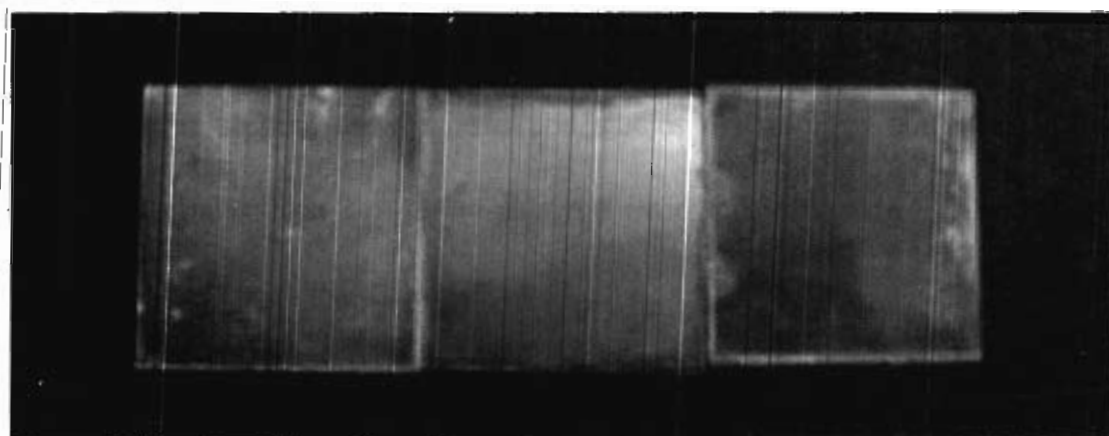
Figure 3.2. Photographs of cholesteric solid films prepared by Tamaoki et al.[35]

Non-covalent interactions, such as hydrogen bonding between molecular species
have been advantageously used in recent years to develop a large variety of LCs.
Formation cholesteric GLCs from hydrogen bonded polymeric materials have been
reported.[12] However, cholesteric GLCs of low molecular weight hetero-
intermolecular hydrogen bonded LCs have not been reported. In this Chapter the

preparation and characterization of hydrogen bonded cholesteric LCs *via* heterointermolecular hydrogen bonding of acids such as 4-*n*-alkyloxybenzoic acids (**5a-e**)[38] as well as 4-*n*-alkyloxycinnamic acids (**9a-e**)[39] with a hydrogen bond acceptor such as cholest-5-en-3-ol-(3β)[4-phenyl,4'-pyridylazo]carbonate (**4**), are described. The ability of these materials to form glassy solids wherein the cholesteric super-structure is maintained has also been explored.

3.3. Results and Discussion

3.3.1. Hydrogen Bonded Assemblies of Cholest-5-en-3-ol-(3β)[4-phenyl-pyridylazo]carbonate (4) with 4-*n*-Alkyloxybenzoic Acids (5a-e)

In this section, the synthesis and studies of hydrogen bonded LCs formed between cholest-5-en-3-ol-(3*β*)[4-phenyl,4'-pyridylazo]carbonate (**4**) and 4-*n*-alkyloxybenzoic acids (**5a-e**) are described.

3.3.1.1. Synthesis and Characterization

Cholest-5-en-3-ol-(3*β*)[4-phenyl,4'-pyridylazo]carbonate (**4**) was synthesized by refluxing cholesteryl chloroformate and 4-hydroxyphenylazopyridine (**2**) in a mixture (1:1) of methanol and chloroform (Scheme 3.1.).

All compounds were characterized on the basis of spectral data and the details are provided in the Experimental Section (3.4.). The hydrogen bonded complexes were synthesized by mixing equimolar quantities of **4** and 4-*n*-alkyloxybenzoic acids

thoroughly above the melting point of the mixtures for a few minutes. The mixture in

each case was then allowed to cool slowly to yield the LC materials **6a-e**.[40-44]

6a-e

a, R = C_4H_9	d, R = $C_{10}H_{21}$
b, R = C_6H_{13}	e, R = $C_{12}H_{25}$
c, R = C_8H_{17}	
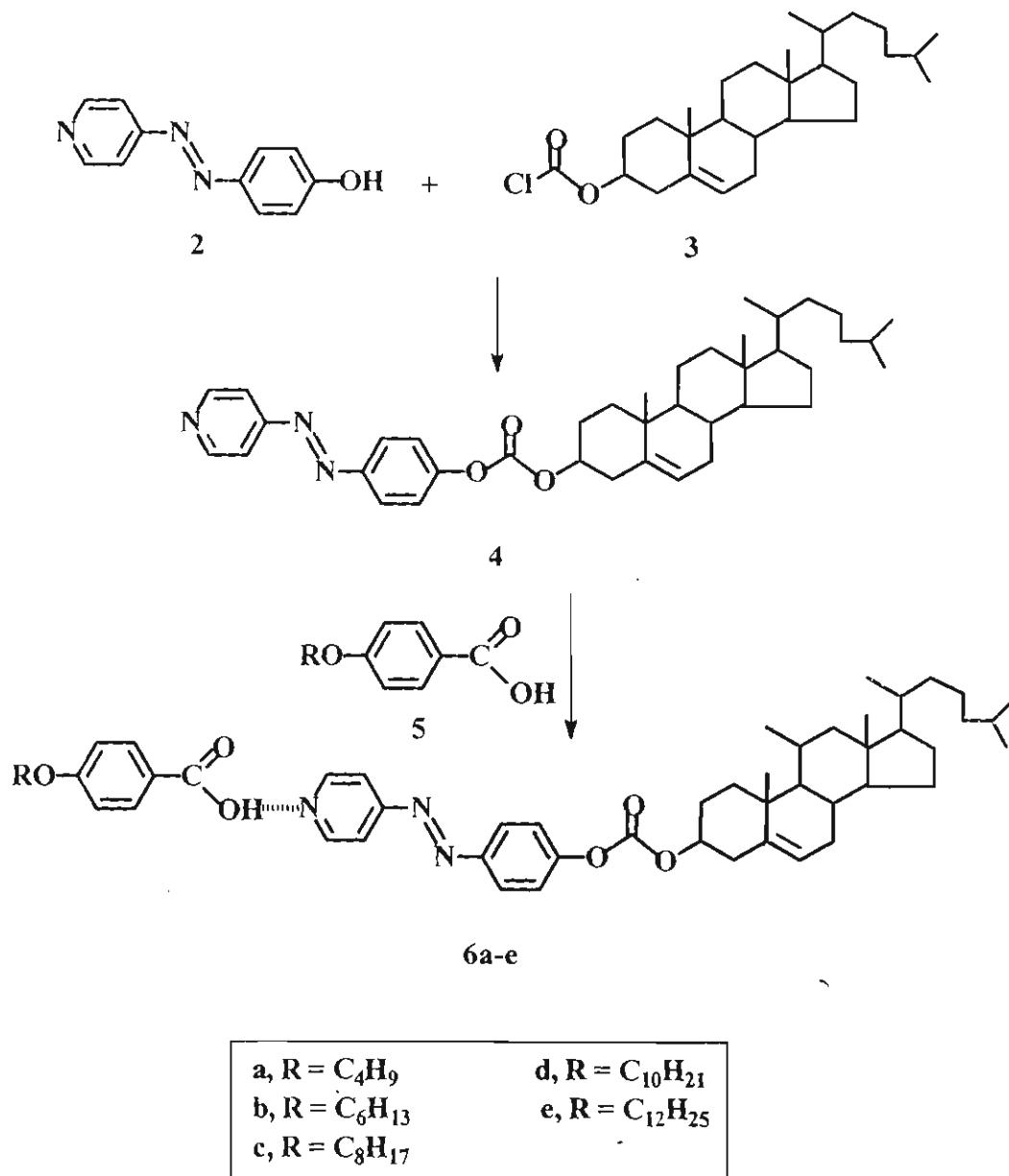
Scheme 3.1.

3.3.1.2. Liquid Crystalline Properties

LC properties of the complexes studied by POM and SAXRD confirm the selective formation of the hydrogen bonded mesogens **6a-e** shown in Scheme 3.1. All the complexes behave as single LC materials and show clear phase transitions. The thermal properties of the complexes are different from those of the individual components. All these supramolecular hydrogen bonded assemblies exhibit S_A LC phase in the heating as well as cooling cycles, which were confirmed from their fan like textures (Figure 3.3.).[45] Phase transition temperatures for the heating and cooling cycles are shown in Table 3.1.

Figure 3.3. Optical photomicrograph of smectic A phase of the hydrogen bonded complex 6a at 170 °C obtained in the cooling cycle.

Table 3.1. Phase transition temperatures of 6a-e.

Compound	Phase transition temperature, °C†	
	Heating	Cooling
6a	K 175.6 S_A 185.6 I	I 185.5 S_A 154.2 K
6b	K 109.9 S_A 158.4 I	I 157.2 S_A 91.2 K
6c	K 108 S_A 155 I	I 155 S_A 108 K
6d	K 109 S_A 144 I	I 140 S_A 70 K
6e	K 130 S_A162 I	I 155 S_A 120 K

†K = crystalline, S_A = smectic A and I = isotropic phase.

The dependence of phase transition temperatures of the complexes on alkyl chain length is shown in Figure 3.4. The temperature range of LC phase was maximum for the complexes with n = 4-6. The observed dependence of the transition points on the length of the alkyl chain (Figure 3.4.) is similar to that reported for well-known smectics.[46] Similar dependence was also reported for smectic liquid crystals generated *via* hydrogen bonding between bipyridyl and 4-*n*-alkyloxybenzoic acids.[40]
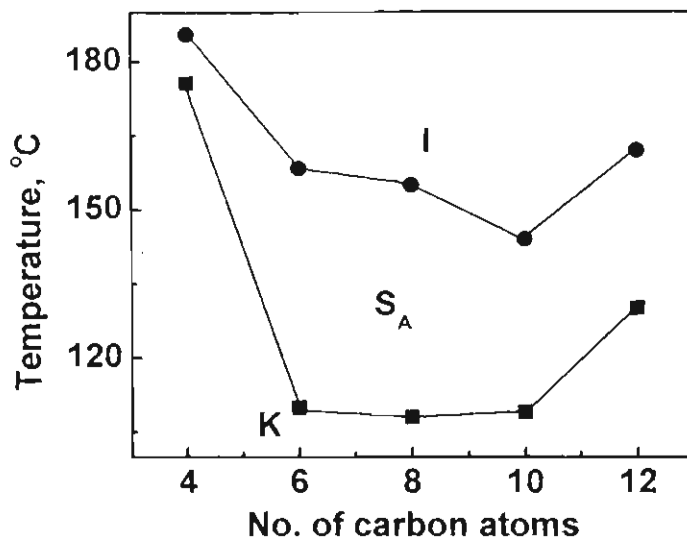
Figure 3.4. Plot of transition temperature against the number of carbon atoms (n) in the alkyl chain for the 1:1 hydrogen bonded complexes, 6a-e.

The S_A phase of compound 6c was also confirmed by X-ray diffraction. Diffraction pattern of 6c at 140 °C showed a sharp ring at 36.7 Å associated with its molecular smectic layers. The length of the supramolecular assembly (6c) in its all *trans* conformation is 37.5 Å (calculated using PC-Spartan software obtained from Wavefunction, Inc., USA, 18401). The slight decrease in the layer spacing may be attributed to the folding of the alkyl chain from its all *trans* conformation. The diffraction pattern also shows a diffused ring at 5.6 Å due to the lateral liquid like correlation of molecules within the layers. The layer spacings were the same at 150 °C.

The O-H bands around 2581 and 1950 cm^{-1} observed for the complexes in the IR spectra are indicative of strong hydrogen bonding.[47,48] These bands replace the O-H band around 3000 cm^{-1}, observed for the weakly hydrogen bonded acid dimers in the pure acid. The absence of the 3000 cm^{-1} band is clearly indicative of the formation of pure 1:1 hydrogen bonded complexes in the 50% mixtures. Compounds mixed at ratios other than 1:1, such as in a mixture containing 30 mol% of **4**, both the O-H bands around 2500 and 1920 cm^{-1} as well as around 3000 cm^{-1} were observed. This is indicative of the coexistence of the hydrogen bonded assemblies with weakly hydrogen bonded dimers.

3.3.1.3. Thermal Properties of the Binary Mixtures of 4 and 5e

The LC properties of the binary mixtures of **4** and **5e** were examined by POM using a heating/cooling rate of 5 °Cmin^{-1}. The binary mixtures containing 10-20 mol% of **4** showed a broken fan texture and a fine four-brush schlieren texture,[45] which clearly indicates the presence of a S$_C$ phase. The focal conic texture observed in 30-60 mol% mixtures confirms the formation of a S$_A$ phase. It is important to note that in all binary mixtures other than 50 mol%, the LC phase coexists with a crystalline phase or an isotropic melt. Additional evidence for the formation of a pure LC material by supramolecular hydrogen bonding in the 50% mixture is provided by the existence of two eutectic points observed for the 30 and

60 mol% mixtures (Figure 3.5.). The melting maximum observed at equimolar mixture also confirms the formation of a pure material.
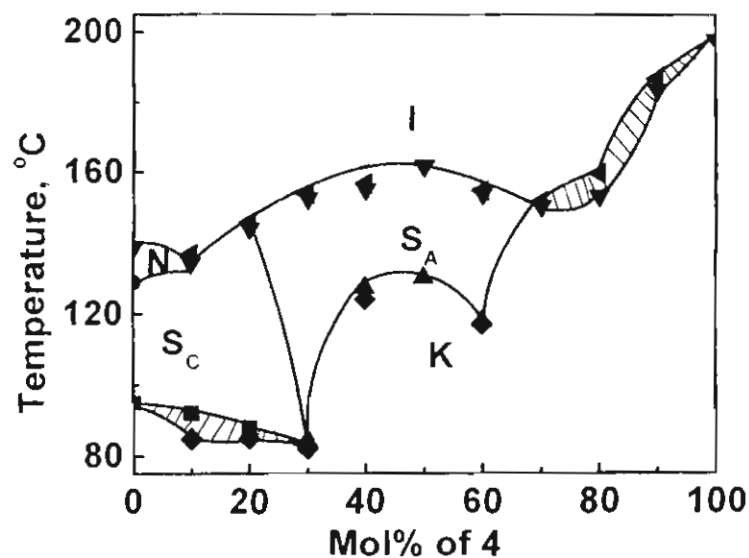
Figure 3.5. **The binary phase diagram of mixtures 4 and 4-*n*-dodecyloxybenzoic acid (shaded regions indicate coexistence of crystal and LC phases or crystal and isotropic phases).**

3.3.2. Hydrogen Bonded Assemblies of Cholest-5-en-3-ol-(3β)|4-phenyl,4'-pyridylazo|carbonate (4) with 4-*n*-Alkyloxycinnamic Acids (9a-e)

The supramolecular hydrogen bonded assemblies formed between cholest-5-en-3-ol-(3β)[4-phenyl,4'-pyridylazo]carbonate **(4)** and 4-*n*-alkyloxybenzoic acids **(5a-e)** did not show chiral mesophases. To study the effect of cinnamic acids on the cholest-5-en-3-ol-(3β)|4-phenyl,4'-pyridylazo]carbonate and its mesophases we have synthesized hydrogen bonded supramolecular assemblies as shown in Scheme 3.2.

$$\text{HO}\!\!-\!\!\langle\text{ring}\rangle\!\!-\!\!\text{CHO} \quad \xrightarrow[\text{DMF}]{\begin{array}{c}\text{RBr}\\ \text{K}_2\text{CO}_3\end{array}} \quad \text{RO}\!\!-\!\!\langle\text{ring}\rangle\!\!-\!\!\text{CHO}$$

7   **8a-e**

$$\begin{array}{c}\text{C}_5\text{H}_5\text{N}\\ \text{C}_5\text{H}_{10}\text{N}\\ \text{CH}_2(\text{CO}_2\text{H})_2\end{array}$$

9a-e

4

10a-e

a, R = C_4H_9	d, R = $C_{10}H_{21}$
b, R = C_6H_{13}	e, R = $C_{12}H_{25}$
c, R = C_8H_{17}	
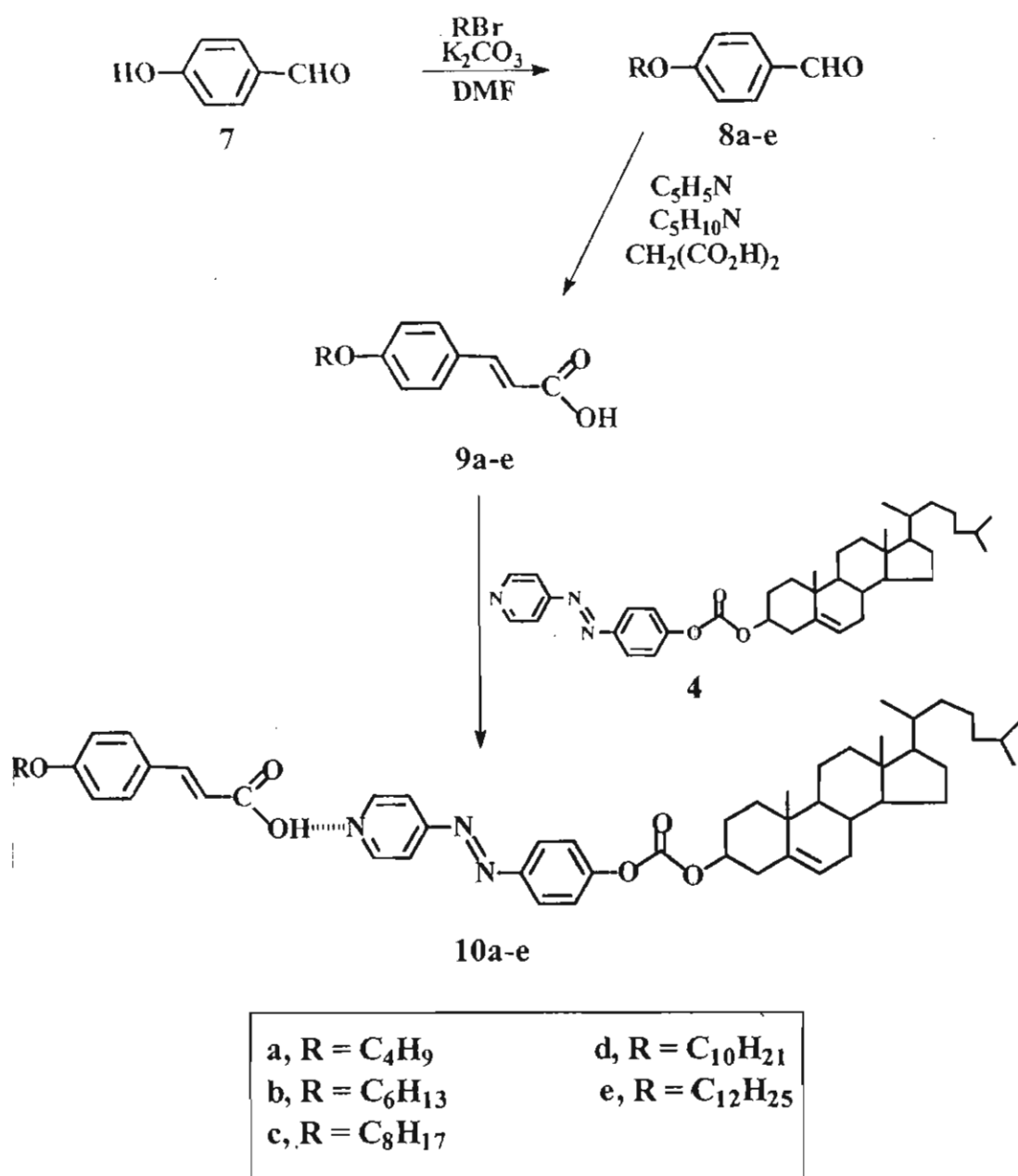
Scheme 3.2.

3.3.2.1. Synthesis and Characterization

The hydrogen bonded supramolecular mesogens described in this section were prepared according to Scheme 3.2. 4-*n*-Alkyloxycinnamic acids (**9a-e**) were synthesized by Doebner reaction. 4-Hydroxybenzaldehyde (**7**) was alkylated with *n*-alkyl bromides and the respective 4-*n*-alkyloxybenzaldehyde (**8a-e**) was treated with malonic acid, pyridine and piperidine. Work-up of the reaction mixture, followed by recrystallization from benzene gave 4-*n*-alkyloxycinnamic acids (**9a-e**) in 70-90% yields.

The hydrogen bonded acceptor, cholest-5-en-3-ol-(3β)[4-phenyl,4'-pyridylazo]carbonate (**4**) was prepared as per Scheme 3.1. All the compounds were characterized on the basis of spectral data and the details are provided in the Experimental Section (3.4.). The hydrogen bonded assemblies (**10a-e**) were synthesized by mixing equimolar quantities of H-bond donor and acceptors thoroughly above the melting point for a few minutes. The mixture was then allowed to cool slowly to yield the LC materials.[42] The formation of the intermolecular hydrogen bonded complexes could be confirmed by IR spectroscopy. The O-H bands observed around 3000 cm^{-1} for the weakly hydrogen bonded dimer in pure acid were replaced by O-H bands around 2500 and 1920 cm^{-1} in the complexes (**10a-e**), indicating strong intermolecular hydrogen bonding.[47,48]

3.2.2. Liquid Crystalline Properties

The heterointermolecular hydrogen bonded complexes (**10a-e**) showed well defined mesophases. The supramolecular assembly **10a** melts at 175.7 °C to form a mesophase ($\Delta H = 19.9$ kJmol^{-1}, $\Delta S = 44.4$ Jmol^{-1}K^{-1}) which becomes isotropic at 197.7 °C ($\Delta H = 1.1$ kJmol^{-1}, $\Delta S = 2.3$ Jmol^{-1}K^{-1}). The Grandjean texture observed under the POM for **10a** suggests the formation of a cholesteric LC phase (Figure 3.6.).[45] This is also consistent with the observation of selective reflections in the visible regions.
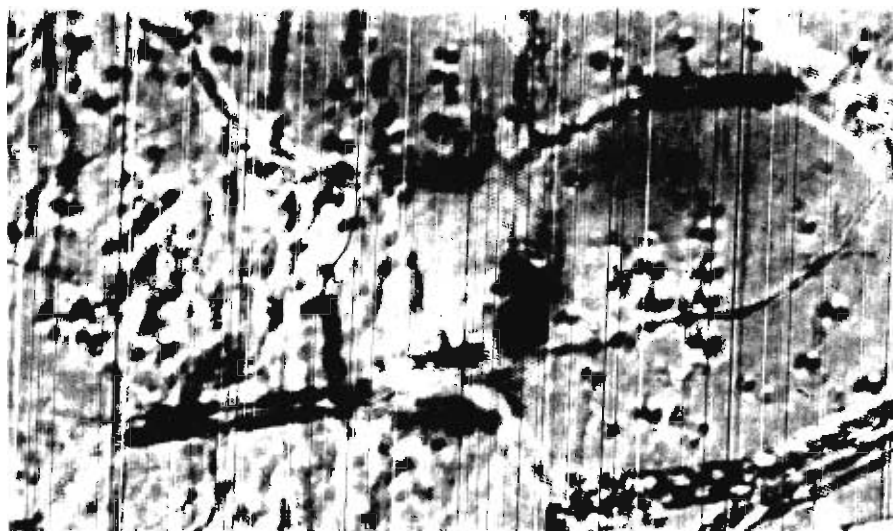

Figure 3.6. Optical photomicrograph of cholesteric Grandjean texture observed for hydrogen bonded complex 10a.

The supramolecular assembly **10b** exhibits similar LC behaviour as **10a**. Hydrogen bonded assemblies **10c** and **10d** show S_A LC phases in the lower temperatures.

which were confirmed from their fan shaped textures containing homeotropic areas (Figure 3.7.). At higher temperatures these assemblies show cholesteric LC phase, which were identified from the characteristic fingerprint as well as single wavelength reflecting Grandjean texture (Table 3.2.).
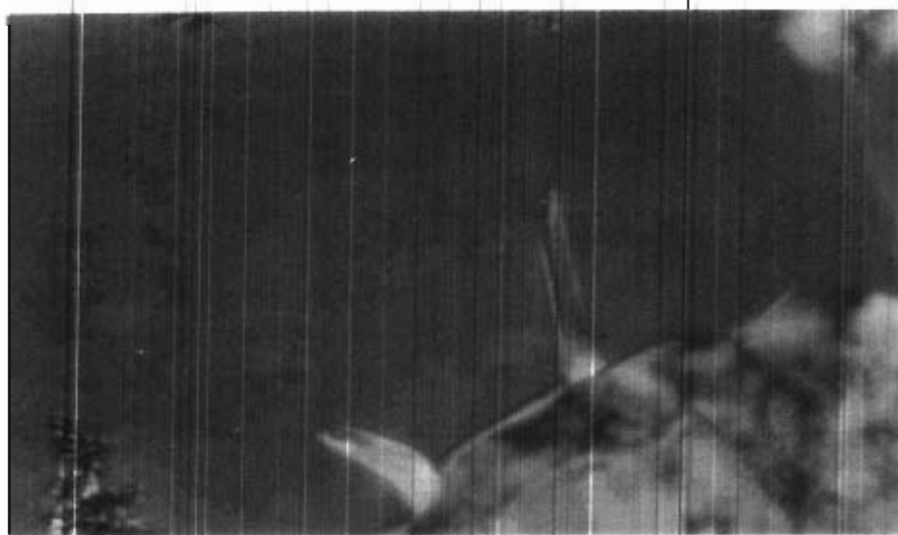

Figure 3.7. Optical photomicrograph of Smectic A phase observed for hydrogen bonded complex 10c.

The complexes **10c** and **10d** also exhibit a S_A^* or twist grain boundary (TGB) phases. S_A^* chiral phases are normally observed in optically active molecules. This phase can be depicted as a series of S_A blocks or grains, which are separated by twist grain boundaries. The director of each block is rotated by a constant angle on going from one grain to the next (Figure 3.8.). These phases were first reported by Goodby *et al.*, in 1989.[49,50]

Table 3.2.   Phase transition temperatures and thermodynamic parameters of 10a-e.

	Phase transition temperature in °C†	ΔH_{K-LC} kJ mol^{-1} (ΔS_{K-LC} JK^{-1}mol^{-1})	ΔH_{LC-I} kJ mol^{-1} (ΔS_{LC-I} JK^{-1}mol^{-1})
10a	K 175.7 Ch 197.7 I	24.0 (44.4)	1.1 (2.3)
10b	K 168.3 Ch 194.8 I	26.4 (59.8)	1.8 (3.9)
10c	K 162.1 S 164.3 TGB 164.7 Ch 189.4 I	26.5 (60.6)	0.7 (1.5)
10d	K 161.2 S 177.6 TGB 178.1 Ch 188.2 I	31.6 (72.8)	0.9 (1.9)
10e	K 156.3 S 174.3 I	24.9 (75.7)	0.7 (1.5)

†K = crystalline, S = smectic A, TGB = twist grain boundary, Ch = cholesteric and I = isotropic phase.

Figure 3.8. Schematic representation of S_A* or twist grain boundary phase.

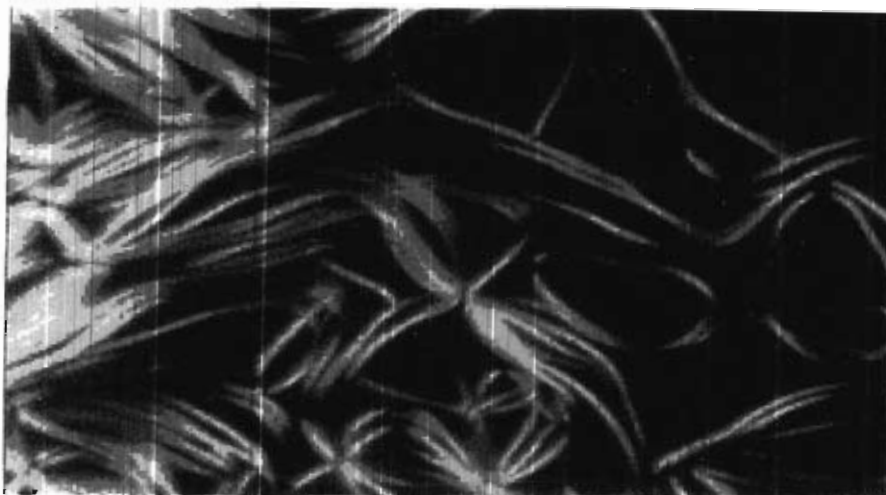TGB phases were identified from their characteristic Vermis texture observed under POM (Figure 3.9.).[51]

Figure 3.9. Optical photomicrograph of TGB phase observed for hydrogen bonded complex 10d at 177.8 °C

On slow heating (0.2 °Cmin⁻¹) the filament structure of the TGB phase grows slowly into the homeotropic regions of the S_A phase and subsequently turns into a cholesteric phase with a fan-shaped structure (Figure 3.10.). Oily streaks were also seen upon subjecting the preparation to mechanical stress.

The hydrogen-bonded complex **10e** does not show any chiral LC phase. It melts to a S_A phase at 156.3 °C (ΔH = 24.9 kJ mol⁻¹, ΔS = 75.7 Jmol⁻¹K⁻¹), which becomes isotropic at 173.9 °C (ΔH = 0.7 kJmol⁻¹, ΔS = 1.5 Jmol⁻¹K⁻¹). The temperatures at which the transition was observed using DSC were similar to those observed by POM. The supramolecular assembly **10b** exhibits two endotherms under the heating cycle which correspond to crystal to cholesteric transition at 168.3 °C (ΔH = 26.4 kJmol⁻¹, ΔS = 59.8 Jmol⁻¹K⁻¹) and cholesteric to isotropic transition at 194.8 °C (ΔH = 1.8 kJmol⁻¹, ΔS = 3.9 Jmol⁻¹K⁻¹) (Figure 3.11.).
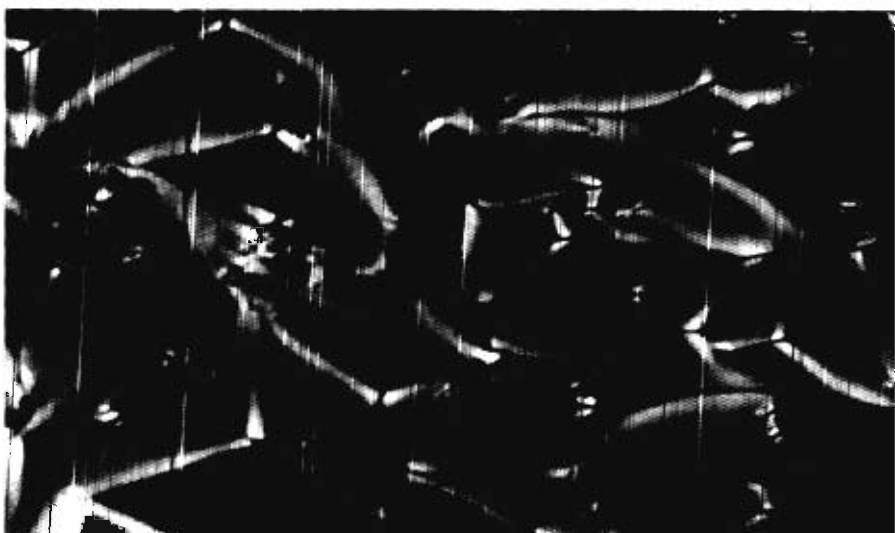
Figure 3.10. Optical photomicrograph of cholesteric focal conic texture observed for hydrogen bonded complex 10d at 181 °C.
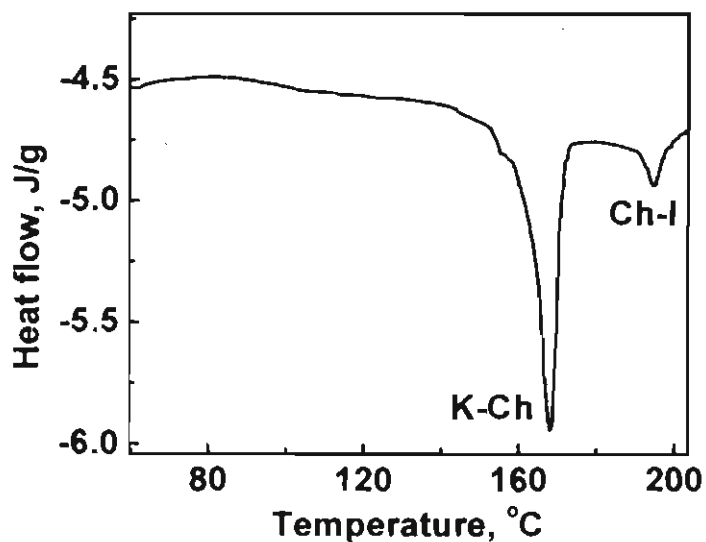
Figure 3.11. DSC thermogram of 10b showing the first heating scan at 5 °Cmin⁻¹.

Similarly, 10d shows three endotherms corresponding to K-S, S-Ch and Ch-I transitions (Figure 3.12.).
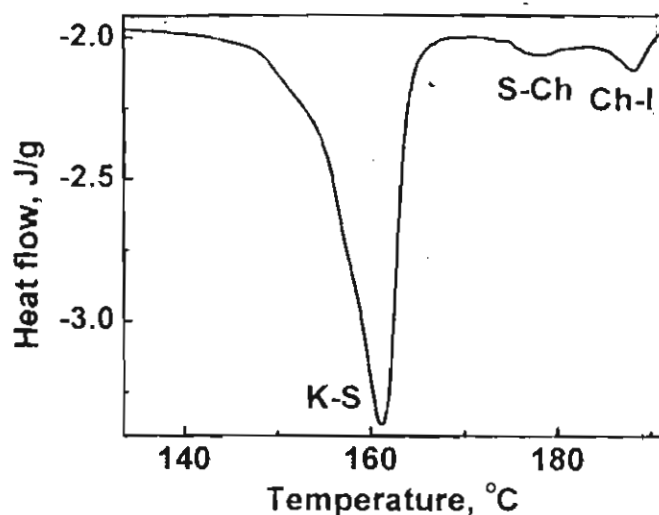
Figure 3.12. DSC thermogram of 10d showing the first heating scan at 5 °Cmin⁻¹.

The phase transition temperatures of these supramolecular assemblies were not reproducible on repeated heating and cooling (Figure 3.13.) and this can be attributed to the thermal instability of these compounds at higher temperatures (Table 3.3.).
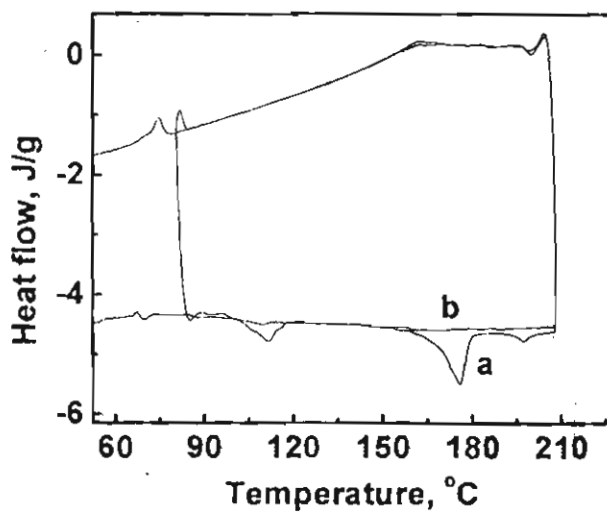
Figure 3.13.   DSC thermogram of 10a showing both the heating and cooling cycles during the (a) first and (b) second run.

Table 3.3. Decomposition temperatures of 10a-e obtained from TGA measurements.

Compound	$T_{1\% \, dec.} \, ^\circ C \S$
10a	180
10b	195
10c	206
10d	199
10e	176

$\S T_{1\% \, dec.} \, ^\circ C$, is the temperature of decomposition of 1% of the compound on heating, obtained from thermo gravimetric analysis.

The dependence of phase transition temperatures of the complexes on chain length of the alkyl group is shown in Figure 3.14.

Figure 3.14. Plot of transition temperature against the number of carbon atoms (n) in the alkyl chain for the 1:1 hydrogen bonded complexes, 10a-e.

Some of the key features of Figure 3.14. are described below. Increase in the number of carbon atoms in the alkyl chain increases the range of the LC phase for the lower homologues (n = 4-6), following which it starts to decrease (n = 10 and 12). Increase of the alkyl chain decreases the isotropization temperatures of the supramolecular a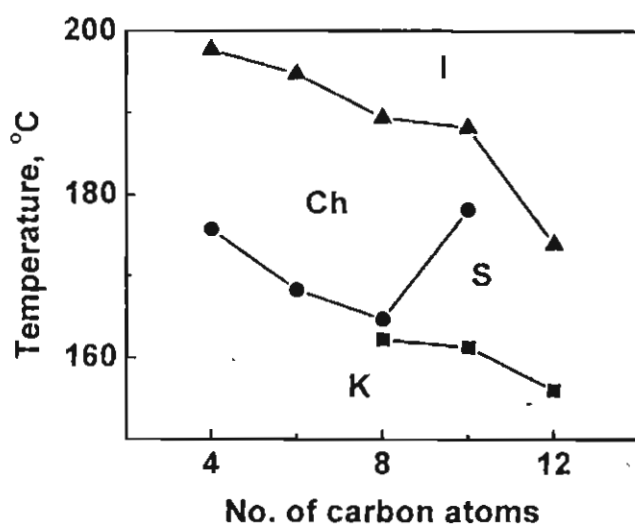ssemblies. The observed dependence of the transition points on alkyl chain is similar to that reported for well-known nematics and cholesterics.[46] Also lower homologues mainly exhibit the cholesteric LC phase (n = 4 and 6). For the complexes with alkyl chain length 8 and 10, the supramolecular assemblies show S_A, TGB and Ch LC phases and for n = 12, the assembly mainly shows an S_A LC phase (Figure 3.14).

3.3.2.3. Thermal Properties of Binary Mixtures of 4 and 9a

Studies on the LC properties of stoichiometric complexes formed between **9a-e** and **4** indicated the formation of unique materials. Further confirmation for the formation of unique materials was obtained by studying the thermal properties of the binary mixture containing cholest-5-en-3-ol-(3β)[4-phenyl,4'-pyridylazo]-carbonate (**4**) and 4-*n*-butyloxycinnamic acid (**9a**) in varying proportions.

The binary mixtures containing 10-90 mol% of **4** exhibit mainly cholesteric phases (Figure 3.15.).
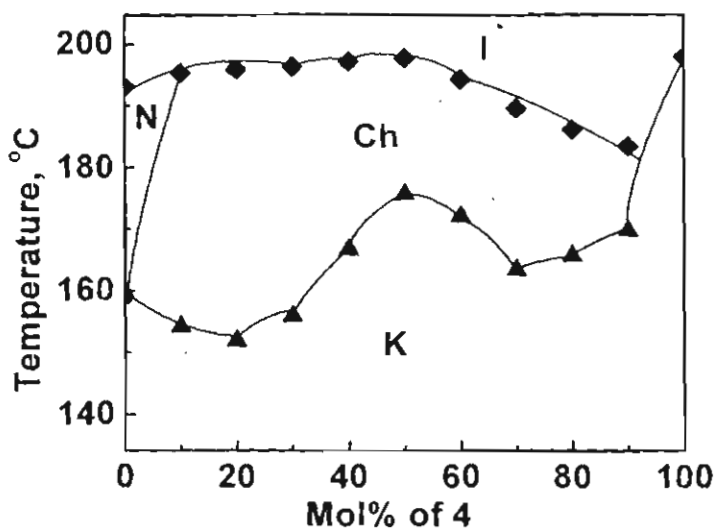
Figure 3.15. The binary phase diagram of 4 and 4-*n*-butyloxycinnamic acid.

The presence of a melting maximum as well as an isotropization maximum for the mixture containing 50mol% of **4** strongly supports the formation of a well defined 1:1 stochiometric compound. Additional support is provided by the presence of two eutectic points at 20 and 70 mol % of **4**.

3.3.2.4. Preparation and Studies of Glassy Cholesteric Solids

On slow cooling (5 °Cmin⁻¹), the complex **10a** exhibits a cholesteric phase from 191.0 °C, which crystallizes at 75.7 °C. On rapid cooling of the cholesteric LC phase to 0 °C, however glassy materials in which the cholesteric colours are retained, were obtained. A green colour reflection (Figure 3.16.a) was observed when the assembly **10a** was suddenly cooled from 150 °C (cooling cycle) to 0 °C and a blue colour reflection was obtained when the assembly was cooled from 180 °C

(heating cycle) to 0 °C (Figure 3.16.b). The Grandjean texture observed at cholesteric temperature was retained in the glassy state, indicating the helical orientation in the glassy solid (Figure 3.17). The glassy materials obtained in this manner are highly stable at room temperature (> 8 months). The colours of the cholesteric glassy LCs (GLCs) were highly angular dependent.

The iridescent colours obtained from the glassy solids can be erased by heating the solid films above 100 °C. The present study shows that the intermolecular hydrogen bonding interaction between suitable donor and acceptor molecules can be conveniently used for the design of materials capable of formation of cholesteric glasses.

(a)   (b)
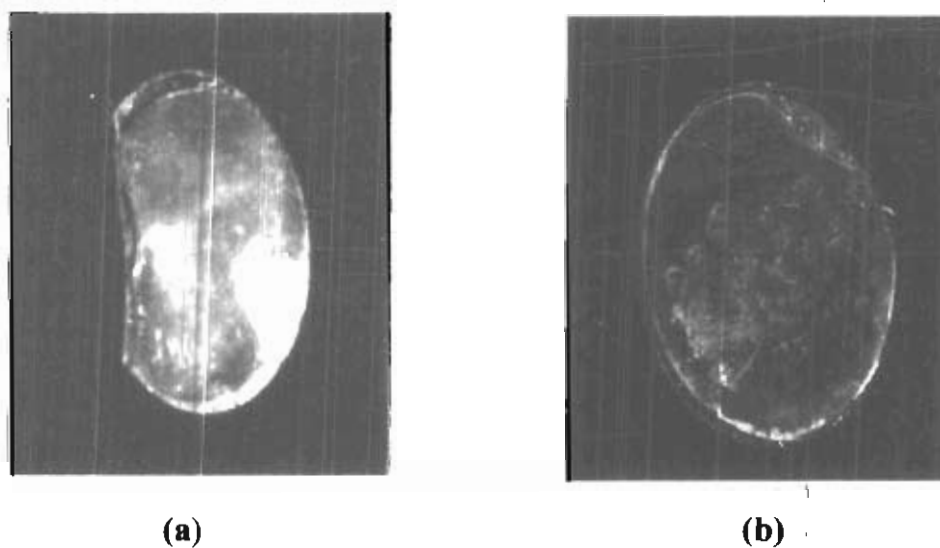
Figure 3.16. Cholesteric GLCs of 10a obtained by sudden cooling from (a) 150 °C (cooling cycle); (b) 180 °C (heating cycle).
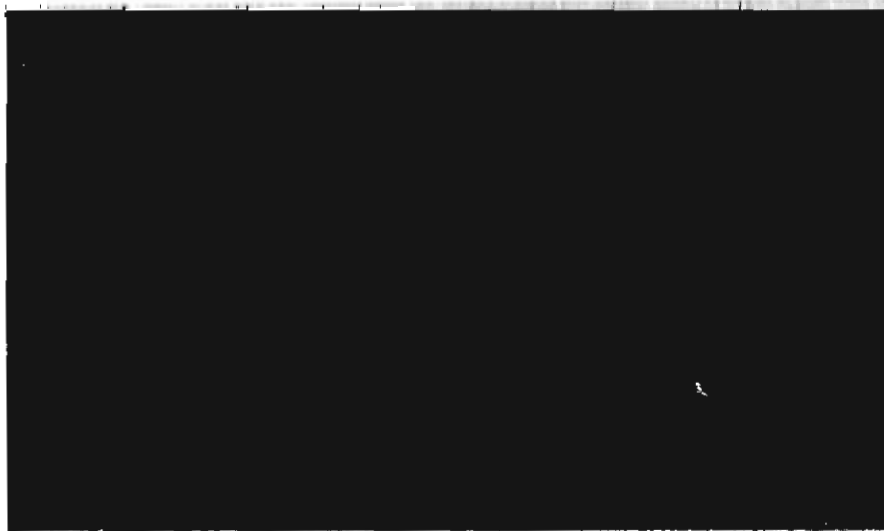
Figure 3.17. Optical photomicrograph of Grandjean texture observed in cholesteric GLC of 10a at room temperature.

3.3.3. Isomerization Studies

Photoisomerization of **4** in ethanol was examined by steady state photolysis using a 200 W high-pressure mercury lamp equipped with 320 nm band pass filter as the light source. The quantum yield of photoisomerization ($\Phi_{trans\text{-}cis}$) was determined using azobenzene as actinometer. The quantum yield of *trans-cis* photoisomerization ($\Phi_{trans\text{-}cis}$) was observed to be 0.11 in ethanol, which is almost similar to that obtained in toluene ($\Phi_{trans\text{-}cis}$ = 0.13). The rates for the thermal conversion of the *cis* isomer to the *trans* isomer following photolysis were determined spectrophotometrically, by monitoring the increase in absorbance of the π-π^* maxima of the *trans* isomer (320 nm) which is accompanied by a decrease

in the absorbance at 450 nm. The *cis-trans* isomerization which occurs in the dark

follows first order kinetics and the rate constants for this process at various

temperatures calculated using the rate equation of the first order kinetics are shown

in Table 3.4. From the plot of log k versus temperature, the activation energy of the

process, calculated using the Arrhenius equation was 90 kJmol^{-1} in ethanol.

The effect of solvents on the rate of the thermal *cis* to *trans* isomerization

for this compound (**4**) was very similar to that observed for 4-pyridylazo,4'-

phenyltetradecanoate described in Chapter 2.

Table 3.4. Rate constants of the *cis-trans* isomerization of 4 in ethanol.

Temperature (K)	$k \times 10^3 \, s^{-1}$
293	1.2
303	2.9
308	7.6
313	11.9
318	19.4
323	28.7

In toluene **4** has an absorption maximum at 323 nm. In alcoholic solvents the

absorption maximum undergoes a progressive hypsochromic shift with increasing

hydrogen bond donating strength of the alcohol (Table 3.5.). However, when acetic acid

was added to the solution of **4** in toluene a progressive bathochromic shift was observed

(Table 3.5.). In order to examine whether this shift could arise due to protonation of the azopyridyl moiety of **4**, we have also studied the effect of addition of hydrochloric acid (> 10 μM) to methanolic solution of **4**. In presence of hydrochloric acid the protonated species of **4** would be formed and this has an absorption maximum centered around 343 nm.

Table 3.5. Rate constants and lifetimes of *cis-trans* isomerization of 4 in hydrogen bonding solvents.

Solvent	λ_{max}, nm	k, s^{-1}	Lifetime, s
Methanol	319	6.2×10^{-4}	1.6×10^2
Ethanol	318	2.0×10^{-3}	500
Trifluoroethanol	314	7.4×10^{-2}	13.5
Toluene:acetic acid (3:2)	325	7.2	0.14
Acetic acid	330	66.8	1.5×10^{-2}
Methanol containing 10 μM hydrochloric acid	343	103.7	7.7×10^{-3}

Cis-trans isomerization of **4** in alcoholic solvents were studied using steady state photolysis and the rate constants for the processes are shown in Table 3.5. It is evident that the rate of *cis-trans* isomerization increases with hydrogen bond donating strength of the solvent.

In the presence of acetic acid however no change could be observed in the absorption spectrum of **4** on steady state photolysis. This is attributed to rapid thermal *cis* to *trans* isomerization. In order to investigate this we have studied the isomerization of **4** in such solvents using nanosecond laser flash photolysis technique. A 320 nm band-pass filter was placed between the sample and the analyzer lamp to prevent secondary photolysis of the *cis* isomer formed in the photoisomerization (Figure 3.18.).

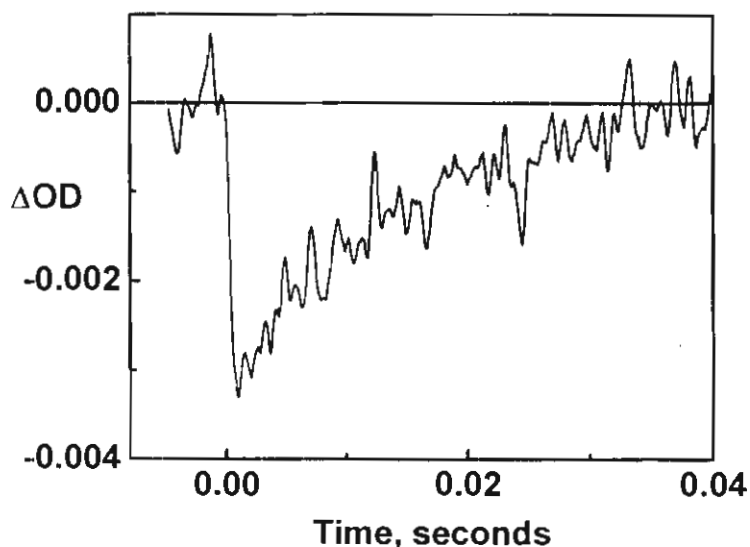**Figure 3.18. Transient absorption-time profile recorded at 330 nm following 355 nm laser pulse excitation of 4 in acetic acid.**

The rate constants for this process measured in solutions of **4** in acetic acid and toluene:acetic acid (3:2) (Table 3.5.) are two to three orders of magnitude higher than that observed in the alcoholic solvents. The rate of isomerization

increases with the concentration of acetic acid. In methanolic solutions of **4** containing hydrochloric acid (10 μM) the rate constant of isomerization was faster (Table 3.5.). These results indicate that both hydrogen bonding as well as protonation results in enhancement in the rate of *cis-trans* isomerization of **4**. The rate constant for the *cis-trans* isomerization observed for **4** was similar to 4-pyridylazo,4'-phenylalkanoates (**9b**, Chapter 2) in the corresponding solvents and was about one order of magnitude slower than for 4-hexyloxyphenyl,4'-azopyridine (**3b**, Chapter 2).

The pKa of acetic acid (4.72) and alkoxybenzoic acids (~4.5) are similar. The absorption spectral shifts of **4** in acetic acid containing solutions are suggestive of partial protonation of the pyridyl moiety. However in the complexes the ratio of **4** to acid is 1:1 and the predominant interaction is expected to be intermolecular hydrogen bonding. Regardless of the exact nature of this interaction the rate of thermal isomerization in the assemblies is expected to be much higher than that of the parent compound.

Due to the rapid thermal *cis-trans* isomerization observed at LC temperatures, photoinduced phase transition of the LC phase of these materials could not be investigated.

3.3.4. Dependence of the Liquid Crystalline Properties of Hydrogen Bonded Complexes on the Chain Length of the Alkyl Spacer of Cholesterol Linked Azo Derivatives

Studies carried out in the previous sections clearly show that the formation of cholesteric LC phases was dependent on the length of the alkyl chain present on the acid derivative (Figure 3.14.). In order to investigate the effect of alkyl chain length of the spacer in the cholesterol linked azo moiety on the phase transition temperatures of the complexes; we have synthesized hydrogen bonded complexes as shown in Chart 3.2.

11a-d

12 a-d

a, n = 2	c, n = 4
b, n = 3	d, n = 5
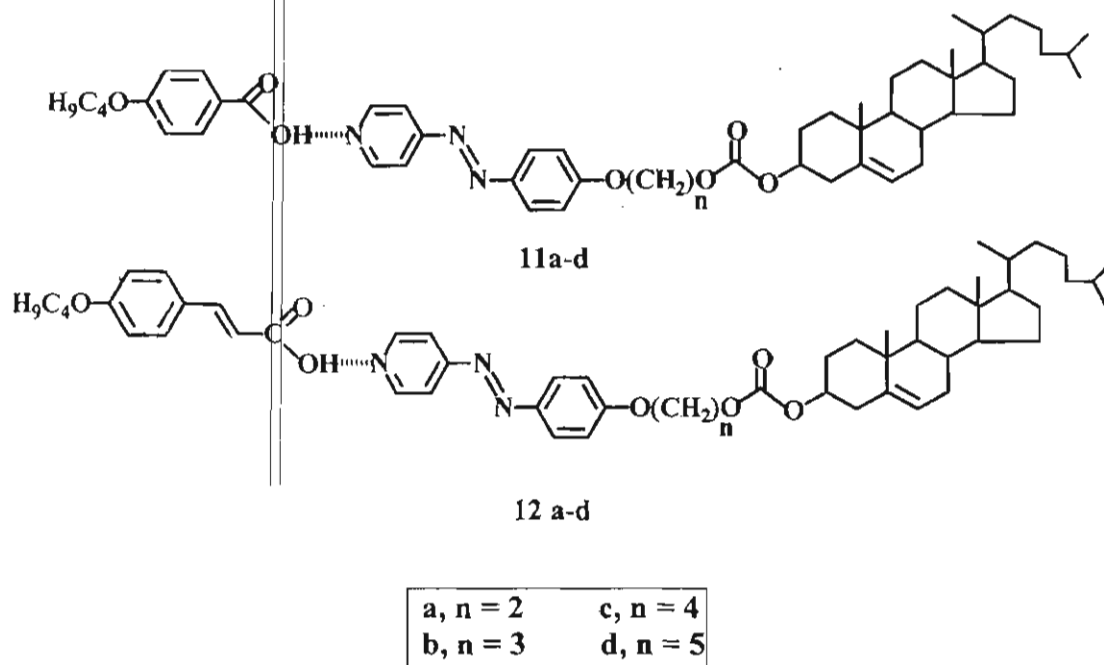
Chart 3.2.

3.3.4.1. Synthesis and Characterization

Cholest-5-en-3-ol-(3β)[4-n-alkyloxyphenyl,4'-pyridylazo]carbonate (**16a-d**)

were synthesized according to Schemes 3.3. and 3.4.

a, n = 2	**c, n = 4**
b, n = 3	
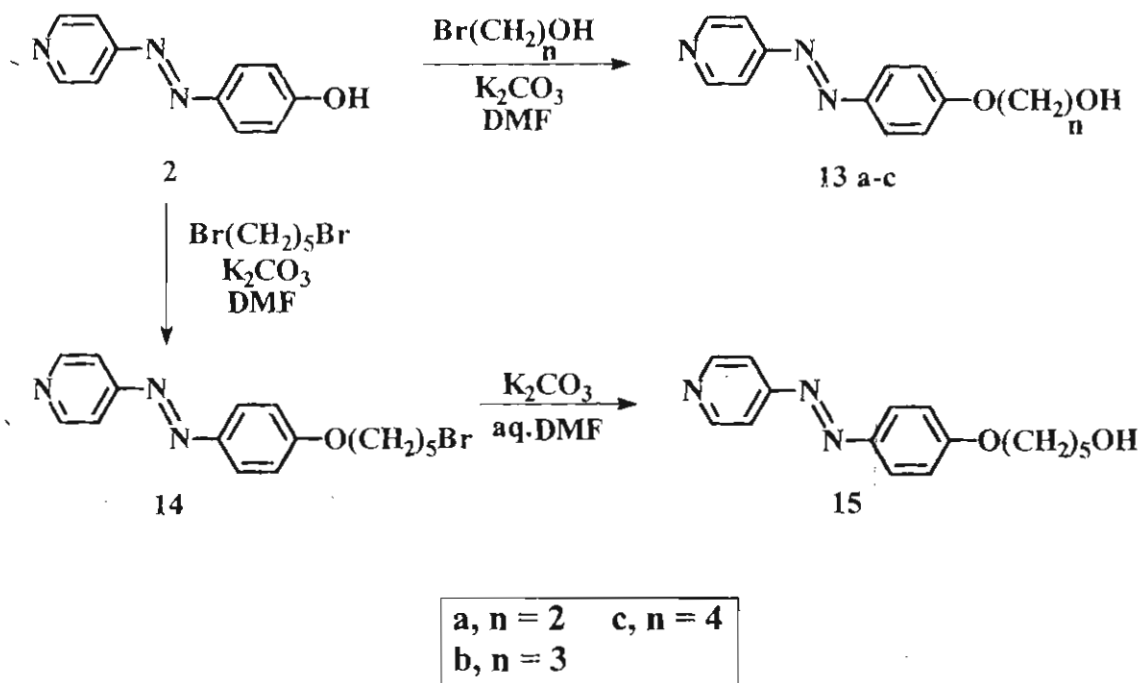
Scheme 3.3.

4-Hydroxyphenyl,4'-azopyridine (**2**) was first reacted with corresponding n-bromoalkanols (for alkyl chain length = 2, 3 and 4) in the presence of potassium carbonate and dimethylformamide to give 4-(hydroxy-n-alkyloxy)phenyl,4'-azopyridine (**13a-c**, Scheme 3.3.). For the synthesis of the derivative containing alkyl chain length 5, 4-hydroxyphenyl,4'-azopyridine (**2**) was reacted with dibromopentane in the presence of potassium carbonate

to yield 4(5-bromo-*n*-pentyloxy)phenyl,4'-azopyridine (**14**). Treatment of **14** with

aqueous dimethylformamide and potassium carbonate gave 4-(5-hydroxy-*n*-

·pentyloxy)phenyl,4'-azopyridine (**15**, Scheme 3.3.). Subsequent refluxing of the 4-

(hydroxy-*n*-alkyloxy)phenyl,4'-azopyridine with cholesteryl chloroformate in

benzene gave **16a-d** (Scheme 3.4.).

16 a-d
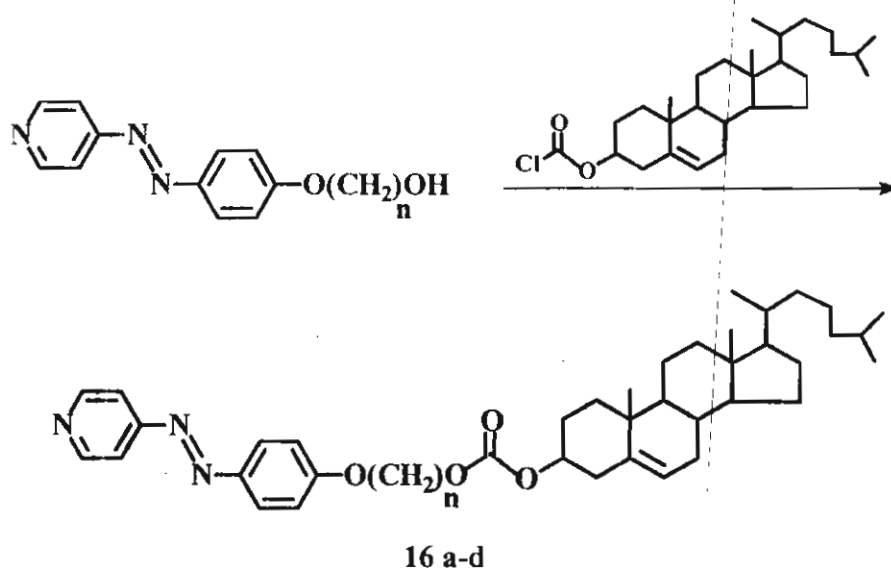
a, n = 2	c, n = 4
b, n = 3	d, n = 5

Scheme 3.4.

All compounds were characterized on the basis of spectral data and the

details are provided in the Experimental Section (3.4.). The hydrogen bonded

complexes were synthesized by mixing equimolar quantities of hydrogen bond

donors and acceptors thoroughly above the melting point of the mixtures for a few

minutes. The mixture, in each case was then allowed to cool slowly to yield the LC materials. Hydrogen bonded assemblies were characterized from IR spectroscopy from the shift observed in the O-H bands of the pure acids and hydrogen bonded complexes. An O-H peak observed at 2500 and 1900 cm^{-1} confirms the formation strong hydrogen bonding between pyridyl moiety and carboxylic acid group.

3.3.4.2. Liquid Crystalline Properties

All heterointermolecular hydrogen bonded complexes, except **11d**, investigated in the present study exhibit smectic A, TGB, and cholesteric LC phases, which were characterized from the textures observed under POM and were confirmed by DSC. **11d** melts to a cholesteric LC phase at 144.5 °C ($\Delta H = 25.4$ kJmol^{-1}, $\Delta S = 60.8$ JK^{-1}mol^{-1}) which becomes isotropic at 167.9 °C ($\Delta H = 4.3$ kJmol^{-1}, $\Delta S = 9.9$ Jmol^{-1}K^{-1}). The LC as well as thermodynamic parameters of **11a-d** and **12 a-d** are shown in Table 3.6. Hydrogen bonded complexes **11a**, **11c**, **12a** and **12d** exhibit an intermediate LC phase (M), which was not readily identifiable. POM studies of these phases indicate a threaded fingerprint like texture (Figure 3.19.), which suggests that a S$_C$* phase may be involved. On heating these phases turn to a S$_A$ phase which is clearly identified by its focal conic texture with homeotropic areas.

Table 3.6. Phase transition and thermodynamic properties observed for 11a-d and 12a-d.

	Phase transition temperature in °C†	$\Delta H_{K\text{-}LC}$ kJ mol^{-1} ($\Delta S_{K\text{-}LC}$ JK^{-1}mol^{-1})	$\Delta H_{LC\text{-}I}$ kJ mol^{-1} ($\Delta S_{LC\text{-}I}$ JK^{-1}mol^{-1})
11a	K 123.6 M 132.6 S$_A$ 150.1 TGB 151.2 Ch 174.1 1	14.6 (36.9)	7.6 (16.9)
·11b	K 142.0 S$_A$ 150.2 TGB 152.3 Ch 170.7 1	24.4 (58.7)	4.4 (10.0)
11c	K 125.7 M 132.6 S$_A$ 145.7 TGB 146.8 Ch 172.8 I	11.5 (28.8)	4.3 (9.7)
11d	K 144.5 Ch 167.9 I	25.4 (60.8)	4.3 (9.9)
12a	K 131.2 M 137.5 S$_A$ 150.5 TGB 151.9 Ch 186.6 1	6.3 (15.6)	5.9 (12.8)
12b	K 144.3 S$_A$ 155.8 TGB 157.7 Ch 179.9 I	30.3 (72.6)	4.7 (10.4)
12c	K 123.3 S$_A$ 149.7 TGB 150.3 Ch 187.1 I	30.3 (76.5)	6.2 (13.4)
12d	K 119.8 M 130.2 S$_A$ 136.5 TGB 138.3 Ch 177.7 I	12.5 (31.7)	‡

†K = crystalline, M = unidentified LC phase S$_A$ = smectic A, TGB = twist grain boundary, Ch = cholesteric and I = isotropic phase.

‡$\Delta H_{LC\text{-}I}$ could not be determined by DSC because energy change was very small.

Figure 3.19. Optical photomicrograph of the unidentified LC phase observed for hydrogen bonded complex **11a** at 128.7 °C.

The DSC thermograms observed for **11d** and **12b** are shown in Figures 3.20 and 3.21, respectively.
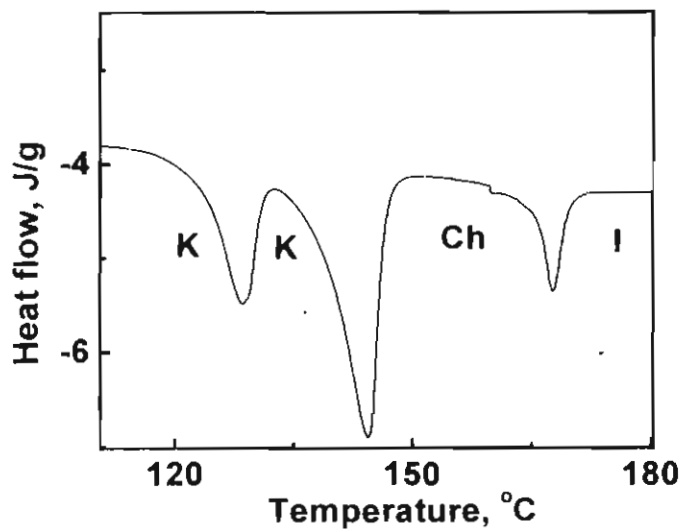

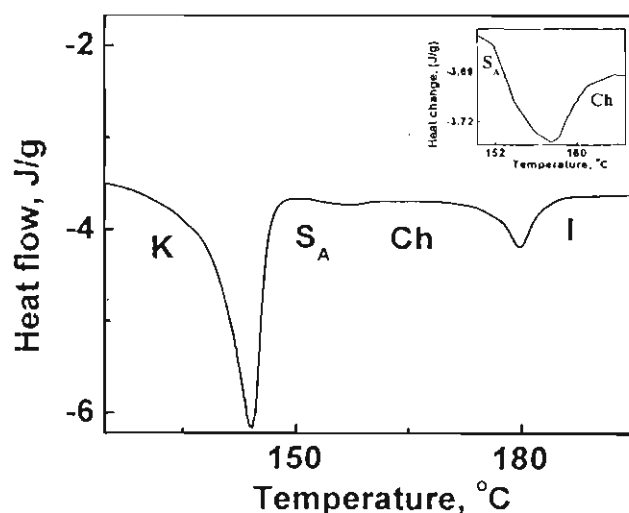**Figure 3.20.** DSC thermogram of **11d** obtained on the first heating scan at 5 °Cmin⁻¹.

Figure 3.21. DSC thermogram of 12b obtained on the first heating scan at 5 °C min⁻¹. Inset shows the expanded scale from 160 to 185 °C.

In the case of **11d**, three endotherms were observed which corresponds to crystal to crystal transition (128.5 °C, ΔH = 10.9 kJmol⁻¹, ΔS = 27.0 Jmol⁻¹K⁻¹) crystal to cholesteric transition (144.5 °C, ΔH = 25.4 kJmol⁻¹, ΔS = 60.8 Jmol⁻¹K⁻¹ and cholesteric to isotropic transition (167.7 °C, ΔH = 4.3 kJmol⁻¹, ΔS = 9.9 Jmol⁻¹K⁻¹, Figure 3.20.). The three endotherms observed in the Figure 3.21. correspond to crystal to S_A (144.0 °C, ΔH = 30.3 kJmol⁻¹, ΔS = 72.6 Jmol⁻¹K⁻¹), S_A to cholesteric (157.5 °C, ΔH = 0.4 kJmol⁻¹, ΔS = 1.0 Jmol⁻¹K⁻¹) and cholesteric to isotropic (179.9 °C, ΔH = 4.7 kJ mol⁻¹, ΔS = 10.4 Jmol⁻¹K⁻¹) transitions.

A plot of the transition temperatures as a function of spacer length indicates an odd-even effects for the isotropization temperatures of **11a-d** and **12a-d** (Figure 3.22. and Figure 3.23.).

Figure 3.22. Plot of transition temperature against the spacer length (n) in the alkyl chain for the 1:1 hydrogen bonded complexes 11a-d (■-● denotes unidentified LC phase).
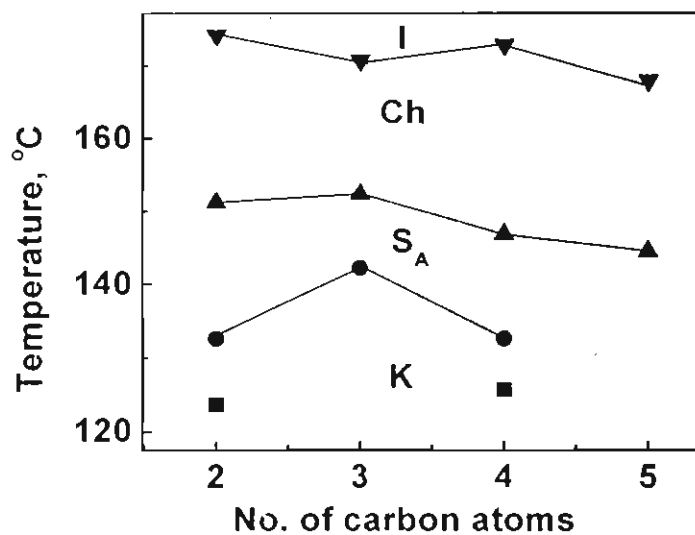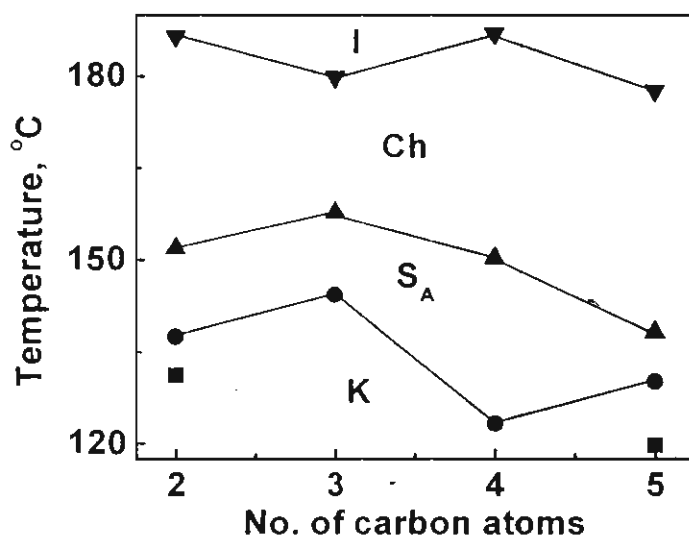

Figure 3.23. Plot of transition temperature against the spacer length (n) in the alkyl chain for the 1:1 hydrogen bonded complexes 12a-d (■-● denotes nnidentified LC phase).

This odd-even effect shown in the isotropization temperatures is similar to that observed for dicarboxylic acid esters of azobenzene derivatives and α,ω-bis(4,4'-cyanobiphenyloxy)alkanes.[46] The odd-even behavior exhibited by LCs can be explained in terms of the packing in the crystal lattice. When the number of methylene group in the spacer is even, the preference of the spacer to adopt an all-*trans* conformation leads to a co-linear arrangement of the mesogens, whereas if the number of methylene units is odd it leads to a biaxial arrangement. Hence in the crystal lattice the even entities can pack more efficiently leading to higher transition temperatures compared to that for odd ones.[52,53]

3.4. Experimental Section

Melting points are uncorrected and were recorded on a Mel-temp II melting point apparatus. Phase transitions were observed using a Nikon HFX 35A Optiphot-2 polarized light microscope, equipped with Linkam THMS 600 heating and freezing stage connected to Linkam TP92 temperature programmer. DSC scans were performed using Du Pont DSC 2010 Differential Scanning Calorimeter attached to Thermal Analyst 2100 data station under air. X-ray diffraction studies were carried out using Cu Kα (λ = 1.54 Å) radiation from a rotating anode X-ray generator (Rigaku) and the diffraction pattern was collected on an image plate detector (Marresearch). IR spectra were recorded on a Perkin Elmer Model 882

infrared spectrophotometer. Electronic spectra were recorded on a Shimadzu Model UV-3101 PC-UV-Vis-NIR Scanning Spectrophotometer. ^{1}H and ^{13}C NMR spectra were recorded on a Bruker DPX 300 MHz FTNMR spectrometer using tetramethylsilane (TMS) as the internal standard. Steady state photolysis was carried out on an ORIEL optical bench using a 200 W high-pressure mercury lamp. Monochromatic light (intensity = 9.3 x 10^{-8} Einsteins min^{-1}) obtained by using a 320 nm band pass filter was used. Nanosecond laser flash photolysis experiments were carried out by employing an Applied Photophysics Model LKS-20 laser kinetic spectrometer using GCR-12 series Quanta Ray Nd:YAG laser. The third harmonic of the laser (355 nm, 60mJ /pulse, pulse width 10 ns) was used for exciting the azo compounds.

3.4.1. Materials

Reagent grade reactants and solvents were used as received from suppliers. Extremely dry solvents were prepared as per standard procedures. Spectroscopic grade solvents were used for all measurements.

3.4.2. Preparation of Cholest-5-en-3-ol-(3β)[4-phenylpyridylazo]-carbonate (4)

To a solution of 4-hydroxyphenylazopyridine, **2** (200 mg, 1 mmol) in methanol (10 mL), pyridine (100 mg, 1.3 mol) was added and refluxed for 30 min. To this, a

solution of cholesteryl chloroformate (450 mg, 1 mmol) in chloroform was added, dropwise. The reaction mixture was refluxed for an additional period of 6 h following which the solvent was removed under reduced pressure. The residue was chromatographed on silica gel (100-200 mesh) using chloroform to give 175 mg (30%) of compound **4**, mp. 197-198 °C.

IR v_{max} (KBr): 2939, 2366, 1766, 1543, 1377, 1251, 1222, 852 cm^{-1}; UV λ_{max} (toluene): 320 nm ($\varepsilon = 14,494$ M^{-1}cm^{-1}); ^{1}H NMR (300 MHz, CDCl$_3$): δ 0.6-2.5 (44H, m, cholesteric), 4.6 (1H, m, OCH), 5.4 (1H, m, vinylic), 6.7-6.9 (2H, d, aromatic), 7.2-7.5 (2H, d, aromatic), 7.8-8.1 (4H, d, aromatic); ^{13}C NMR (75 MHz, CDCl$_3$): δ 11.81, 18.67, 19.18, 21.00, 22.52, 22.76, 23.83, 24.22, 27.65, 27.92, 28.16, 31.80, 35.74, 36.16, 36.48, 36.78, 37.89, 39.47, 39.68, 40.15, 42.24, 49.94, 56.15, 56.59, 78.59, 121.31, 124.95, 139.36, 151.74, 152.36, 152.57.

3.4.3. General Procedure for the Preparation of 4-*n*-Alkyloxycinnamic Acids (9a-e)

4-Hydroxybenzaldehyde (8.2 mmol), *n*-alkyl bromide (8.2 mmol) and potassium carbonate (3.5 g, 25.3 mmol) were dissolved in dimethylformamide (25 mL) and heated at 120 °C for 10 h. The reaction mixture was cooled and added to water. It was extracted with ether and the solvent was evaporated. The

residue was chromatographed on silica gel (100-200 mesh) using a mixture (1:16) of ethyl acetate and petroleum ether to give pure products.

4-*n*-Alkyloxybenzaldehyde (**8a-e**, 3.5 mmol) and malonic acid (7.6 mmol) were dissolved in a mixture of pyridine (3 mL) and piperidine (30 mg). The reaction mixture was refluxed for 90 min. It was added to water and the precipitated solid was washed with water and recrystallized from benzene to give the respective 4-*n*-alkyloxybenzoic acids (**9a-e**).

4-*n*-Butyloxybenzaldehyde (8a)

Yield 85%; IR v_{max} (neat): 2926, 2862, 2741, 1706, 1604, 1583, 1516, 1472, 1431, 1395. 1315, 1256, 1216, 1160, 1019, 834 cm^{-1}; ^{1}H NMR (300 MHz, CDCl$_3$): δ 0.9 (3H, t, CH$_3$), 1.4-1.5 (2H, m, OCH$_2$-CH$_2$-CH$_2$), 1.7-1.8 (2H, m, OCH$_2$-CH$_2$), 3.9 (2H, t, OCH$_2$), 6.9 (2H, d, aromatic), 7.7 (2H, d, aromatic), 9.8 (1H, s, CHO); ^{13}C NMR (75 MHz, CDCl$_3$): δ 13.89, 19.29, 31.27, 67.98, 114.61, 129.61, 131.84, 164.15, 190.63.

4-*n*-Butyloxycinnamic acid (9a)

Mp. K 159.1°C N 192.9 °C I; Yield 95%; IR v_{max} (KBr): 3467, 2956, 2874, 1676, 1601, 1307, 1283, 1245, 958 cm^{-1}; ^{1}H NMR (300 MHz, CDCl$_3$): δ 0.9 (3H, t, CH$_3$), 1.4-1.5 (2H, m, OCH$_2$-CH$_2$-CH$_2$), 1.7-1.8 (2H, m, OCH$_2$-CH$_2$),

4.0 (2H, t, OCH$_2$), 6.3 (1H, d, vinylic), 6.9 (2H, d, aromatic), 7.4 (2H, d, aromatic), 7.7 (2H, d, aromatic); ^{13}C NMR (75 MHz, CDCl$_3$): δ 13.89, 19.29, 31.27, 67.98, 114.30, 115.00, 126.69, 130.16, 146.85, 161.49, 172.10.

4-*n*-Hexyloxybenzaldehyde (8b)

Yield 87%; IR ν$_{max}$ (neat): 2939, 2865, 2745, 1702, 1606, 1582, 1514, 1472, 1426, 1398, 1315, 1261, 1163, 1111, 1020, 833 cm^{-1}; ^{1}H NMR (300 MHz, CDCl$_3$): δ 0.8 (3H, t, CH$_3$), 1.3-1.4 (6H, m, OCH$_2$-CH$_2$-CH$_2$), 1.7-1.8 (2H, m, OCH$_2$-CH$_2$), 4.0 (2H, t, OCH$_2$), 6.9 (2H, d, aromatic), 7.7 (2H, d, aromatic), 9.8 (1H, s, CHO); ^{13}C NMR (75 MHz, CDCl$_3$): δ 13.92, 22.49, 25.56, 28.94, 31.45, 68.32, 114.65, 129.68, 131.84, 164.18, 190.57.

4-*n*-Hexyloxycinnamic acid (9b)

Mp. K 151.8 °C N 183.1 °C I; Yield 95%; IR ν$_{max}$ (KBr): 3443, 2918, 2850, 1676, 1601, 1307, 1239, 983 cm^{-1}; ^{1}H NMR (300 MHz, CDCl$_3$): δ 0.9 (3H, t, CH$_3$), 1.2-1.4 (6H, m, OCH$_2$-CH$_2$-CH$_2$), 1.7-1.8 (2H, m, OCH$_2$-CH$_2$), 3.9 (2H, t, OCH$_2$), 6.2 (1H, d, vinylic), 6.8 (2H, d, aromatic), 7.4 (2H, d, aromatic), 7.7 (2H, d, aromatic); ^{13}C NMR (75 MHz, CDCl$_3$): δ 14.00, 22.58, 25.65, 29.08, 31.53, 68.18, 114.30, 114.88, 126.51, 130.51, 146.92, 172.44.

4-*n*-Octyloxybenzaldehyde (8c)

Yield 85%; IR v_{max} (neat): 2926, 2862, 2741, 1706, 1604, 1583, 1516, 1472, 1431, 1395, 1315, 1256, 1216, 1160, 1019, 834 cm^{-1}; ^{1}H NMR (300 MHz, CDCl$_3$): δ 0.9 (3H, t, CH$_3$), 1.2-1.4 (9H, m, OCH$_2$-CH$_2$-CH$_2$), 1.8-1.9 (2H, m, OCH$_2$-CH$_2$), 4.0 (2H, t, OCH$_2$), 7.0 (2H, d, aromatic), 7.8 (2H, d, aromatic), 9.9 (1H, s, CHO); ^{13}C NMR (75 MHz, CDCl$_3$): δ 13.97, 22.53, 25.85, 28.94, 29.02, 29.18, 31.68, 68.30, 114.63, 129.61, 131.86, 164.18, 190.70.

4-*n*-Octyloxycinnamic acid (9c)

Mp. K 144.4 ^{o}C N 176.9 ^{o}C I; Yield 90%; IR v_{max} (KBr): 3474, 2930, 2856, 1676, 1601, 1426, 1283, 970 cm^{-1}; ^{1}H NMR (300 MHz, CDCl$_3$): δ 0.9 (3H, t, CH$_3$), 1.3-1.5 (10H, m, OCH$_2$-CH$_2$-CH$_2$), 1.8-1.9 (2H, m, OCH$_2$-CH$_2$), 4.0 (2H, t, OCH$_2$), 6.3 (1H, d, vinylic), 6.9 (2H, d, aromatic), 7.3 (2H, d, aromatic), 7.5 (2H, d, aromatic), 7.8 (1H, d, vinylic); ^{13}C NMR (75 MHz, CDCl$_3$): δ 14.10, 22.66, 26.01, 29.15, 29.23, 29.34, 31.81, 68.22, 114.33, 126.57, 130.09, 146.78, 161.40, 171.89.

4-*n*-Decyloxybenzaldehyde (8d)

Yield 85%; IR v_{max} (neat): 2934, 2860, 2735, 1700, 1605, 1581, 1516, 1474, 1432, 1396, 1315, 1262, 1217, 1161, 1111, 1019, 832 cm^{-1}; ^{1}H NMR (300 MHz, CDCl$_3$):

δ 0.8 (3H, t, CH₃), 1.3-1.4 (14H, m, OCH₂-CH₂-CH₂), 1.7-1.8 (2H, m, OCH₂-CH₂), 4.0 (2H, t, OCH₂), 6.9 (2H, d, aromatic), 7.7 (2H, d, aromatic), 9.8 (1H, s, CHO); ^{13}C NMR (75 MHz, CDCl₃): δ 14.01, 22.49, 25.85, 28.94, 29.22, 29.28, 29.44, 31.45, 31.79, 68.29, 114.61, 129.61, 131.84, 164.15, 190.63.

4-*n*-Decyloxycinnamic acid (9d)

Mp. K 133.1 °C S$_C$ 151.7 °C N 172.1 °C I; Yield 90%; IR ν$_{max}$ (KBr): 3443, 2918, 2850, 1676, 1601, 1307, 1239, 983 cm^{-1}; ^{1}H NMR (300 MHz, CDCl₃): δ 0.8 (3H, t, CH₃), 1.2-1.4 (6H, m, OCH₂-CH₂-CH₂), 1.7-1.8 (2H, m, OCH₂-CH₂), 3.9 (2H, t, OCH₂), 6.2 (1H, d, vinylic), 6.9 (2H, d, aromatic), 7.5 (2H, d, aromatic), 7.7 (2H, d, aromatic); ^{13}C NMR (75 MHz, CDCl₃): δ 14.09, 22.66, 25.97, 29.12, 29.30, 29.34, 29.38, 29.45, 31.87, 68.20, 114.89, 126.51, 130.09, 146.91, 161.42, 172.15.

4-*n*-Dodecyloxybenzaldehyde (8e)

Yield 85%; IR ν$_{max}$ (neat): 2922, 2861, 2742, 1694, 1608, 1582, 1515, 1472, 1431, 1396, 1314, 1260, 1217, 1162, 1111, 1016, 832 cm^{-1}; ^{1}H NMR (300 MHz, CDCl₃): δ 0.9 (3H, t, CH₃), 1.3-1.5 (18H, m, OCH₂-CH₂-CH₂), 1.7-1.8 (2H, m, OCH₂-CH₂), 4.0 (2H, t, OCH₂), 6.9 (2H, d, aromatic), 7.7 (2H, d, aromatic), 9.8 (1H, s, CHO); ^{13}C NMR (75 MHz, CDCl₃): δ 13.95, 22.54,

25.81, 28.90, 29.21, 29.31, 29.42, 29.45, 29.50, 31.45, 31.79, 68.29, 114.61, 129.61, 131.84, 164.10, 190.52.

4-*n*-Dodecyloxycinnamic acid (9e)

Mp. K 131.5 °C S$_C$ 155.1 °C 1; Yield 90 %; IR (KBr): v_{max} 3443, 2918, 2850, 1676, 1601, 1307, 1239, 983 cm^{-1}; ^{1}H NMR (300 MHz, CDCl$_3$): δ 0.9 (3H, t, CH$_3$), 1.2-1.5 (18H, m, OCH$_2$-CH$_2$-CH$_2$), 1.8 (2H, m, OCH$_2$-CH$_2$), 3.9 (2H, t, OCH$_2$), 6.3(1H, d, vinylic), 6.9 (2H, d, aromatic), 7.5 (2H, d, aromatic), 7.8 (2H, d, vinylic); ^{13}C NMR (75 MHz, CDCl$_3$): δ 14.12, 22.70, 26.01, 29.16, 29.36, 29.41 29.59, 29.65, 29.72, 31.87, 31.93 68.20, 114.93, 126.62, 130.08, 146.74, 161.42, 171.77.

3.4.4. General Procedure for the Preparation of 4-Hydroxy-*n*-alkyloxy-phenyl,4'-azopyridine (13a-c)

To a solution of 4-hydroxy,4'-pyridylazobenzene (2) and potassium carbonate in dimethylformamide, *n*-bromoalkanol was added dropwise. The mixture was heated at 100 °C for 12 h. The reaction mixture was cooled, added to ice-cold water and extracted with dichloromethane. The organic layer was washed with water and dried over anhydrous sodium sulfate. The crude product was chromatographed on silica gel (100-200 mesh) using chloroform to give the pure product.

4(2-Hydroxy-*n*-ethyloxy)phenyl,4'-azopyridine (13a)

Mp. 165-167 °C (yield 50%); IR ν_{max} (KBr): 3207, 2936, 2865, 1595, 1489, 1412, 1252, 1142, 1102, 1043, 998, 915, 840 cm^{-1}; UV λ_{max} (toluene): 353 nm (ε = 22,667 M^{-1}cm^{-1}); ^{1}H NMR (300 MHz, CDCl$_3$): δ 1.9 (1H, s, -OH), 3.9 (2H, t, CH$_2$OH), 4.1(2H, t, OCH$_2$), 7.0 (2H, d, aromatic), 7.6 (2H, d, aromatic), 7.9 (2H, d, aromatic), 8.7 (2H, d, aromatic); ^{13}C NMR (75 MHz, CDCl$_3$): δ 47.99, 53.40, 117.36, 119.81, 128.04, 146.27, 148.15, 160.79, 165.25.

4(3-Hydroxy-*n*-propyloxy)phenyl,4'-azopyridine (13b)

Mp. 125 °C (yield 68%); IR ν_{max} (KBr): 3260, 2927, 2880, 1597, 1487, 1412, 1314, 1251, 1143, 1067, 1014, 839 cm^{-1}; UV λ_{max} (toluene): 354 nm (ε = 22,713 M^{-1}cm^{-1}); ^{1}H NMR (300 MHz, CDCl$_3$): δ 2.1 (2H, m, CH$_2$-CH$_2$), 3.9 (2H, t, CH$_2$OH), 4.1(2H, t, OCH$_2$), 7.0 (2H, d, aromatic), 7.7 (2H, d, aromatic), 8.0 (2H, d, aromatic), 8.8 (2H, d, aromatic); ^{13}C NMR (75 MHz, DMSOd$_6$): δ 47.99, 53.40, 117.36, 119.81, 128.04, 146.27, 148.15, 160.79, 165.25.

4(4-Hydroxy-*n*-butyloxy)phenyl,4'-azopyridine (13c)

Mp. 131-132 °C (yield 18 %); IR ν_{max} (KBr): 3288, 2926, 1828, 1597, 1505, 1467, 1412, 1314, 1252, 1143, 1053, 1007, 964, 838 cm^{-1}; UV λ_{max}

(toluene): 354 nm ($\varepsilon = 17,495$ M^{-1}cm^{-1}): ^{1}H NMR (300 MHz, CDCl$_3$): δ 2.1 (4H, m, CH$_2$-CH$_2$), 3.9 (2H, t, CH$_2$OH), 4.1(2H, t, OCH$_2$), 7.0 (2H, d, aromatic), 7.6 (2H, d, aromatic), 8.0 (2H, d, aromatic), 8.7 (2H, d, aromatic); ^{13}C NMR (75 MHz, DMSOd$_6$): δ 25.67, 29.27, 62.41, 68.19, 114.86, 116.21, 125.62, 146.77, 151.01, 157.49, 162.67.

3.4.5. Preparation of 4(5-Bromo-*n*-pentyloxy)phenyl,4'-azopyridine (14)

To a solution of 4-hydroxyphenyl,4'-azopyridine (**2**, 300 mg, 1.5 mmol) and potassium carbonate (1.25 g, 9 mmol) in dimethylformamide was added dibromopentane (0.3 mL, 2.3 mmol). The mixture was heated at 100 °C for 12 h. The reaction mixture was cooled and added to ice-cold water followed by extraction with dichloromethane. The organic layer was washed with water and dried over anhydrous sodium sulfate. The residue was chromatographed on silical gel (100-200 mesh) using chloroform to give 38 mg (yield 50%) of **14**, mp. 85-87 °C.

^{1}H NMR (300 MHz, CDCl$_3$): δ 1.5-1.9 (6H, m, CH$_2$), 3.7 (2H, t, CH$_2$Br), 4.1(2H, t, OCH$_2$), 7.0 (2H, d, aromatic), 7.6 (2H, d, aromatic), 7.9 (2H, d, aromatic), 8.7 (2H, d, aromatic); ^{13}C NMR (75 MHz, CDCl$_3$): δ 22.35, 28.90, 32.37, 62.67, 68.30, 114.88, 116.30, 125.68, 146.77, 150.71, 157.69, 162.92.

3.4.6. Preparation of 4(5-Hydroxy-*n*-pentyloxy)phenyl,4'-azopyridine (15)

A mixture of 4(5-bromo-*n*-pentyloxy)phenyl,4'-azopyridine (**14**, 50 mg, 0.1 mmol) and potassium carbonate (200 mg, 1.4 mmol) in dimethylformamide (aqueous, 1%) was heated at 100 °C for 12 h. The reaction mixture was cooled, and added to cold water and extracted with dichloromethane. The organic layer was washed with water and dried over anhydrous sodium sulfate. The crude mixture was chromatographed on silica gel (100-200 mesh) using chloroform to give a product 7 mg (25%), mp. 97-98 °C.

IR v_{max} (KBr): 3284, 2934, 2869, 1597, 1467, 1416, 1325, 1251, 1138, 1063, 915, 840 cm^{-1}; UV λ_{max} (toluene): 354 nm ($\varepsilon = 18,686$ M^{-1}cm^{-1}); ^{1}H NMR (300 MHz, CDCl$_3$): δ 1.5-1.9 (6H, m, CH$_2$), 3.9 (2H, t, CH$_2$OH), 4.1(2H, t, OCH$_2$), 7.0 (2H, d, aromatic), 7.6 (2H, d, aromatic), 7.9 (2H, d, aromatic), 8.7 (2H, d, aromatic); ^{13}C NMR (75 MHz, CDCl$_3$): δ 22.35, 28.90, 32.36, 62.69, 68.28, 114.86, 116.23, 125.63, 146.74, 150.97, 157.69, 162.83.

3.4.7. General Procedure for the Preparation of Cholest-5-en-3-ol-(3β)[4-(*n*-alkyloxy)phenylpyridylazo]carbonate (16a-d)

To a solution of 4-(hyroxy-*n*-alkyloxy)phenyl,4'-azopyridine in benzene, cholesteryl chloroformate in benzene was added. The reaction mixture was refluxed for 2 h. It was cooled to room temperature and filtered. The filtrate was

concentrated and it was purified by column chromatography (silica gel 100-200 - mesh) using benzene as eluent.

Cholest-5-en-3-ol-(3β)[4-(*n*-ethyloxy)phenylpyridylazo]carbonate (16a)

Mp. 130 °C (yield 36%); IR v_{max} (KBr): 2951, 1744, 1601, 1456, 1251, 1146, 1004, 841 cm^{-1}; UV λ_{max} (toluene): 349 nm (ε = 18,504 M^{-1}cm^{-1}); ^{1}H NMR (300 MHz, CDCl$_3$): δ 0.6-2.4 (44H, m, cholesteric), 4.3 (2H, t, CH$_2$), 4.5 (3H, cholesteric 1H and 2H -OCH$_2$), 5.4 (1H, m, vinylic), 7.1 (2H, d, aromatic), 8.0 (2H, d, aromatic), 8.2 (2H, d, aromatic), 8.8 (2H, d, aromatic); ^{13}C NMR (75 MHz, CDCl$_3$): δ 11.83, 19.23, 22.53, 22.79, 23.79, 27.98, 31.81, 35.75, 39.49, 42.29, 49.98, 56.12, 56.67, 65.27, 115.33, 118.31, 123.12, 126.80, 139.17, 145.33, 147.26, 154.33, 163.58.

Cholest-5-en-3-ol-(3β)[4-(*n*-propyloxy)phenylpyridylazo]carbonate (16b)

Mp. 125 °C (yield 50%); IR v_{max} (KBr): 2956, 1742, 1628, 1597, 1501, 1464, 1403, 1330, 1254, 1141, 1049, 959, 840 cm^{-1}; UV λ_{max} (toluene): 352 nm (ε = 17,600 M^{-1}cm^{-1}); ^{1}H NMR (300 MHz, CDCl$_3$): δ 0.6-2.4 (46H, m, aliphatic), 4.3 (2H, t, CH$_2$), 4.5(3H, cholesteric 1H and 2H -OCH$_2$), 5.4 (1H, m, vinylic), 7.1 (2H, d, aromatic), 8.0 (2H, d, aromatic), 8.2 (2H, d, aromatic), 8.8 (2H, d, aromatic); ^{13}C NMR (75 MHz, CDCl$_3$): δ 11.81, 18.67, 19.21, 20.99,

22.52, 22.77, 23.78, 24.23, 27.66, 27.96, 28.57, 31.79, 31.86, 35.73, 36.14, 36.49, 39.47, 39.66, 49.94, 56.64, 64.11, 64.52, 76.56, 76.98, 77.40, 77.97, 114.87, 116.24, 122.99, 125.61, 128.29, 139.22, 146.88, 150.84, 154.43, 162.43.

Cholest-5-en-3-ol-(3β)[4-(*n*-butyloxy)phenylpyridylazo]carbonate (16c)

Mp. 139-140 °C (yield 31%); IR v_{max} (KBr): 2957, 2866, 1741, 1596, 1502, 1462, 1390, 1315, 1262, 1137, 1025, 957, 839, 798 cm^{-1}; UV λ_{max} (toluene): 354 nm (ε = 23,404 M^{-1}cm^{-1}); ^{1}H NMR (300 MHz, CDCl$_3$): δ 0.6-2.0 (46H, m, aliphatic), 2.2 (2H, m, CH$_2$), 4.1 (2H, t, OCH$_2$), 4.3 (2H, t, OCH$_2$), 4.5(1H, m, OCH), 5.4 (1H, m, vinylic), 7.1 (2H, d, aromatic), 7.7 (2H, d, aromatic), 7.9 (2H, d, aromatic), 8.7 (2H, d, aromatic); ^{13}C NMR (75 MHz, CDCl$_3$): δ 11.84, 18.70, 22.54, 25.44, 25.61, 31.84, 38.03, 39.50, 39.71, 42.30, 56.14, 56.68, 67.16, 67.75, 114.94, 116.57, 122.97, 125.83, 139.32, 146.88, 150.09, 154.58, 162.91.

Cholest-5-en-3-ol-(3β)[4-(*n*-pentyloxy)phenylpyridylazo]carbonate (16d)

Mp. 131-132 °C (yield 73%); IR v_{max} (KBr): 2951, 1746, 1596, 1504, 1468, 1407, 1326, 1265, 1137, 1023, 959, 842, 792 cm^{-1}; UV λ_{max} (toluene): 352 nm (ε = 20,439 M^{-1}cm^{-1}); ^{1}H NMR (300 MHz, CDCl$_3$): δ 0.6-2.0 (48H, m, aliphatic), 2.2 (2H, m, CH$_2$), 4.1 (2H, t, OCH$_2$), 4.3 (2H, t, OCH$_2$), 4.5(1H, m, OCH), 5.4 (1H, m, vinylic), 7.0 (2H, d, aromatic), 7.7 (2H, d, aromatic), 7.9 (2H, d, aromatic),

8.8 (2H, d, aromatic); ^{13}C NMR (75 MHz, CDCl$_3$): δ 11.84, 18.69, 19.24, 22.44, 22.54, 22.80, 23.80, 27.99, 28.20, 28.43, 28.73, 31.82, 31.88, 35.77, 36.17, 39.50, 39.70, 42.29, 49.98, 56.13, 56.67, 67.46, 68.11, 114.86, 116.33, 122.94, 125.70, 139.33, 146.76, 150.73, 154.62, 162.85.

3.5. Conclusions

Hydrogen bonded mesomorphic materials were prepared from cholesterol containing a hydrogen bond acceptor such as cholest-5-en-3-ol-(3β)[4-phenyl,4'-pyridylazo]carbonate (4) with a series of hydrogen bond donors such as 4-*n*-alkyloxybenzoic acids (5a-e) and 4-*n*-alkyloxycinnamic acids (9a-e). These heterointermolecular supramolecules (6a-e, 10a-e) exhibit well defined mesophases, which were confirmed by POM as well as DSC. The assemblies 6a-e show S$_A$ phases over a wide range of temperatures, whereas in 10a-d, the lower homologues (n = 4 and 6) show cholesteric LC phases, and when n = 8 and 10, S$_A$, TGB and cholesteric phases were observed. Sudden cooling of the complexes (10a-d) from cholesteric temperatures to 0 °C resulted in the formation of stable glasses. The glassy phases thus formed show the characterstic cholesteric colours, which were extremely stable at room temperature (> eight months). In conclusion, the present study shows, for the first time, that low molecular weight cholesteric GLCs can be conveniently

generated *via* heterointermolecular hydrogen bonding between suitable donor and acceptor molecules.

3.6. References

1.   F. Reinitzer, *Monatsh* **1888**, *9*, 421.

2.   H. L. de Vries, *Acta. Cryst.* **1951**, *4*, 219.

3.   J. L. Fergason, *Mol. Cryst.* **1966**, *1*, 293.

4.   H. Stegemeyer, K. J. Mainusch, *Chem. Phys. Lett.* **1970**, *6*, 5.

5.   J. L. Fergason, *Appl. Opt.* **1968**, *7*, 1729.

6.   W. E. Haas, J. Adams, *Appl. Opt.* **1968**, *7*, 1203.

7.   G. H. Heilmeier, J. E. Goldmacher, *Appl. Phys. Lett.* **1968**, *13*, 132.

8.   J. L. Fergason, *Scientific American* **1964**, *211*, 77.

9.   J. L. Fergason, *Mol. Cryst.* **1966**, *1*, 309.

10.   W. E. Haas, J. Adams, J. Wysocki, *Mol. Cryst. Liq. Cryst.* **1969**, *7*, 371.

11.   W. E. Haas, K. F. Nelson, J. E. Adams, G. A. Dir, *J. Electrochem. Soc.* **1974**, *121*, 1667.

12.   Mathew George, V. A. Mallia, P. K. S. Antharjanam, M. Saminathan, S. Das, *Mol. Cryst. Liq. Cryst.* **2001**, *350*, 125.

13.   H-K. Lee, K. Doi, H. Hirada, O. Tsutsumi, A. Kanazawa, T. Shiono, T. Ikeda, *J. Phys. Chem. B.* **2000**, *104*, 7023.

14.   P. N. Keating, *Mol. Cryst. Liq. Cryst.* **1969**, *8*, 315.

15.   J. L. Fergason, N. N. Goldberg, R. J. Nadalin, *Mol. Cryst.* **1966**, *1*, 309.

16.   O. S. Selawry, H. S. Selawry, J. F. Holland, *Mol. Cryst.* **1966**, *1*, 495.

17.   W. E. Woodmansee, *Appl. Optics* **1968**, *7*, 1721.

18.   J. Hansen. J. L. Fergason, A. Okaya, *Appl. Optics* **1964**, *3*, 987.

19.   F. Keilmann, *Appl. Optics* **1970**, *9*, 1319.

20.   K. Iizuka, *Electronics Lett.* **1969**, *5*, 26.

21.   S. Chandrasekhar, B. R. Ratna, *Mol. Cryst. Liq. Cryst.* **1976**, *35*, 109.

22.   P. H. Keyes, H. T. Weston, W. B. Daniels, *Phys. Rev. Lett.* **1973**, *31*, 628.

23.   R. Shashidhar, S. Chandrasekhar, *J. de Physique* **1975**, *36*, C1.

24.   G. Friedel, *Ann. Physique.* **1922**, *18*, 273.

25.   J. Adams, W. E. Haas, *Mol. Cryst. Liq. Cryst.* **1971**, *15*, 27.

26.   J. Adams, W. E. Haas, J. Wysocki, *J. Phys. Rev. Lett.* **1969**, *22*, 92.

27.   T. Nakagiri, H. Kodama, K. K. Kobayashi, *Phys. Rev. Lett.* **1971**, *27*, 564.

28.   A. D. Buckingam, G. P. Ceaser, M. B. Dunn, *Chem. Phys. Lett.* **1969**, *3*, 540.

29.   F. D. Saeva, *Mol. Cryst. Liq. Cryst.* **1973**, *23*, 171.

30.   P. J. Shannon, *Macromolecules* **1984**, *17*, 1873.

31.   H. Finkelmann, J. Koldehoff, H. Ringsdorf, *Angew. Chem. Int. Ed. Engl.* **1978**, *17*, 935.

32. W. Mahler, M. Panar, *J. Am. Chem. Soc.* **1972**, *94*, 7195.

33. T. Tachibana, E. Oda, *Bull. Chem. Soc. Jpn.* **1973**, *46*, 2583.

34. K. Tsuji, M. Sorai, S. Seki, *Bull. Chem. Soc. Jpn.* **1971**, *44*, 1452.

35. N. Tamaoki, A. V. Parfenov, A. Masaki, H. Matsuda, *Adv. Mater* **1997**, *9*, 1102.

36. N. Tamaoki, G. Kruk, H. Matsuda, *J. Mater. Chem.* **1999**, *9*, 2381.

37. P. Palffy-Muhoray, *Nature* **1998**, *391*, 745.

38. V. A. Mallia, S. Das, *Liq. Cryst.* **2001**, *28*, 259.

39. V. A. Mallia, P. K. S. Antharjanam, S. Das, *Chem. Lett.* **2001**, 000.

40. T. Kato, J. M. J. Frechet, P. G. Wilson, T. Saito, T. Uryu, A. Fujishima, C. Jin, F. Kaneuchi, *Chem. Mater.* **1993**, *5*, 1094.

41. T. Kato, J. M. J. Frechet, *J. Am. Chem. Soc.* **1989**, *111*, 8533.

42. Z. Sideratou, C. M. Paleos, *Mol. Cryst. Liq. Cryst.* **1995**, *265*, 19.

43. Z. Sideratou, D. Tsiourvas, C. M. Paleos, A. Skoulios, *Liq. Cryst.* **1997**, *22*, 51.

44. C. M. Paleos, D. Tsiourvas, *Angew. Chem. Int. Ed. Engl.* **1995**, *34*, 1696.

45. D. Demus, L. Richter, *Texture of Liquid Crystals*, Weinheim, New York, **1978**.

46. H. Kelker, R. Hatz, *Handbook of Liquid Crystals*, Verlag Chemie, Weinheim, **1980**.

47. S. L. Johnson, K. A. Rumon, *J. Phys. Chem.* **1965**, *69*, 74.

48. S. E. Odinokov, A. A. Mashkovsky, V. P. Glazunov, A. V. Iogansen, B. V. Rassadin, *Spectrochemica Acta* **1976**, *32A*, 1355.

49. J. W. Goodby, M. A. Waugh, S. M. Stein, E. Chin, R. Pindak, J. S. Patel, *Nature* **1989**, *337*, 449.

50. J. W. Goodby, M. A. Waugh, S. M. Stein, E. Chin, R. Pindak, J. S. Patel, *J. Am. Chem. Soc.* **1989**, *111*, 8119.

51. S. W. Cha, J-I. Jin, M. Laguerre, M. F. Achard, F. Hardouin, *Liq. Cryst.* **1999**, *26*, 1325.

52. A. Abe, H. Furuya, R. N. Shimizu, S. Y. Nam, *Macromolecules* **1995**, *28*, 96.

53. A. Abe, S. Y. Nam, *Macromolecules* **1995**, *28*, 90.

CHAPTER 4

SYNTHESIS AND STUDIES OF SOME HYDROGEN BONDED SUPRAMOLECULAR DENDRIMERIC SYSTEMS

4.1. Abstract

First- and second-generation supramolecular dendrimeric moieties have been synthesized and characterized. These assemblies were prepared by the intermolecular hydrogen bonding interaction between hydrogen bond donors such as 3,4,5-tri-*n*-dodecyloxybenzoic acid and 3,4,5-tris[3',4',5'-tris(*n*-dodecane-1-yloxy)-benzyloxy]benzoic acid with hydrogen bond acceptors such as 4,4'-azobipyridine (ABP), 4,4'-bipyridylethylene (BPE) and 4,4'-bipyridine (BP). The first-generation dendrimeric assemblies obtained by complexing 3,4,5-tri-*n*-dodecyloxybenzoic acid with ABP, BPE and BP did not possess LC phases. The second-generation hydrogen bonded assemblies however show cubic LC phases, which were characterized by POM, DSC and SAXRD. Sudden cooling of these materials from their LC temperature in an ice bath resulted in the formation of highly transparent ordered glassy phases, which were extremely stable at room

temperature (> 1 year). Photochemical transformations of the azo and stilbene chromophores of the hydrogen bonded assemblies in the cubic glassy liquid crystalline phases were also explored.

4.2. Introduction

Molecules possessing highly branched structures are labeled as dendrimers or cascade molecules. The term cascade molecule indicates that such compounds usually originate from a stepwise synthetic procedure whereas the word dendrimer is a combination of the Greek word dendron (tree branch) and meron (part).[1-4] Evolving around a core atom or molecule, dendrimers possess repeating generations. The number of publications on this topic has been steadily increasing[1-73]since the first cascade molecules were reported about twenty years ago.[20] Dendrimers were first reported in 1979 by Denkewalter et al., in a patent on branched molecules based on amino acids.[23] In 1990 Tomalia revived the concept of highly branched monodisperse molecules from polyamidoamine (PAMAM).[62] Subsequently polyalcohol,[39] polyaryl[71] and polypropylene-based dendrimers[16] have been reported. Xu et al., have succeeded in preparing a soluble dendrimer with molecular weight 30,000 emu.[72] The heaviest dendrimer so far reported has a molecular weight of more than 3 million emu.[61]

Dendrimeric molecules can be synthesized using two fundamentally

different strategies known as the divergent and convergent methods. In the divergent method, one branching unit after another is successively attached to the core molecule. Hence the multiplicity of the number of peripheral group is dependent on the branching multiplicity. This way the dendrimer can be built up step by step until steric effects prevent further reactions of the end groups. This effect is labelled as starburst effect.[63] In the convergent method, the skeleton is constructed stepwise starting from the outer end groups towards the inside and the branched structure is finally reacted with a core molecule to yield the dendrimer. The advantage of the convergent method over the divergent approach is that the dendrimers formed will be free from defects. In the case of the divergent method, as the branching of the dendrimers increases a large number of the reactions have to be performed on a single molecule. This increases the chance of forming byproducts, which are difficult to separate. However, both types of synthetic methodologies have been successfully used to synthesize a large variety of dendrimeric molecules.

Recent studies indicate that dendrimers may find application in a number of areas including energy harvesting, host-guest chemistry, drug release, ion sensing, catalysis, magnetic imaging and also in information technology.[1,3,4] Two topics of current interest in the study of dendrimers are (a) preparation of photoactive

dendritic molecules and (b) synthesis and study of dendrimeric mesogens.

Jung and McGrath have reported the synthesis and studies of benzyl aryl ether dendrimers containing azobenzene central linkers. Photoinduced isomerization of the azobenzene moiety of these molecules has been investigated.[29] Recently, Jiang and Aida have reported the photoisomerization of dendrimers by harvesting low energy photons by the branched units of dendrimers.[27] Several studies have been carried out on the photoisomerization of azobenzene groups attached to the periphery of dendrimers.[5,8,9,29,67] More recently, photoactive dendritic LCs containing azobenzene[17] as well as cinnamoyl[18] moieties have been reported.

In the solution state it is well known that dendrimers adopt a spherical shape. Studies on the melt state of dendrimeric molecules suggest that intermolecular interaction between dendritic molecules result in the formation of spherical or rod shape LCs.[41,44,46] Examples of rod shaped structures can be found in the studies on hyperbranched polymers by Percec *et al.*.[34,45] They have synthesized a series of hyperbranched polymers through the polyetherification of branched monomers under heterogeneous conditions, followed by *insitu* alkylation of the products with aliphatic or benzyl bromides (Chart 4.1.).[34,45]
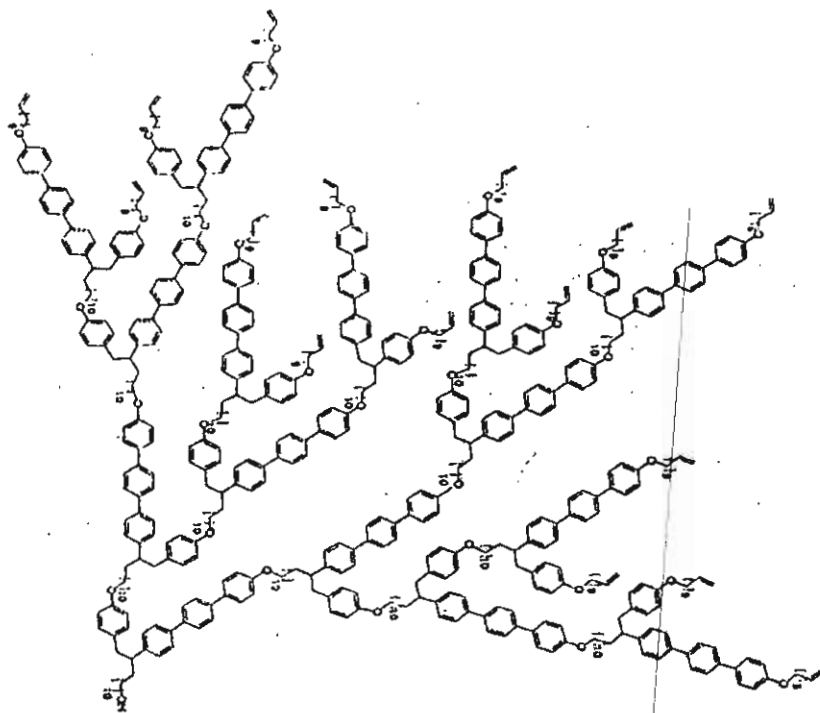
Chart 4.1.

The proposed rod arrangement of such molecules in the nematic phase is shown in Figure 4.1.[34,45] Smectic and cholesteric LC phases also have been reported in dendrimeric molecules.[13,14,35,37,59]
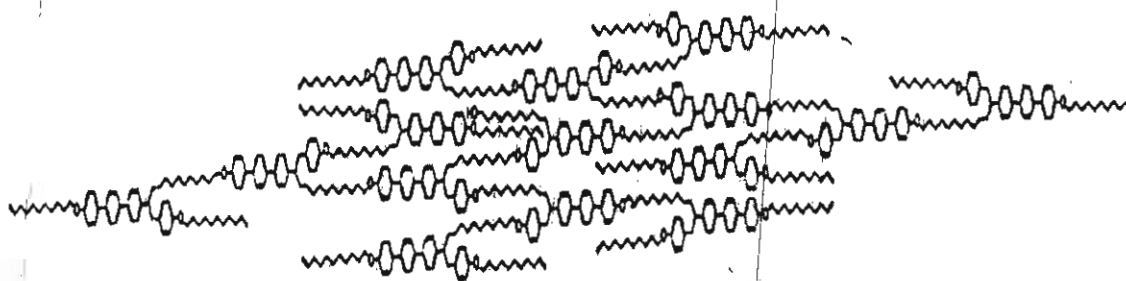

Figure 4.1. The proposed rod shape of nematic hyperbranched polymer.

Percec and coworkers have tried to elucidate the supramolecular structure of dendrimers in their LC states. They described the properties of dendrons in terms of tapered shapes and focal receptor moieties (Figure 4.2.).
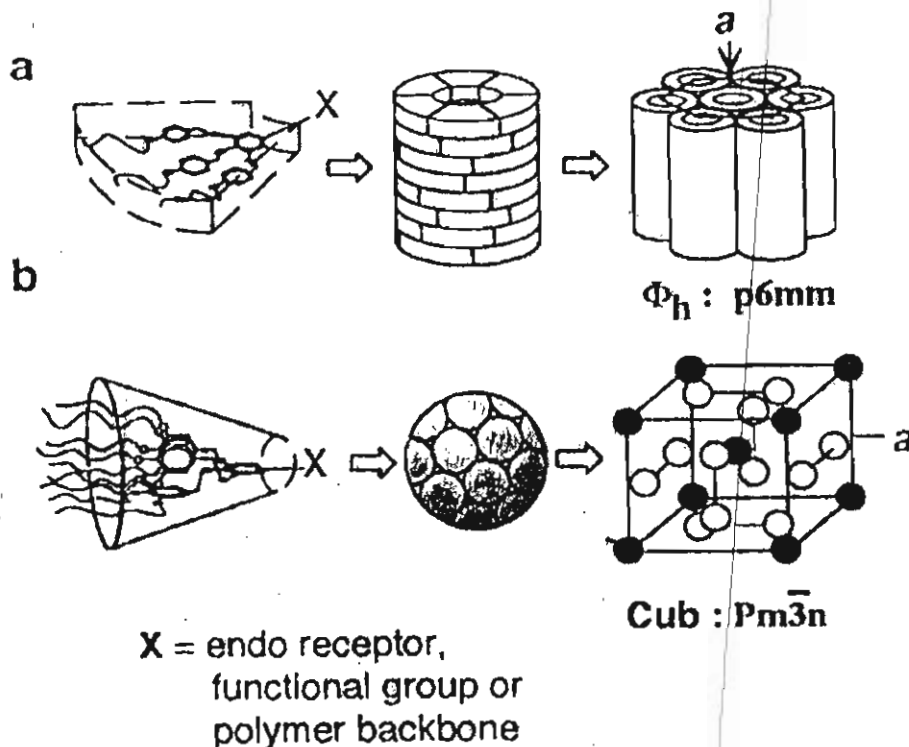

Figure 4.2. Self-organization of structurally different dendron in the LC phase (adapted from reference 73).

They have used gallic acid with long alkyl chains as the branching unit. In the melt these substances show columnar LC behaviour. They have been able to tune the LC properties of such dendrimers by attaching different suitable functional groups at the focal positions of the gallic acid derivatives (Figure 4.2.). Recently, Percec *et al.*, have found a correlation between the macromolecular

superstructure of the dendrimer and degree of polymerization (Figure 4.3.).[50] Low

degree of polymerization results in the formation of a spherical molecule, whereas

a higher degree of polymerization results in the formation of cylindrical molecules.

In this manner, the macroscopic architecture could be synthetically controlled
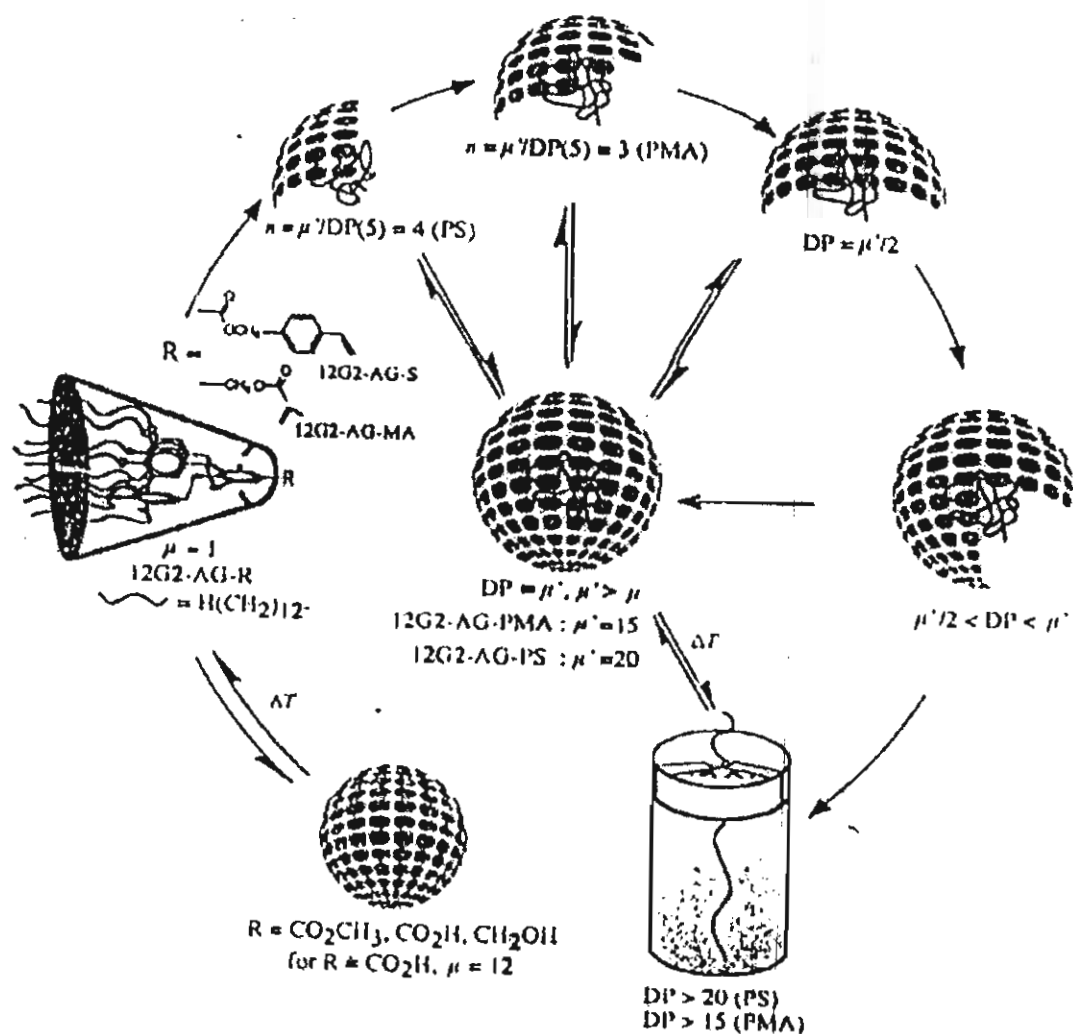
(Figure 4.3.).[11,40,42,43,45,47-57,66,73]

Figure 4.3. Control of shape of dendritic polymers in LC phase (adapted from reference 50).

In this Chapter, the preparation and characterization of hydrogen bonded dendrimeric molecules are described. These molecules were prepared *via* hydrogen bonding between branched benzoic acid derivatives and hydrogen bond acceptors such as 4,4'-azobipyridine (ABP), 4,4'-bipyridylethylene (BPE) and 4,4'-bipyridine (BP). LC properties of these dendrimeric hydrogen bonded supramolecular assemblies have been examined in detail. Photochemical properties of these materials containing photoactive groups have been investigated.

4.3. Results and Discussion

4.3.1. First-Generation Dendrimeric Assemblies

Supramolecular assemblies were prepared by complexing 3,4,5-tri-*n*-dodecyloxybenzoic acid with hydrogen bonded acceptors such as ABP, BPE and BP. Hydrogen bonded supramolecular assemblies investigated in this section are shown in Chart 4.2.

4.3.1.1. Synthesis and Characterization

3,4,5-Tri-*n*-dodecyloxybenzoic acid (6) was synthesized as per reported procedure[74] (Scheme 4.1.). Gallic acid was first reacted with methanol in the presence of sulphuric acid to obtain methyl gallate (5, Scheme 4.1.) Alkylation of the hydroxyl

groups of the ester by *n*-dodecyl bromide yielded 3,4,5-tri-*n*-dodecylether of methyl gallate (7, Scheme 4.1.). The ester (7) was subsequently hydrolyzed in the presence of ethanolic potassium hydroxide which on acidification with concentrated hydrochloric acid gave the compound 6.
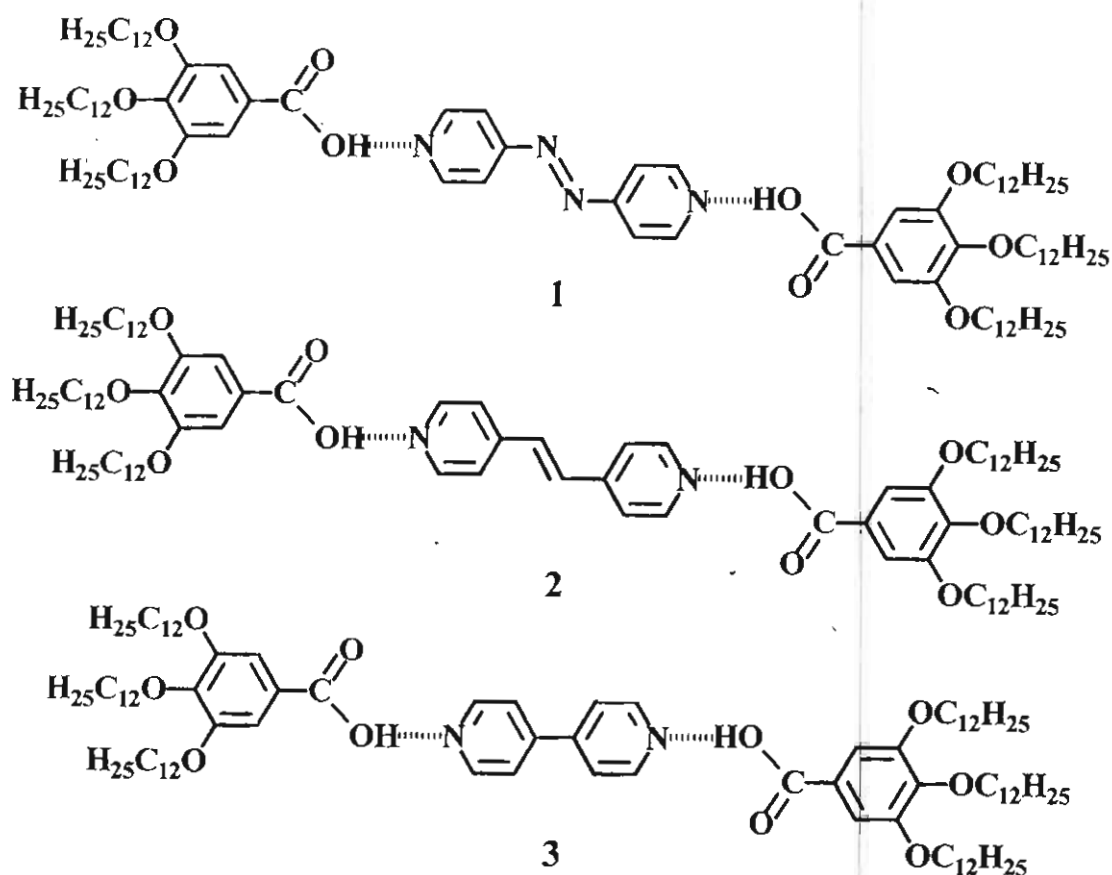

Chart 4.2.

All compounds described here were characterized on the basis of spectral data and the details are provided under the Experimental Section (4.4.). The hydrogen bonded

complexes were synthesized by mixing 2:1 molar quantities of **6** with ABP, BPE and BP thoroughly above the melting point of the mixtures for a few minutes.[75] The mixture was then allowed to cool slowly to yield the LC materials **1-3** (Chart 4.2.).
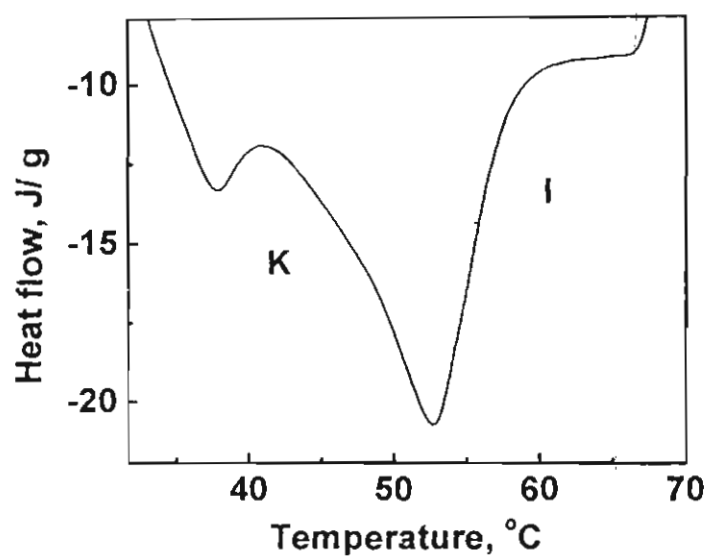

$R = C_{12}H_{25}$
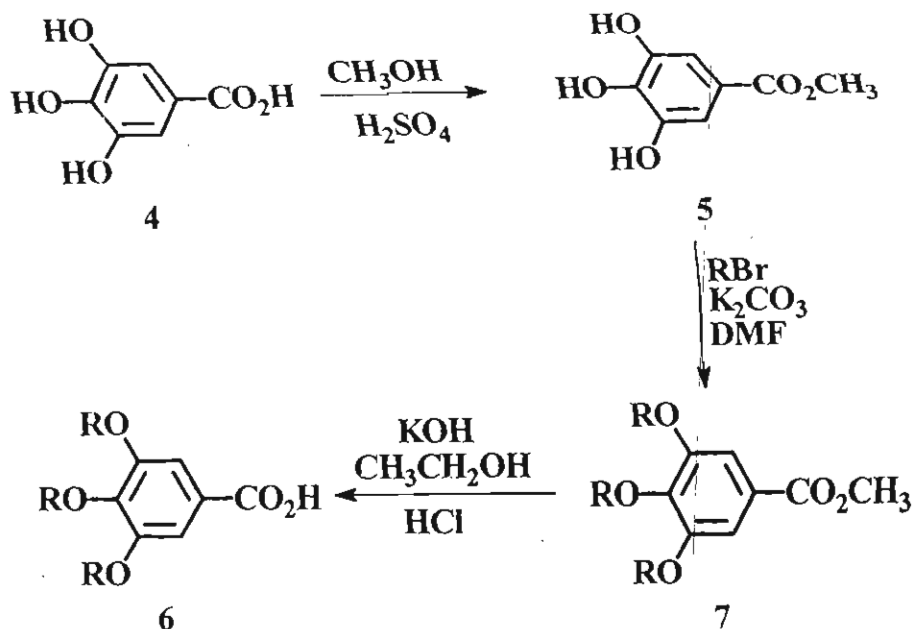
Scheme 4.1.

POM and DSC studies reveal that these hydrogen bonded assemblies did not show any LC Phases. The DSC plot obtained for **1** shows two endotherms, characteristic of crystal to crystal transition at 30 °C and crystal to isotropic transition at 55 °C (Figure 4.4.). The melting temperatures of these assemblies are summarized in Table 4.1.
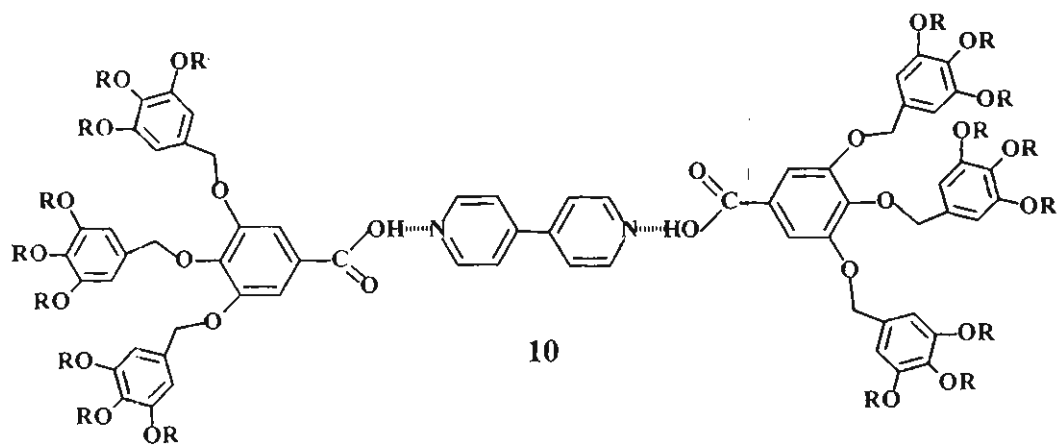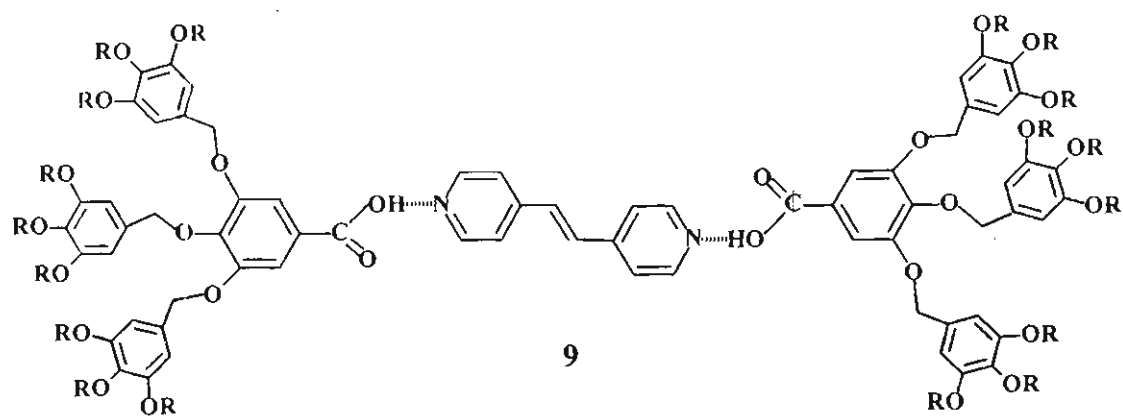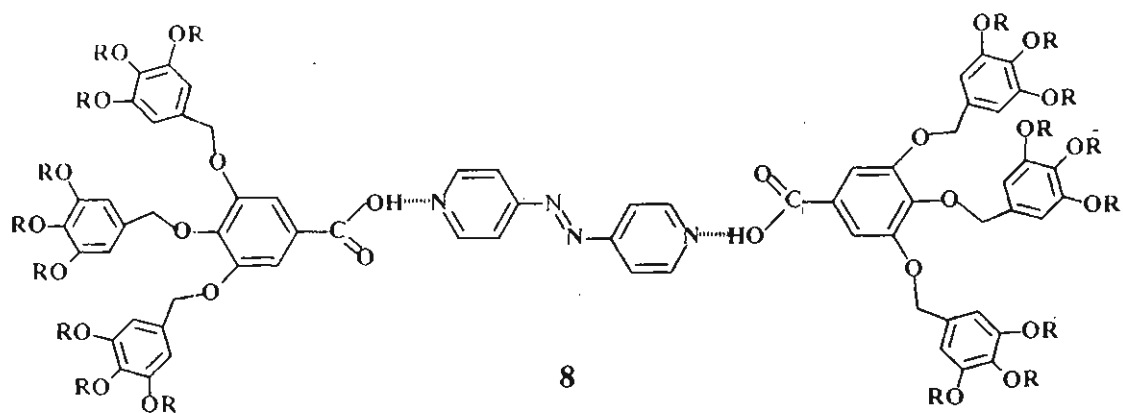
Table 4.1. Phase transition temperatures of 1-3.

	Melting temperature in °C
1	K 55 I
2	K 50 I
3	K 53 I

Figure 4.4. DSC thermogram of 1 showing first heating scan.

4.3.2. Second-Generation Dendrimeric Assemblies

The second-generation dendrimeric assemblies investigated in the present study are shown in Chart 4.3.
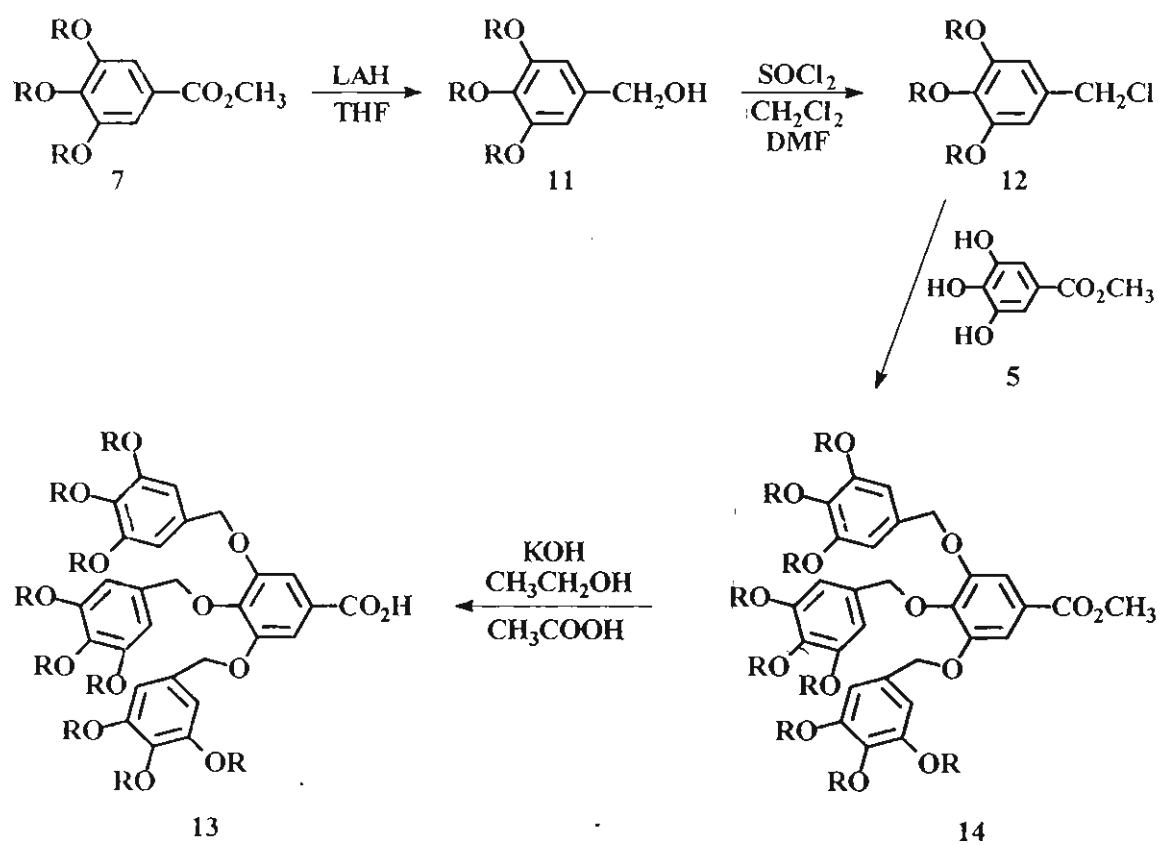
8

9

10

$$R = C_{12}H_{25}$$

Chart 4.3.

4.3.2.1. Synthesis and Characterization

The gallic acid derivative **13**, required for the preparation of the hydrogen bonded assemblies shown in Chart 4.3. was synthesized according to the reported procedure[11] (Scheme 4.2.).

$$R = C_{12}H_{25}$$

Scheme 4.2.

The ester group of the 3,4,5-tri-*n*-dodecylether of methyl gallate (**7**, Scheme 4.2.) was reduced using lithium aluminium hydride to give the

corresponding benzyl alcohol (**11**, Scheme 4.2.). Chlorination of the alcohol (**11**) with thionyl chloride in the presence of catalytic amounts of dimethylformamide resulted in the formation of 3,4,5-tri-*n*-dodecyloxybenzyl chloride (**12**, Scheme 4.2.). The second-generation ester of gallic acid was obtained by the alkylation of methyl gallate by 3,4,5-tri-*n*-dodecyloxybenzyl chloride (**12**) in the presence of potassium carbonate in dimethylformamide. Purification by column chromatography followed by recrystallization gave **14** (Scheme 4.2.). The ester (**14**, Scheme 4.1.) was hydrolyzed by refluxing in ethanolic potassium hydroxide (10 N) for 3.5 h. Acidification with acetic acid gave **13** (Scheme 4.2.).

All the compounds described here were characterized on the basis of spectral data and the details are provided in the Experimental Section (4.4.). The hydrogen bonded complexes were synthesized by mixing 2:1 molar quantities of **13** with ABP, BPE and BP thoroughly above the melting point of the mixtures for a few minutes. The mixture was then allowed to cool slowly to yield the LC materials **8-10** (Chart 4.3.).

4.3.2.2. Liquid Crystalline Properties

The phase transition behaviour of the supramolecular assemblies were characterized using polarizing optical microscopy (POM) and differential scanning calorimetry (DSC). The phase was finally confirmed based on the X-ray diffraction techniques. POM studies of **8** shows that the supramolecular assembly

melts at 82.2 °C to an isotropic phase. Under the POM, 8 did not show any

characteristic birefringent LC textures. However, DSC studies of 8 indicate two

endotherms at 82.27 (ΔH = 128.7 kJmol^{-1}, ΔS = 357.4 JK^{-1}mol^{-1}) and 108.5 °C (ΔH =

16.8 kJmol^{-1}, ΔS = 43.9 JK^{-1}mol^{-1} (Figure 4.5.)). This strongly suggests the

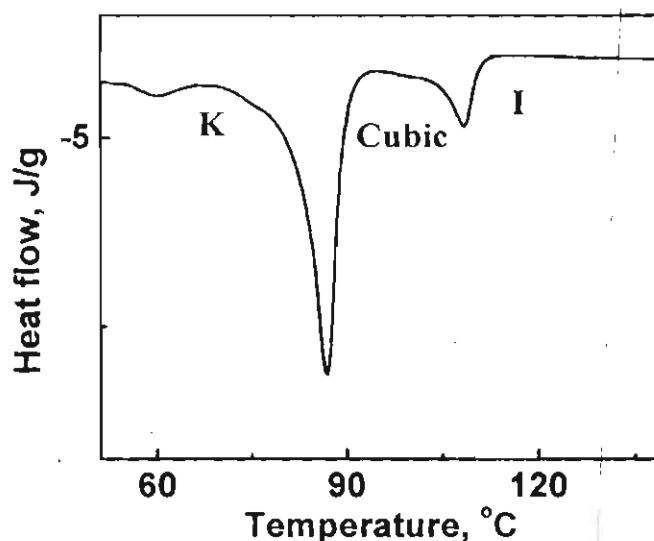existence of a cubic mesophase in the range 82.27 °C to 108.5 °C.

Figure 4.5. DSC thermogram of 8 showing the first heating scan.

Cubic LC phases, which are generally observed in lyotropic LCs can exist either

as cubic array of micelles (I phases) or as bicontinuous phases (V phases). These phases

possess a cubic symmetry. Due to the absence of anisotropy in these phases they do not

show the characteristic birefrigent texture under the POM, which is normally observed

for the other LC phases. The structure of cubic phases have been described using three

models, namely the micellar model, the interconnecting rod model and infinite periodic

minimal surface model (IPMS). The first one describes the formation of micellar cubic phases in lyotropic systems and the latter two are more applicable to the so called bicontinuous lyotropic cubic phases and cubic phases of most thermotropic systems. In lyotropic systems the rods are presumed to consist of polar head groups, with the chains filling the space between. Extending this model to thermotropic system suggests that the rods consist of the central, rigid part of the molecule, with the chains extending to fill the space in between. In the IPMS model, the arrangement of the rods is related to the minimal surfaces since the minimal surfaces divide the space into parts.

Earlier reports [76,77] show that calamitic materials can also form cubic LCs (Chart 4.4.).
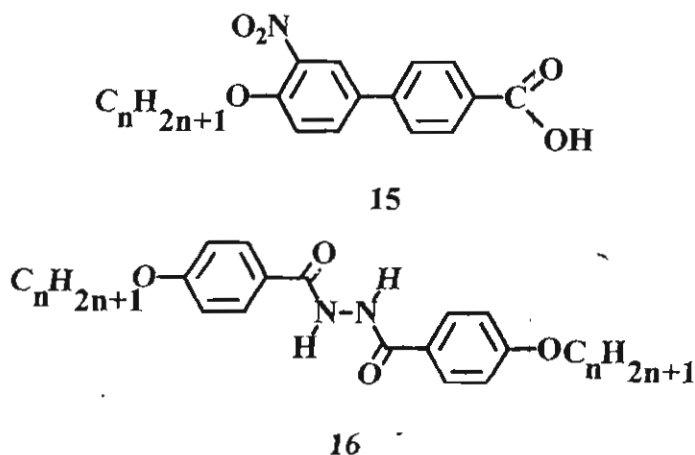

15

16

Chart 4.4.

Recent reports by Lee *et al.*[78] and Nishikawa *et al.*[79] show that hydrogen bond mediated rod-coil copolymers also exhibit cubic LC phases (Chart 4.5.).
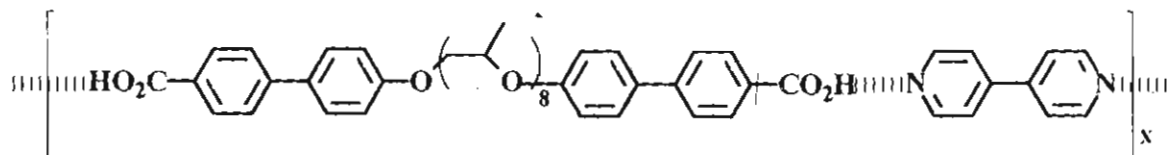
Chart 4.5.

The cubic LC phase of the supramolecular assemblies (Chart 4.2.) were confirmed by X-ray diffraction techniques. X-ray diffraction patterns of **8** at 105 °C displayed a sharp reflection in the small angled region (Figure 4.6.).
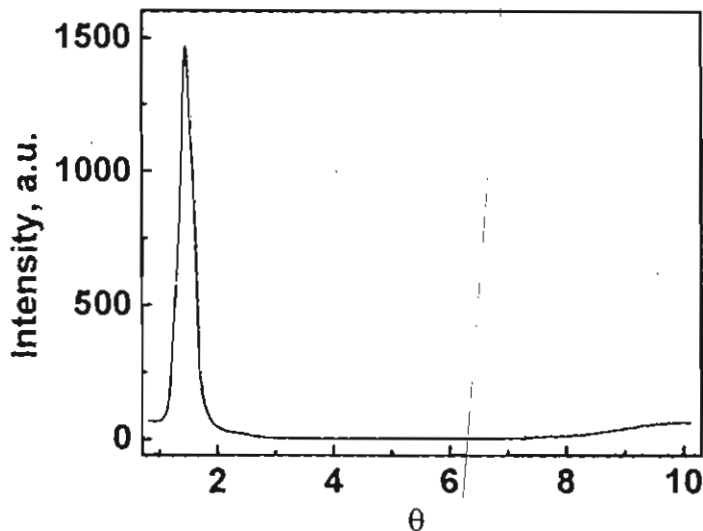
Figure 4.6. X-ray diffraction pattern of 8 at 105 °C.

At a wide angle, only a diffuse halo was observed as evidence of lack of any positional long-range order other than the three dimensional cubic packing of supramolecular units. The combination of the optical isotropy observed under

the POM and presence of sharp reflection confirms the presence of a cubic
LC phase. The supramolecular assembly **9** melts to an isotropic phase at
80.32 °C (ΔH = 197.3 kJmol^{-1}, ΔS = 557.7 JK^{-1}mol^{-1}). The DSC curve of **9** shows
only one peak at 80.32 °C (Figure 4.7.). This may be due to the energy change in
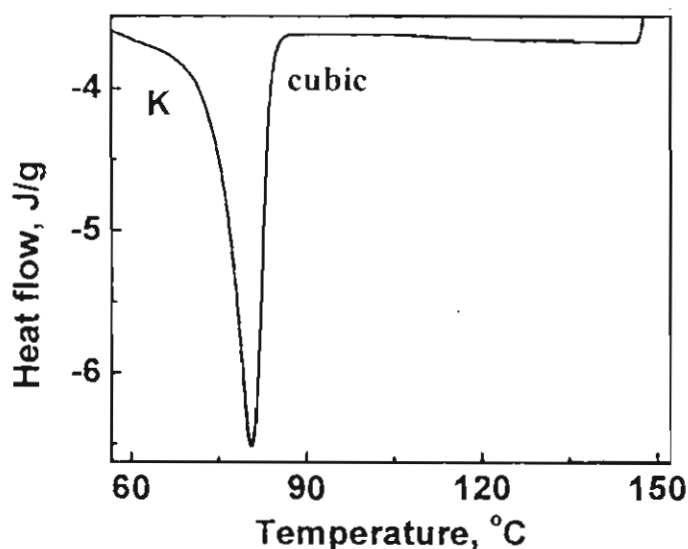the melting of cubic to isotropic being very small.

Figure 4.7. DSC thermogram of 9 showing the first heating scan.

The sharp reflection observed at 90 °C in the small angle X-ray diffraction
studies however confirms the formation of cubic LC phase (Figure 4.8.). The
phase transition temperatures as well as thermodynamic parameters of these
supramolecular dendrimeric mesogens are summarized in the Table 4.2.
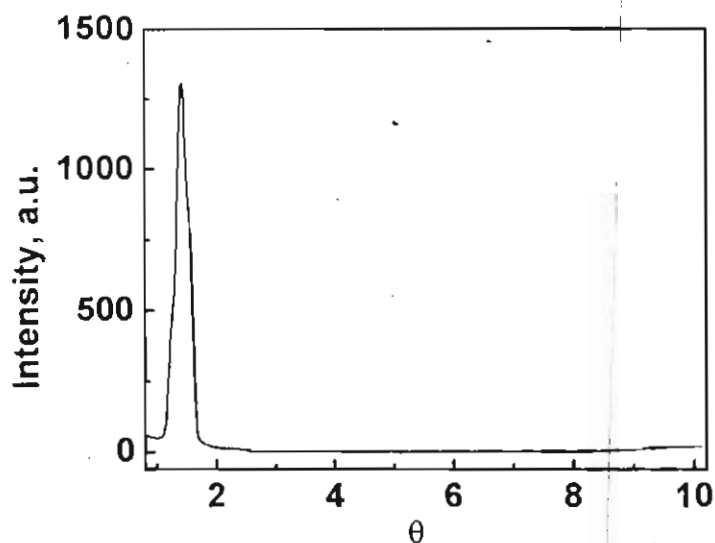
Figure 4.8. Xray diffraction pattern of 9 at 90 °C.

Table 4.2. Phase transition temperatures and thermodynamic parameters of 8-10.

	Phase transition temperature in °C†	$\Delta H_{K\text{-}LC}$ kJ mol^{-1} ($\Delta S_{K\text{-}LC}$ JK^{-1}mol^{-1})	$\Delta H_{LC\text{-}I}$ kJ mol^{-1} ($\Delta S_{LC\text{-}I}$ JK^{-1}mol^{-1})
8	K 87.3 Cubic 108.5 I	128.7 (357.3)	16.76 (43.9)
9	K 80.7 Cubic ‡	197.3 (557.7)	✿
10	K 83.5 Cubic 147.1 I	128.8 (349.6)	✿

† K = crystalline, cubic = cubic LC phase and I = isotropic phase.

‡ The isotropic point could not be determined by DSC. This may be because energy change is very small.

✿ $\Delta H_{LC\text{-}I}$ could not be determined by DSC, this may be because energy change is very small.

Similarly POM, DSC and SAXRD studies of **10** confirm the formation of cubic LC phase (Figures 4.9. and 4.10.).

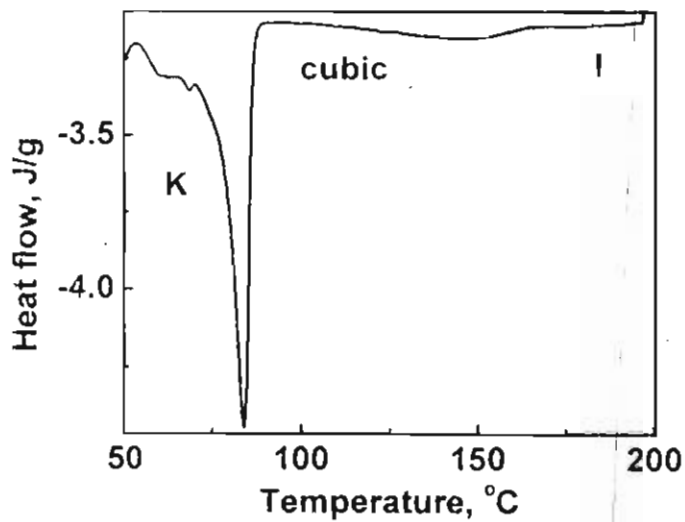
Figure 4.9. DSC thermogram of 10 showing the first heating scan.
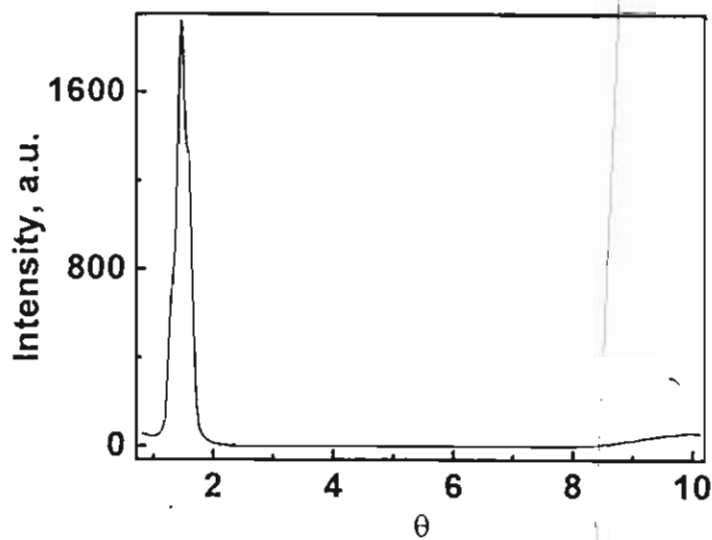
Figure 4.10. X-ray diffraction pattern of 10 at 100 °C.

4.2.2.3. Preparation and Studies of Cubic Glassy Solids

Rapid cooling of the dendritic hydrogen bonded assemblies (**8-10**) from their LC temperature in a n ice bath resulted in the formation of highly transparent ordered glassy liquid crystalline solids. These glassy LCs (GLCs) were found to be extremely stable at room temperature (> 1 year). Figure 4.11. shows the texture of the cubic glassy liquid crystal observed under the POM. This glassy solid was obtained by rapid cooling of **8** from 90 °C in an ice bath.

Figure 4.11. Optical photomicrograph of isotropic texture observed in cubic GLC of 8 at room temperature.

4.3.2.4. Photolysis of the Dendritic Supramolecular Liquid Crystals

A preliminary investigation on the effect of light on these dendritic LC materials has been carried out and these results are briefly described below.

The azopyridine moiety present in the dendritic molecule **8** and stilbyl

chromophore present in **9** can undergo phototransformations, which could result in light induced phase changes of the LC materials. Photolysis of **8** and **9** in their LC phases using UV light source however did not result in any phase change, which could be detected under a POM. A change in phase from cubic LC to crystalline phase, on photolysis could be ruled out because such a change would have been detectable under the POM. A change of phase from cubic LC to isotropic melt could however not be ruled out, since such a change would not be detectable under the POM.

The photochemical transformations of the chromophores in **8** and **9** were investigated in their GLC phase. Photoisomerization of **8** in its cubic GLC phase at ambient temperature (~25 °C) was examined by steady state photolysis, using a 200 W high-pressure mercury lamp equipped with a 325 nm band-pass filter as light source. On photolysis, the absorption around 320 nm decreases while that around 440 nm, due to the n-π^* transition of the *cis* form increases. A photostationary state was reached within 7 minutes of photolysis (Figure 4.12). The photoinduced changes in the absorption spectra were thermally fully reversible within 60 minutes of photolysis. In the case of dendrimeric supramolecular assembly **9**, photolysis for 5 minutes using 320 nm wavelength light led to permanent changes in its absorption spectrum (Figure 4.13).

Figure 4.12. Absorption spectra of 8 in cubic glassy LC, at different time intervals of photolysis using 320 nm light. Time of photolysis: (a) 0 min, (b) 2 min, (c) 4 min, (d) 7 min. Inset shows the expanded scale spectrum from 350 to 460 nm.
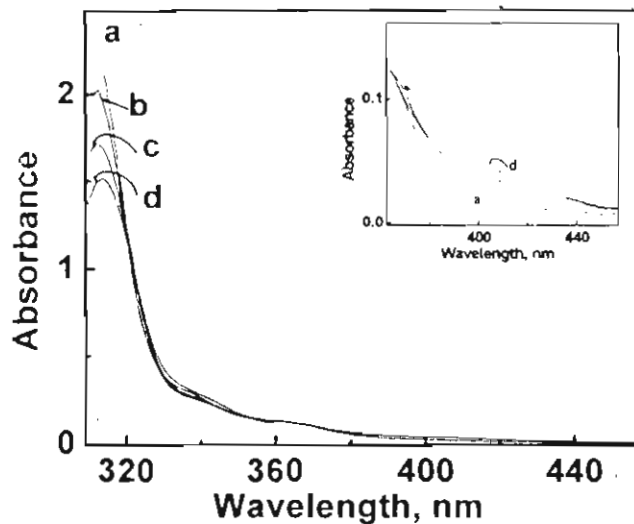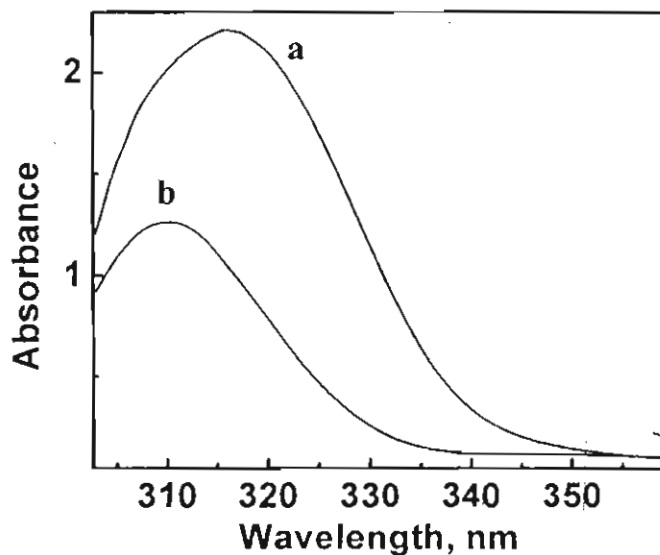

Figure 4.13. Absorption spectra of 9 in cubic glassy LC, at different time intervals of photolysis using 320 nm light. (a) Before photolysis, (b) after photolysis for 5 min.

Stilbene derivatives are known to undergo [2+2] cycloaddition,[80-82] which could lead to permanent changes in its absorption spectrum and similar processes may be occurring here.

4.4. Experimental Section

Melting points are uncorrected and were recorded on a Mel-temp II melting point apparatus. Phase transitions were observed using a Nikon HFX 35A Optiphot-2 polarized light microscope, equipped with Linkam THMS 600 heating and freezing stage connected to Linkam TP92 temperature programmer. DSC scans were performed using Du Pont DSC 2010 Differential Scanning Calorimeter attached to Thermal Analyst 2100 data station under air. The heating rate was 10 °Cmin⁻¹ in all cases. X-ray diffraction studies were carried out using Cu Kα (λ = 1.54 Å) radiation from a rotating anode X-ray generator (Rigaku) and the diffraction pattern was collected on an image plate detector (Marresearch). IR spectra were recorded on a Perkin Elmer Model 882 infrared spectrophotometer. The electronic spectra were recorded on a Shimadzu Model UV-3101 PC UV-Vis-NIR Scanning Spectrophotometer. The ^{1}H and ^{13}C NMR spectra were recorded on a Bruker DPX 300 MHz FTNMR spectrometer using tetramethylsilane (TMS) as the internal standard. Steady state photolysis was carried out on an ORIEL optical

bench using a 200 W high-pressure mercury lamp. Monochromatic light (intensity = 9.3×10^{-8} Einsteins min^{-1}) obtained by using a 320 nm band pass filter was used.

4.4.1. Materials

Reagent grade reactants and solvents were used as received from suppliers. Extremely dry solvents were prepared as per standard procedures. Spectroscopic grade solvents were used for all measurements.

4.4.1. Preparation of Methyl Gallate (5)

Gallic acid (5g, 30 mmol), sulphuric acid (concentrated, 5 mL) and methanol (50 mL, dry) were refluxed for 10 h. Excess methanol was distilled off and the reaction mixture was added to water. It was extracted with ether and the organic layer was washed with sodium bicarbonate (10%, aqueous) solution. The solvent was evaporated and the product was recrystallized from benzene to give 4g (71%) of 5, mp. 199-201 °C.

IR v_{max} (KBr): 3529, 3379, 3266, 1702, 1626, 1589, 1455 cm^{-1}; ^{1}H NMR (300 MHz, CDCl$_3$): δ 2.5 (3H, s, -OH), 3.7(3H, t, OCH$_3$), 6.9 (2H, s, aromatic);^{13}C NMR (75 MHz, CDCl$_3$): δ 49.92, 107.39, 118.27, 136.72, 143.88, 165.08.

4.4.2. Preparation of Methyl (3,4,5-Tridodecyloxy)benzoate (7)

A mixture of methyl gallate (5, 1.75g, 9.5 mmol), *n*-bromododecane (10g, 11.8 mmol) and potassium carbonate (10g, 72.4 mmol) was refluxed in cyclohexanone (80 mL) for 40 h. The reaction mixture was cooled to room temperature and the solvent was distilled off. The product was purified by column chromatography using a mixture of ethyl acetate and petroleum ether (1:19) as an eluent to give 5 g (90%) of a pure product (7), which melted at 43 °C.

IR v_{max} (KBr): 2935, 2863, 1729, 1690, 1394, 1388, 1339 cm^{-1}; ^{1}H NMR (300 MHz, CDCl$_3$): δ 0.8 (9H, t, CH$_3$), 1.2-1.4 (60H, m, OCH$_2$-CH$_2$), 3.7 (3H, t, OCH$_3$), 4.1 (6H, t, OCH$_2$), 7.2 (2H, d, aromatic); ^{13}C NMR (75 MHz, CDCl$_3$): δ 14.10, 22.69, 26.07, 26.14, 29.36, 29.38, 29.63, 29.68, 30.32, 31.93, 52.09, 69.16, 73.48, 107.97, 152.81.

4.4.3. Preparation of 3,4,5-Tridodecyloxybenzoic Acid (6)

Methyl (3,4,5-tridodecyloxy)benzoate (7, 500 mg, 0.7 mmol) and potassium hydroxide (100 mg, 1.8 mmol) were dissolved in ethanol (10 mL) and the mixture was refluxed for 4 h. To the reaction mixture, hydrochloric acid (concentrated, 4 mL) was added. The precipitated product was filtered and purified by column chromatography using a mixture of ethyl acetate and petroleum ether (1:4). The

product was further purified by recrystallization using ethanol (96%) to give 300 mg (61%) of white crystalline compound, mp. 58 °C.

IR v_{max} (KBr): 2929, 2862, 1689, 1618, 1505, 1490, 1438, 1381, 1333, 1276, 1221, 1123 cm^{-1}; ^{1}H NMR (300 MHz, CDCl$_3$): δ 0.8 (9H, t, CH$_3$), 1.2-1.4 (54H, m, OCH$_2$-CH$_2$-CH$_2$), 1.7-1.8 (6H, m, OCH$_2$-CH$_2$), 4.0 (6H, t, OCH$_2$), 7.3 (2H, d, aromatic); ^{13}C NMR (75 MHz, CDCl$_3$): δ 14.20, 22.79, 26.17, 39.38, 29.48, 29.73, 29.79, 30.42, 32.02, 69.30, 73.65, 108.67, 123.63. 142.23, 152.95, 170.93.

4.4.4. Preparation of 3,4,5-Tridodecyloxybenzyl Alcohol (11)

Lithium aluminum hydride (170 mg, 4 mmol) was taken in a round bottom flask and tetrahydrofuran (10 mL) was added dropwise under nitrogen atmosphere. Methyl (3,4,5-tridodecyloxy)benzoate (7, 3g, 4 mmol) dissolved in tetrahydrofuran (15 mL) was added to it and the reaction mixture was stirred for 1 h. The reaction mixture was quenched by the addition of water and was filtered. The filtrate was extracted with ether and the solvent was evaporated to give a product, which was recrystallized from hot acetone to give 2.6 g (93%) of a pure product (11), mp. 49-50 °C.

^{1}H NMR (300 MHz, CDCl$_3$): δ 0.8 (9H, t, CH$_3$), 1.4-1.6 (54H, m, OCH$_2$-CH$_2$-CH$_2$), 1.8 (6H, m, OCH$_2$-CH$_2$) 4.1 (6H, t, OCH$_2$), 4.6 (2H, s, CH$_2$OH), 7.3 (2H, d, ortho);

^{13}C NMR (75 MHz, CDCl$_3$): δ 14.10, 22.69, 26.07, 26.14, 29.36, 29.38, 29.63, 29.68, 30.32, 31.93, 52.09, 69.16, 73.48, 105.10, 136.24, 152.81.

4.4.5. Preparation of 3,4,5-Tridodecyloxybenzyl Chloride (12)

To a solution of 3,4,5-tridodecyloxybenzyl alcohol, **11** (1.6 g, 2.4 mmol), in dichloromethane (15 mL, dry), a catalytic amount of dimethylformamide (2 mL), followed by thionyl chloride (500 mg, 4.2 mmol) was added with stirring. It was stirred at room temperature for 1h. The solvent and excess thionyl chloride was distilled under reduced pressure. The resulting white solid was dissolved in diethyl ether and washed with water and the organic layer was dried over sodium sulfate. The crude product was purified by column chromatography using a mixture of ethyl acetate and hexane (1:19) to give 91% of product (**12**), mp. 47 °C.

IR v_{max} (KBr): 2928, 2859, 1786, 1742, 1684, 1663, 1606, 1472, 1391, 1336, 1244, 1121, 931 cm^{-1}; ^{1}H NMR (300 MHz, CDCl$_3$): δ 0.8 (9H, t, CH$_3$), 1.2-1.6 (54H, m, OCH$_2$-CH$_2$-CH$_2$), 1.8 (6H, m, OCH$_2$-CH$_2$), 3.9 (6H, t, OCH$_2$), 4.5 (2H, s, CH$_2$Cl), 6.6 (2H, d, ortho); ^{13}C NMR (75 MHz, CDCl$_3$): δ 14.10, 22.69, 26.07, 26.14, 29.36, 29.38, 29.63, 29.68, 30.32, 31.93, 46.97, 69.16, 73.48, 107.10, 132.34, 138.24, 153.21.

4.4.6. Preparation of Methyl 3,4,5-T.ris[3',4',5'-tris(*n*-dodecan-1-yloxy)-benzyoxy]benzoate (14)

A mixture of potassium carbonate (250 mg, 1.8 mmol) in dimethylformamide (25 mL, dry) purged with nitrogen. Methyl 3,4,5-trihydroxybenzoate (35 mg, 0.2 mmol) was added and the mixture was heated at 65 °C. A solution of 3,4,5-tris(*n*-dodecan-1-yloxy)benzyl chloride (386 mg, 0.6 mmol) in dimethylformamide (10 mL) was added rapidly. After 3.5 h, the completed reaction mixture was poured into cold water. The precipitated product was filtered and was purified by column chromatography using a mixture of petroleum ether and ethyl acetate (19:1). The compound was further purified by recrystallization from a mixture of dichloromethane and methanol to give **14**, mp. 57 °C.

IR v_{max} (KBr): 2928, 2861, 1735, 1676, 1598, 1517, 1439, 1333, 1241, 1119, 823 cm^{-1}; ^{1}H NMR (300 MHz, CDCl$_3$): δ 0.8 (27H, t, CH$_3$), 1.2-1.6 (162H, m, OCH$_2$-CH$_2$-CH$_2$), 1.8 (18H, m, OCH$_2$-CH$_2$), 3.8 (11H, CH$_3$ and OCH$_2$) 3.9 (6H, t, OCH$_2$), 5.0 (6H, s, Ar-CH$_2$-OAr), 6.6 (2H, d, aromatic), 7.4 (2H, s, aromatic); ^{13}C NMR (75 MHz, CDCl$_3$): δ 14.10, 22.54, 26.23, 26.34, 29.36, 29.38, 29.63, 29.68, 30.32, 31.93, 52.36, 69.16, 71.72, 73.48, 75.16, 105.72, 106.83, 109.10, 125.14, 131.76, 132.34, 137.76, 142.14, 152.56, 153.00, 153.21, 166.54.

4.4.7. Preparation of 3,4,5-Tris[3',4',5'-tris(*n*-dodecan-1-yloxy)benzyoxy]-benzoic Acid (13)

3,4,5-Tris[3',4',5'-tris(*n*-dodecan-1-yloxy)benzyoxy]benzoate (**14**, 200 mg, 0.064 mmol) was suspended in a mixture of ethanol (95%, 10 mL) and potassium hydroxide (10 N, 1 mL), heated and maintained at a gentle reflux for 3h. After cooling to room temperature ethanol was decanted and the solid residue was dissolved in tetrahydrofuran (hot) and neutralized with acetic acid (50%). The precipitate was filtered and washed well with water to give 130 mg of pure product **13** (96%), mp. 117 °C.

IR v_{max} (KBr): 2919, 2853, 1686, 1586, 1507, 1467, 1434, 1367, 1328, 1235, 1116, 1003, 811 cm^{-1}; ^{1}H NMR (300 MHz, CDCl$_3$): δ 0.8 (27H, t, CH$_3$), 1.2-1.6 (162H, m, OCH$_2$-CH$_2$-CH$_2$), 1.7-1.9 (18H, m, OCH$_2$-CH$_2$), 3.7 (8H, t, OCH$_2$) 3.9 (6H, t, OCH$_2$), 5.0 (6H, s, Ar-CH$_2$-OAr), 6.6 (2H, d, aromatic), 7.4 (2H, s, aromatic); ^{13}C NMR (75 MHz, CDCl$_3$): δ 14.10, 22.69, 26.07, 26.14, 29.36, 29.38, 29.63, 29.68, 30.32, 31.93, 69.16, 71.76, 73.51, 75.48, 105.84, 106.17, 110.13, 124.23, 131.58, 132.32, 137.94, 143.44, 152.64, 153.00, 153.31, 171.54.

4.5. Conclusions

Dendrimeric supramolecular hydrogen bonded assemblies were prepared from dendrimeric hydrogen bond donors such as 3,4,5-tri-*n*-dodecyloxybenzoic acid and 3,4,5-tris[3',4',5'-tris(*n*-dodecane-1-yloxy)benzyl-oxy]benzoic acid with hydrogen bond acceptors like 4,4'-azobipyridine (ABP), 4,4'-bipyridylethylene (BPE) and 4,4'-bipyridine (BP). The first- generation hydrogen bonded assemblies did not show any LC properties, whereas, hydrogen bonded assemblies prepared between 3,4,5-tris[3',4',5'-tris(*n*-dodecane-1-yloxy)benzyloxy]benzoic acid with hydrogen bond acceptors like 4,4'-azobipyridine (ABP), 4,4'-bipyridylethylene (BPE) and 4,4'-bipyridine (BP) exhibit cubic LC phases over a wide range of temperatures. LC phases were confirmed from POM, DSC and SAXRD. Dendrimeric supramolecules obtained from the second-generation benzoic acid derivative form a highly transparent ordered cubic glassy phases at room temperatures. These glassy superstructures were found to be extremely stable at room temperature (> 1 year).

4.6. References

1. A. Archut, F. Vögtle, *Chem. Soc. Rev.* **1998**, *27*, 233.

2. M. Freemantle, *Chem. Eng. News* **1999**, 27.

3. M. Fisher, F. Vögtle, *Angew. Chem. Int. Ed. Engl.* **1999**, *38*, 885.

4. S. Hecht, J. M. J. Frechet, *Angew. Chem. Int. Ed. Engl.* **2001**, *40*, 74.

5. A. Adronov, J. M. J. Frechet, *Chem. Commun.* **2000**, 1701.

6. R. Anwander, *Angew. Chem. Int. Ed. Engl.* **1998**, *37*, 599.

7. A. Archut, F. Vögtle, L. D. Cola, G. C. Azzellini, *Chem. Eur. J.* **1998**, *4*, 699.

8. A. Archut, G. C. Azzellini, V. Balzani, L. D. Cola, F. Vögtle, *J. Am. Chem. Soc.* **1998**, *120*, 12187.

9. A. Archut, F. Vögtle, L. De Cola, G. C. Azzellini, V. Balzani, R. H. Berg, P. S. Ramanujam, *Chem. Eur. J.* **1998**, *4*, 83.

10. M. W. P. L. Baars, S. H. M. Sontjens, H. M. Fischer, H. W. I. Peerlings, E. W. Meijer, *Chem. Eur. J.* **1998**, *4*, 2456.

11. V. S. K. Balagurusamy, G. Ungar, V. Percec, G. Johansson, *J. Am. Chem. Soc.* **1997**, *119*, 1539.

12. V. Balzani, S. Campagna, G. Denti, A. Juris, S. Serroni, M. Venturi, *Acc. Chem. Res.* **1998**, *31*, 26.

13. J. Barbera, M. Marcos, J. L. Serrano, *Chem. Eur. J.* **1999**, *5*, 1834.

14. S. Bauer, H. Fischer, H. Ringsdorf, *Angew. Chem. Int. Ed. Engl.* **1993**, *32*, 1589.

15. U. Beginn, G. Zipp, M. Moller, *Chem. Eur. J.* **2000**, *6*, 2016.

16. E. M. M. de Brabander-van den Berg, E. W. Meijer, *Angew. Chem. Int. Ed. Engl.* **1993**, *32*, 1308.

17. A. Y. Bobrovsky, A. A. Pakhomov, X. M. Zhu, N. I. Boiko, V. P. Shibaev, *Polymer Science, Ser. A.* **2001**, *43*, 431.

18. N. Boiko, X. Zhu, A. Bobrovsky, V. Shibaev, *Chem. Mater.* **2001**, *13*, 1447.

19. M. Brewis, G. J. Clarkson, A. M. Holder, N. B. Mckeown, *Chem. Commun.* **1998**, 969.

20. E. Buhieier, W. Wehner, F. Vögtle, *Synthesis* **1978**, 155.

21. P. Busson, J. Ortegren, H. Ihre, U. W. Gedde, A. U. Hult, *Macromolecules* **2001**, *34*, 1221.

22. C. G. Clark Jr, K. L. Wooley, *Polym. Pre.* **1999**, 484.

23. R. G. Denkewalter, J. F. Kole, W. J. Lukasavage, *US Patent 4,410,688* **1983**,

24. A. W. Freeman, J. M. J. Frechet, *Polym. Pre.* **1999**, 856.

25. M. A. Hearshaw, J. R. Moss, *Chem. Commun.* **1999**, 1.

26. D-L. Jiang, T. Aida, *Chem. Commun.* **1996**, 1523.

27. D-L. Jiang, T. Aida, *Nature* **1997**, *388*, 454.

28. R-H. Jin, T. Aida, S. Inoue, *J. Chem. Soc. Chem. Commun.* **1993**, 1260.

29. D. M. Jung, D. V. McGrath, *J. Am. Chem. Soc.* **1999**, *121*, 4912.

30. J. W. Kriesel, S. Konig, M. A. Freitas, A. G. Marshall, J. A. Leary, T. D. Tilley, *J. Am. Chem. Soc.* **1998**, *120*, 12207.

31. M. R. Leduc, C. J. Hawker, J. Dao, J. M. J. Frechet, *J. Am. Chem. Soc.* **1996**, *118*, 11111.

32. M. R. Leduc, W. Hayes, J. M. J. Frechet, *J. Polym. Sci. A* **1998**, *36*, 1.

33. J. W. Leon, M. Kawa, J. M. J. Frechet, *J. Am. Chem. Soc.* **1996**, *118*, 8847.

34. J. F. Li, K. A. Crandall, P. W. Chu, V. Percec, R. G. Petschek, C. Rosenblatt, *Macromolecules* **1996**, *29*, 7813.

35. K. Lorenz, H. Frey, B. Stuhn, R. Mulhaupt, *Macromolecules* **1997**, *30*, 6860.

36. J-P. Majoral, A-M. Caminade, *Chem. Rev.* **1999**, *99*, 845.

37. M. Markos, R. Gimenez, J. L. Serrano, B. Donnio, B. Heinrich, D. Guillon, *Chem. Eur. J.* **2001**, *7*, 1006.

38. H. Meier, M. Lehmann, U. Kolb, *Chem. Eur. J.* **2000**, *6*, 2462.

39. G. R. Newkome, C. N. Moorefield, G. R. Baker, *Aldrichimica Acta* **1992**, *25*, 31.

40. V. Percec, J. Heck, *J. Polym. Sci. A* **1991**, *29*, 591.

41. V. Percec, M. Kawasumi, *Polym. Prepr.* **1992**, *33*, 221.

42. V. Percec, J. Heck, D. Tomazos, F. Falkenberg, H. Blackwell, G. Ungar, *J. Chem. Soc. Perkin Trans. I* **1993**, 2799.

43. V. Percec, G. Johansson, J. Heck, G. Ungar, S. V. Batty, *J. Chem. Soc. Perkin Trans. I* **1993**, 1411.

44. V. Percec, P. W. Chu, M. Kawasumi, *Macromolecules* **1994**, *27*, 4441.

45. V. Percec, P. Chu, G. Ungar, J. Zhou, *J. Am. Chem. Soc.* **1995**, *117*, 11441

46. V. Percec, *Pure Appl. Chem.* **1995**, 2031.

47. V. Percec, G. Joharnsson, G. Ungar, J. Zhou, *J. Am. Chem. Soc.* **1996**, *118*, 9855.

48. V. Percec, C.-H. Ahn, B. Barbolu, *J. Am. Chem. Soc.* **1997**, *119*, 12978.

49. V. Percec, D. Schlueter, *Macromolecules* **1997**, *30*, 5783.

50. V. Percec, C.-H. Ahn, G. Ungar, D. J. P. Yeardley, M. Moller, S. S. Sheiko, *Nature* **1998**, *391*, 161.

51. V. Percec, D. Schlueter, G. Ungar, S. Z. D. Cheng, A. Zhang, *Macromolecules* **1998**, *31*, 1745.

52. V. Percec, W. -D. Cho, P. E. Mosier, G. Ungar, D. J. P. Yeardley, *J. Am. Chem. Soc.* **1998**, *120*, 11061.

53. V. Percec, C. -H. Ahn, W. -D. Cho, A. M. Jamieson, J. Kim, T. Leman, M. Schmidt, M. Gerle, M. Möller, S. A. Prokhorova, S. S. Sheiki, S. Z. D. Cheng, A. Zhang, G. Ungar, D. J. P. Yeardley, *J. Am. Chem. Soc.* **1998**, *120*, 8619.

54. V. Percec, C. -H. Ahn, T. K. Bera, G. Ungar, D. J. P. Yeardley, *Chem. Eur. J.* **1999**, *5*, 1070.

55. V. Percec, W-D. Cho, G. Ungar, D. J. P. Yeardley, *Angew. Chem. Int. Ed. Engl.* **2000**, *39*, 1598.

56. V. Percec, W-D. Cho, G. Ungar, *J. Am. Chem. Soc.* **2000**, *122*, 10273.

57. V. Percec, W. -D. Cho, M. Möller, S. A. Prokhorova, G. Ungar, D. J. P. Yeardley, *J. Am. Chem. Soc.* **2000**, *122*, 4249.

58. D. J. Pesak, J. S. Moore, *Angew. Chem. Int. Ed. Engl.* **1997**, *36*, 1636.

59. S. A. Ponomarenko, E. A. Rebrov, A. Y. Bobrovsky, N. I. Boiko, A. M. Muzafarov, V. P. Shibaev, *Liq. Cryst.* **1996**, *21*, 1.

60. R. Sadamoto, N. Tomioka, T. Aida, *J. Am. Chem. Soc.* **1996**, *118*, 3978.

61. M. Slany, M. Bardaji, A. -M. Caminade, B. Chaudret, J. P. Majoral, *Inorg. Chem.* **1997**, *36*, 1939.

62. D. A. Tomalia, A. M. Naylor, W. A. Goddard, *Angew. Chem. Int. Ed. Engl.* **1990**, *29*, 138.

63. D. A. Tomalia, *Adv. Mater.* **1994**, *6*, 529.

64. Y. Tomoyose, D-L. Jiang, R-H. Jin, T. Aida, T. Yamashita, K. Horie, *Macromolecules* **1996**, *29*, 5236.

65. C. Tschierske, *J. Mater. Chem.* **1998**, *8*, 1485.

66. G. Ungar, V. Percec, M. N. Holerca, G. Johansson, J. A. Heck, *Chem. Eur. J.* **2000**, *6*, 1258.

67. F. Vögtle, S. Gestermann, C. Kauffmann, P. Ceroni, V. Vicinelli, I. De Cola, V. Balzani, *J. Am. Chem. Soc.* **1999**, *121*, 12161.

68. R. Wang, Z. Zheng, *J. Am. Chem. Soc.* **1999**, *121*, 3549.

69. H. Wang, Z. Shen, J. J. Ge, S. Z. D. Cheng, F. W. Harris, *Polym. Pre.* **1999**, 486.

70. S. E. Webber, *Chem. Rev.* **1990**, *90*, 1469.

71. K. L. Wooley, C. J. Hawker, J. M. J. Frechet, *J. Am. Chem. Soc.* **1991**, *113*, 4252.

72. Z. Xu, J. S. Moore, *Angew. Chem. Int. Ed. Engl.* **1993**, *32*, 1354.

73. D. J. P. Yeardley, G. Ungar, V. Percec, M. N. Holerca, G. Johansson, *J. Am. Chem. Soc.* **2000**, *122*, 1684.

74. A. R. A. Palmans, J. A. J. M. Vekemans, H. Fischer, *Chem. Eur. J.* **1997**, *3*, 300.

75. Z. Sideratou, C. M. Paleos, *Mol. Cryst. Liq. Cryst.* **1995**, *265*, 19.

76. G. W. Gray, B. Jones, F. Marson, *J. Chem. Soc.* **1957**, 393.

77. S. Kutsumizu, M. Yamada, S. Yano, *Liq. Cryst.* **1994**, *16*, 1109.

78. M. Lee, B.-K. Cho, Y.-S. Kang, W. -C. Zin, *Macromolecules* **1999**, *32*, 8531.

79. E. Nishikawa, E. T. Samulski, *Liq. Cryst.* **2000**, *27*, 1457.

80. H. I. Bernstein, W. C. Quimby, *J. Am. Chem. Soc.* **1943**, *65*, 1845.

81. V. Ramamurthy, K. Venkatesan, *Chem. Rev.* **1987**, *87*, 433.

82. Z. Savion, D. L. Wernick, *J. Org. Chem.* **1993**, *58*, 2424.